UTILIZATION OF INFLUENZA VACCINATION AS AN INTRATUMORAL

IMMUNOTHERAPY FOR CANCER

By

JENNA NEWMAN

A dissertation submitted to the

School of Graduate Studies

Rutgers, The State University of New Jersey

In partial fulfillment of the requirements

For the degree of

Doctor of Philosophy

Graduate Program in Microbiology and Molecular Genetics

Written under the direction of

Andrew Zloza

And approved by

_____

_____

_____

_____

New Brunswick, New Jersey

October 2019

ABSTRACT OF THE DISSERTATION

Utilization of influenza vaccination as an intratumoral immunotherapy for cancer

by JENNA NEWMAN

Dissertation Director:

Andrew Zloza

In recent years, immunotherapy for cancer has yielded unprecedented response rates and increased survival in patients. Despite progress, a significant fraction of patients exhibit progression of tumor growth during immunotherapy treatment. One barrier to response is the tumor microenvironment; patients who lack immune infiltration of their tumors or exhibit infiltration of suppressive cell subsets often do not respond to immunotherapy. In an effort to infiltrate the tumor microenvironment with pro-inflammatory cells (such as $CD8^+$ T cells) that are correlated with response to immunotherapy in the clinic, inactivated influenza was administered intratumorally in immunocompetent mice. This vaccination slowed tumor growth when compared to that of mock-treated controls, and yielded an increased proportion in the tumor of dendritic cells, cross-presenting dendritic cells, $CD8^+$ T cells, and tumor-reactive $CD8^+$ T cells –all critical for anti-tumor immunity. Moreover, analysis of RNA from the vaccinated tumor revealed an upregulation in transcripts indicative of an inflamed tumor microenvironment, relative to that observed in mock-treated controls. Intratumoral influenza vaccination administered in combination with checkpoint blockade (αPD-L1) immunotherapy resulted in superior tumor control relative to that observed with either therapy alone. Further benefit derived from the intratumoral vaccination was protection from influenza infection. Interestingly, one vaccine formulation tested contained a

squalene-based adjuvant; this vaccine did not slow tumor growth and failed to reduce the proportion of suppressive B regulatory cells (Bregs) in the tumor. Depletion of Bregs enabled the adjuvanted influenza vaccine to slow tumor growth. The research discussed in this dissertation indicates that intratumoral influenza vaccination may be used in the future as an immunotherapy for cancer; clinical trials are currently in preparation.

ACKNOWLEDGEMENTS

Kohlhapp FJ, *et al.* (2016) Non-oncogenic Acute Viral Infections Disrupt Anti-cancer Responses and Lead to Accelerated Cancer-Specific Host Death. *Cell Reports* 17(4): 957-965.

The past four years have been replete with learning, scientific growth, personal growth, encouragement, friendship, and mentorship. There are countless individuals and groups that have enriched every day of my experience; my gratitude for the richness of this experience and the accompanying support is endless.

I would like to start by thanking the members of the Zloza Laboratory for providing a wonderful setting for conducting scientific research. To Shengguo, who tirelessly ensured that our laboratory was always experiment-ready and who provided great support, encouragement, and advice throughout my course in the lab. To Fred, Brent, Natalie, Praveen, Sachin, Sal, Russell, Rico, and all others who worked alongside me in the lab, thank you for fostering a great community in the lab and for our friendship. To Nora and Stuti, thank you for being wonderful lab partners; mentoring you has been among my greatest moments as a Ph.D. student. Thank you to my advisor, Dr. Andrew Zloza, for providing unending support and encouragement throughout the past 4 years. I am immensely grateful for your efforts in familiarizing me with the field of tumor immunology (by encouraging my attendance at workshops and top conferences), providing insights on what it means to become an excellent scientist, and navigating the world of postdoctoral fellowships and beyond. I have been further energized and excited by science in these past 4 years, and I am looking forward to carrying the Zloza lab spirit to the next stage!

I am endlessly grateful to the Denzin and Sant'Angelo labs for graciously welcoming me into their labs for the past 9 months as I completed the work for this dissertation. Thank you for providing a wonderful, friendly, and supportive environment for me that always felt like home. Thank you to Lou, Dani, Jen, Neelam, Austin, Agata, Patrick, Josh, and Aditya for being great labmates and friends; you truly have enriched my experience here. Thank you to Dr. Lisa Denzin, for so kindly integrating me as a member of the lab, and for your support and wonderful mentorship through this process. Thank you to Dr. Arnold Rabson, for generously incorporating me into the CHI community and for excellent mentorship. Thank you to Dr. Lori Covey, for teaching me immunology and providing great insights and excellent mentorship. I am forever grateful.

Thank you to the staff of the Cancer Institute of New Jersey and Child Health Institute of New Jersey for providing the resources and support for conducting my research; from core resources to the vivarium, it has been a pleasure working with you.

Thank you to the NIH-Rutgers-Biotechnology Training Program, which I have been a member of for the past 4 years. Our sessions and symposiums have been extremely educational and have prepared me for a career in biomedical research. I have so often emerged from these meetings incredibly inspired to pursue science. Thank you to Drs. Ann Stock and Martin Yarmush for coordinating such a wonderful program and for your excellent mentorship and encouragement.

Thank you to the Molecular Biosciences and Microbiology & Molecular Genetics Ph.D. programs for providing an encouraging, supportive environment for graduate students. I have greatly benefitted from the courses and career workshops that are

My experience as a Ph.D. student would have been significantly less enriching if it hadn't included meeting and befriending my phenomenal classmates. Since day 1, we have been in the PhD process together; from studying amino acid side chains together, to rehearsing our qualifying exam proposals, to getting dinner together in the midst of our most jam-packed research days, you have been the glue that cements this great experience. Thank you to Austin, Agata, Brandon, Christen, Eve, Larry, Praveen, Vaidhy, Victor and Vrushank for being wonderful friends and classmates. Thank you to Eve for being an awesome friend throughout these years and my thesis writing (and ice cream, of course) buddy! I will cherish these memories and fondly look back upon my graduate years thinking of all of you.

Thank you to my family, who has always provided me with extraordinary support and encouragement. Throughout these past 4 years, you have guided me, provided advice, and have been my biggest cheerleaders. Thank you for constantly listening to my research updates, and for patiently understanding when an experiment ran a little late or

coincided with a holiday weekend. To my sisters, Kimberly and Heather, thank you for always being available—whether it be in person or our "sister love" group chat—for me to share my graduate school experience with you. Thank you to my mother for wholeheartedly supporting me through this process and providing the most wise advice and feedback known to humankind!

I would like to dedicate this dissertation to my father, who provided me with the best example of what it means to be a kind and passionate person who lives life to the fullest. When I was young, you opened my mind and spurred my imagination; you loved answering my questions about how the world worked and inspired and encouraged me to explore further. I am forever inspired by your love of knowledge and adventure; this has driven me throughout my graduate school years and will always stay with me.

TABLE OF CONTENTS

TABLE OF FIGURES

TABLE OF FIGURES (ADDENDUM)

TABLE OF TABLES

TABLE OF TABLES (ADDENDUM)

TABLE OF SCHEMES (ADDENDUM)

CHAPTER 1: INTRODUCTION

Immunotherapy for Cancer: The Challenge of the Tumor Microenvironment

Immunotherapy has emerged in recent years as an approach towards cancer treatment in response to the ineffectiveness of chemotherapy, radiation therapy and surgery in a notable fraction of cancer patients[1]. While there are several diverse treatment strategies under investigation (ranging from cytokine therapy to blockade of inhibitory immune checkpoints to oncolytic viruses to chimeric antigen receptor (CAR) T cells)[1,2], a nearly universal prerequisite for (successful) immunotherapy treatment is the ability of immune cells to navigate to and enter the tumor[3]. The tumor microenvironment presents a significant barrier that restricts immune responses against tumors and limits the efficacy of currently available immunotherapies as treatments for cancer[3]. A significant proportion of patients harbor an immunologically "cold" tumor microenvironment that is either devoid of immune cell infiltration (an "immune desert") or that is predominantly infiltrated by suppressive regulatory cell subtypes (including regulatory T cells [Tregs] and myeloid-derived suppressor cells [MDSCs])[3,4]. In both environments, cancer growth is immunologically unchecked and recruitment of inflammatory immune cells into such tumors is imperative. However, immune infiltration of tumors, especially by CD8^{+} T cells, has been shown to correlate with augmented responses to immunotherapy and improved survival[4-8]. An immunologically inflamed ("hot") tumor microenvironment exhibits robust antigen presentation and T cell activation, contributing to the development of tumor-specific CD8^{+} T cell functionality that can acutely eliminate cancer cells, generate systemic tumor-specific immunity, and form long-term anti-tumor memory responses[8,9]. However, responses to such therapies—particularly commonly prescribed

checkpoint blockade therapies (αPD-1/αPD-L1) that reduce tumor growth by alleviation of T cell exhaustion[10]—have been demonstrated to be effective only in select patients, particularly those who harbor a "hot" tumor microenvironment[11]. Therefore, to increase response rates to immunotherapy, innovative solutions are needed to convert "cold" tumor microenvironments to "hot" by increasing infiltration of inflammatory immune cells that can serve as targets for immunotherapies in tumors devoid of pro-inflammatory immune infiltration and can overcome local immunosuppression in tumors infiltrated by regulatory cells.

Pathogen-based Strategies for Inflammation of the Tumor Microenvironment

One approach to inflame the tumor microenvironment, and ultimately reduce tumor growth, could be to introduce an infection by a pathogen. Since antiquity, it has been noted that infection of a tumor can lead to tumor regression[12-14]. In ancient Egypt, a physician named Imhotep discovered that if an incision was made into a tumor, that the tumor would become infected and sometimes regress[12-15]. Other examples throughout history have been documented; for instance, a priest in Italy was recorded to have a tumor in his leg so large that it compromised the adjacent skin tissue and emerged forth[12,13]. Subsequently, the tumor became inflamed and completely disappeared[12, 13]. In the late nineteenth century, Dr. William Coley, of what is now Memorial Sloan Kettering Cancer Center in New York City, observed regression of a previously treatment-resistant tumor in a patient who acquired the bacterial infection *Streptococcus pyogenes*[13]. In response to this incident, Dr. Coley began to systematically test whether bacterial infection could lead to tumor regression; due to adverse reactions to infection (at a time in which antibiotics were not available), Dr. Coley switched to using a cocktail of inactivated *Streptococcus*

pyogenes and *Serratia marcescens* bacteria[12,13,16,17]. Upon induction of a fever, some patients would exhibit complete regression of their tumor(s)[13,17]. The mechanisms leading to tumor regression in response to Coley's toxin are not well-documented due to technological limitations of the time; however, better understanding of immunology in recent years has led to conjectures of how Coley's toxin may promote anti-tumor immunity, and ultimately, reduction of tumor growth. Foreign genetic material or cellular components from pathogens can serve as pattern-associated molecular patterns (PAMPs) that bind to toll-like receptors (TLRs) on cells of the innate immune system (macrophages, dendritic cells), subsequently initiating a signaling cascade that triggers an inflammatory response designed to eliminate the pathogen[18]. Licensed dendritic cells will acquire local antigens—some of which may be tumor-derived—and interact with T cells[18]. Activated tumor-reactive T cells, particularly $CD8^+$ T cells, can directly target tumor cells for death. Upregulation of cytokines, such as IFN-γ, IL-12 and TNF-α, will further contribute to inflammation and expansion of pro-inflammatory, anti-tumor immune cell subsets[18]. In summation, these changes induced by exposure to a pathogen could reverse the immunosuppression of the tumor microenvironment.

The Demise of Coley's Toxin: The Discovery of Oncogenic Pathogens

In the twentieth century, the advent of chemotherapy and radiation therapy halted advancement of Coley's toxin in the clinic, as these treatments were viewed as more consistent in their targeting of tumors, and were easily standardizable in terms of both production and administration in clinics[18]. Further, the early twentieth century brought forth advancements in our knowledge of pathogens that were paradigm-shifting—and alarming. In 1911, Rockefeller Institute (now Rockefeller University in New York City)

pathologist Francis Peyton Rous demonstrated that sarcomas developed in chickens that were administered supernatant of tumor extracts from sarcomas originating in other chickens of the same variety[19]. Tumor extracts were suspended in sterile sand and Ringer's solution and subjected to multiple rounds of centrifugation, convincing Rous that tumor extracts injected into naïve animals were indeed cell-free[19]. Rous proposed that the transmissible, cancer-causing agent was a "minute parasitic organism" or a "chemical stimulant elaborated by the neoplastic cells"[19]. However, contemporaries dismissed these ideas and insisted that the tumor extracts were not completely cell-free and/or that the masses Rous identified were infectious granulomata rather than tumors[20]. The importance of the Rous sarcoma virus (RSV), cancer-causing agent derived from the cell-free supernatant of chicken tumor extracts, was overlooked until 1958, when Howard Temin and Harry Rubin demonstrated that RSV could convert a chicken fibroblast into a cell with an embryonic cell phenotype[20, 21]. This key experiment brought forth a revival of the study of RSV, and Rous was awarded the Nobel Prize in Physiology and Medicine in 1966[20]. In 1970, Howard Temin, Satoshi Mizutani, and David Baltimore discovered that the RSV virion harbored an RNA-dependent DNA polymerase, in addition to its single-stranded RNA genome[22, 23]. Viruses possessing the capability of converting RNA to DNA, now called retroviruses, were later shown to use an enzyme called integrase to insert viral DNA into the host genome[24]. RSV was found to contain in its genome an avian-derived oncogene[25], src, and the integration of src into a host cell genome was demonstrated to be the mechanistic driver of oncogenesis by RSV[26]. Apart from such integration of a host cell-derived oncogene into the host genome, it has been widely acknowledged that another mechanism of retroviral-induced carcinogenesis is integration

of the viral genome in regions of proto-oncogenes or tumor suppressor genes. Disruptions

in such genes may yield hyperactivity of a proto-oncogene or loss of function of tumor

suppressor gene products[27]. RSV is an example of an oncogenic virus, that is, a virus

causally linked to the development of cancer. The cancer-causing genetic alterations

induced by RSV infection constitute a direct mechanism for oncogenesis. While RSV

serves as a classic example by which viruses can promote tumor development by

introduction of an oncogene into the host genome, there are countless other oncogenic

infections that induce cancer development by indirect means.

Oncogenic viruses are not just limited to retroviruses and vary widely in the

mechanisms by which they induce tumorigenesis. Another significant, albeit indirect,

mechanism by which viruses can cause cancer is via damage induced by the

inflammation and perpetual cell turnover associated with chronic infection[28]. Hepatitis B

virus (HBV) and hepatitis C virus (HCV), both implicated in the development of

hepatocellular carcinoma (HCC), are two viruses that are oncogenic, mainly as a

consequence of chronic inflammation in the liver[29]. Typically, HCC arises in patients

infected with hepatitis for two decades or longer, who usually present with cirrhosis or

severe fibrosis prior to HCC diagnosis[30]. Research has shown that cytokines that are

present at constitutively high levels as a product of chronic inflammation, such as TNF-α

and IL-6, may promote tumor cell proliferation[31]. IL-6 operates as a growth factor for

cancer via its downstream activation of the transcription factor STAT3[31]. Interestingly,

IL-6 has been implicated as a predictor of whether a patient with chronic viral hepatitis

infection progresses to HCC, with patients exhibiting higher serum levels of IL-6 more

frequently developing HCC than those harboring lower levels[32]. Although the indirect

mechanism of chronic inflammation as an agent of tumorigenesis is believed to be a main

driver of HCC development in individuals with chronic HBV or HCV infection, there is

some evidence that these viruses mediate oncogenesis directly. For example, the HBx

protein encoded by HBV is known to upregulate the MAP/ERK pathway and lead to

genomic instability[33]. Nevertheless, the inflammation brought forth by chronic infection

is a clinically significant mechanism of oncogenic virus-mediated tumorigenesis. In fact,

inflammation as a mediator of cancer development is not limited to oncogenic viral

infection. Individuals with Crohn's disease have an elevated risk of developing colorectal

cancer[34], and those infected with the bacterium Helicobacter pylori are at higher risk than

the general population for developing stomach cancer[35].

While commonly referenced as classic mechanisms by which viruses can cause

cancer, retroviral integration into the host genome and inflammation and cell turnover

caused by chronic viral infection are only two of the several mechanisms by which viral

infection can impact tumor development. Epstein-Barr virus (EBV) has been linked to

nasopharyngeal carcinoma and several subtypes of lymphoma, including Burkitt's

lymphoma and Hodgkin's lymphoma[36]. EBV is a double-stranded DNA gammaherpes

virus that infects B cells and later establishes latency[36]. EBV-infected B lymphocytes

acquire an activated phenotype, engaging survival-promoting B cell signaling, and

consequently, leading to tumorigenesis[36]. Merkel cell polyomavirus, the virus responsible

for most Merkel cell carcinomas observed in humans, has been shown to induce

transformation in rodents, in vivo, under certain conditions[37]. One mechanism by which

polyomaviruses promote the development of cancer is by inducing the host cell to

transition into the S phase of the cell cycle, promoting host cell division, and

consequently, viral replication[38]. Another double-stranded DNA virus, human

papillomavirus (HPV)[39], which can cause cervical cancer and head and neck cancer,

mediates tumorigenesis by other mechanisms. Specifically, degradation of the pro-

apoptotic protein Bak is mediated by HPV protein E6, conditioning pre-cancerous cells

for survival[40]. Furthermore, E6 is believed to disrupt normal functioning of tumor

suppressors, such as p53[40].

Oncogenic infections can also increase the incidence of cancer in the context of

immunosuppression. The best-known example of this is observed in individuals infected

by human immunodeficiency virus (HIV). Patients with HIV have elevated incidence of

several cancers referred to as acquired immunodeficiency syndrome (AIDS)-defining

cancers (ADCs) subsequent to HIV infection including Kaposi's sarcoma, primary

central nervous system lymphoma (PCNSL), cervical cancer, and non-Hodgkin's

lymphoma[41]. Additionally, other types of cancers referred to as non-AIDS-defining

cancers (NADCs) such as lung, liver, anal, and melanoma are increased in HIV-infected

individuals and are major contributors to morbidity and mortality in this patient

population. In the context of HIV infection-induced global immunosuppression,

oncogenic viruses such as EBV can establish chronic infection, leading to stimulation of

B cells that can drive the development of lymphoma, as previously discussed[41].

Approximately 80–100% of Hodgkin's lymphomas and PCNSLs in AIDS patients can be

attributed to EBV infection[41]. Hepatitis B and hepatitis C infections, as well as human

papillomavirus infections, have been reported at high frequency in AIDS patients, and

observed in conjunction with hepatocellular and cervical cancers, respectively[41]. These

data illustrate that loss of immunological control of viral infection is strongly linked to

the development of cancer, indicating the major role that pathogens play in promoting tumorigenesis. Furthermore, it should be noted that the emergence of cancer in AIDS individuals can be partially attributable to the inability of an immunocompromised individual to mount functional anti-tumor immune responses against tumors in their nascent, subclinical stages[42]. The ability of the immune system to detect abnormal-self cells is dependent upon several physiological factors, including the presence or absence of viral infection, as is discussed in the sections below. [This section is a direct passage from Newman JH and Zloza A (2017) Infection: a Cause of and Cure for Cancer. Current Pharmacology Reports 3(6): 315-320.]

Oncogenic pathogens are diverse in their mechanisms of promoting tumor growth; after a century of investigation, we now have a basic understanding of the genetic and immunological programs that trigger and support oncogenesis. Armed with knowledge, the fear of oncogenic pathogens has quieted, allowing for a revisiting of the idea of developing modernized and optimized Coley's toxins for the treatment of cancer.

Oncolytic Viruses: Employing Viruses to Target Tumors

In the present age of immunotherapy, there has been a resurgence of interest in utilizing pathogens to reverse the suppression of the tumor microenvironment and stimulate anti-tumor immunity. Currently, the focus mainly has been centered on use of oncolytic viruses—viruses that selectively replicate in and lyse tumor cells[2]. Mechanistically, it is thought that the therapeutic potential of oncolytic virus infection relies on two main actions of such viruses, first being preferential lysis of tumor cells and the second being the resultant priming of a systemic anti-tumor immune response

subsequent to cell lysis-mediate release of tumor antigens in the context of inflammation[2]. Defective interferon and toll-like receptor signaling in tumor cells allows for successful viral replication, while non-cancerous cells equipped with functional interferon signaling and other viral recognition pathways effectively thwart viral replication, thereby mainly limiting oncolytic viral infection to tumor cells[2,43]. Failure to clear virus from tumor cells can result in activation of apoptosis, necrosis, or pyroptosis, yielding lysis of such tumor cells[2]. Upon lysis, tumor neoantigens, pattern-associated molecular patterns (PAMPs; such as viral proteins and genomic material), and damage-associated molecular patterns (DAMPs) such as ATP, calreticulin, and uric acid, are released from the cell[2]. Released antigens are engulfed and presented by antigen presenting cells, which interact with the TCRs on T cells, ultimately leading to the activation of IL-2-secreting $CD4^+$ T lymphocytes[2]. Engagement of IL-2 by the IL-2 receptor on cytotoxic T ($CD8^+$) lymphocytes yields activation of CTLs reactive to tumor antigens[2]. Cytokines such as TNF-α, IFN-γ, and IL-12 released from lysed tumor cells can engage cytokine receptors on natural killer (NK) and $CD8^+$ T cells, promoting destruction of tumor cells that downregulate major histocompatibility complex (MHC) antigen-presentation molecules and tumor cells expressing neoantigens, respectively[2]. In summation, oncolytic viruses can promote tumor cell death by inducing lysis of infected cells, exposing tumor-associated antigens, neoantigens, and danger signals that can subsequently initiate and propagate anti-tumor immune responses.

In the clinic, oncolytic viruses have demonstrated efficacy in curtailing tumor growth. In October 2015, the United States Food and Drug Administration (FDA) approved Imlygic (Amgen, Inc.), a modified herpes simplex-1 (HSV-1) oncolytic virus

therapy[44]. Imlygic, also called talimogene laherparepvec (T-VEC), harbors a deletion in the ICP34.5 neurovirulence gene and the ICP47 gene, which obstructs antigen presentation by binding to the transporter of antigen presentation (TAP) protein, consequently preventing binding interactions between TAP and peptide that are necessary for an operational MHC Class I presentation pathway[45, 46]. Further, an insertion of the granulocyte macrophage-colony stimulating factor (GM-CSF) gene yields infiltration of macrophages and dendritic cells into the infected tumor, thereby strengthening the anti-tumor immune response[45]. The results of a 436-patient clinical trial comparing intratumoral administration of T-VEC to subcutaneously delivered GM-CSF in patients with stage IIIb to IV melanoma, published in 2015, indicated that 16.3% of T-VEC-treated patients had a durable response to therapy, compared to the 2.1% durable response rate observed for GM-CSF treatment[47]. Further, median survival was increased in the T-VEC-treated arm. Together, these data demonstrate that T-VEC can be employed as a treatment for melanoma, without an excess of detrimental side effects[47].

Oncolytic virus therapies utilizing other classes of virus and various genetic modifications are currently under investigation and in clinical trial. Coxsackievirus, vaccinia virus, adenovirus, reovirus, Newcastle disease virus, measles virus, and others have been candidates for oncolytic virus therapy of cancer[48]. Cytokines and molecular mediators of the immune system that can augment the immune response initiated by oncolytic viral infection include IL-2, IL-12, IL-15, IFN-α, and 4-1BB. Genes encoding these cytokines have been explored as potential candidates for insertion into oncolytic viral genomes. In China, a modified adenovirus, H101, was approved in 2006 for head and neck squamous cell carcinoma[49]. Coxsackievirus A21 (CVA21) has been tested as an

oncolytic viral therapy for melanoma with one clinical trial already demonstrating that 19.3% of patients exhibit a durable response, and 75.4% of patients survive 1 year after beginning treatment[50]. Additionally, an attenuated poliovirus (PVSRIPO) harboring the internal ribosome entry site of human rhinovirus type 2 (HRV2) is currently under investigation for the treatment of glioblastoma[51]. Glioblastoma cells largely express CD155 (the receptor for poliovirus), rendering them a good target for PVSRIPO oncolytic virus therapy[52]. In conjunction with use of other immunotherapies, such as PD-1 and CTLA-4 blockade, oncolytic viruses have the potential to become even more effective treatments for cancer. For a summary of select clinical trials of oncolytic viruses with clinical and immune outcomes data, please see the following reviews[53, 54]. While oncolytic viruses have had some success in the clinic, they are limited in application, for several reasons, including inability to infect the entire spectrum of (tumor) cell types[53] and limits on mode of delivery[55]. [This section is a direct passage from Newman JH and Zloza A (2017) Infection: a Cause of and Cure for Cancer. Current Pharmacology Reports 3(6): 315-320.]

The Impact of Non-oncogenic, Non-oncolytic Pathogens on the Development and Progression of Cancer

The subsets of oncogenic and oncolytic pathogens are small and defined by a few well-studied examples (see above); most pathogens that have been characterized are neither oncogenic nor oncolytic, and will therefore be referred to as non-oncogenic, non-oncolytic pathogens. The impact of such pathogens on tumor development and progression is unclear. In the literature, there are conflicting reports regarding the role of infection in cancer. In one report, immunocompetent C57BL/6 (B6) mice were challenged with A/PR8/H1N1 influenza 60 days prior to intradermal Lewis Lung

Carcinoma (LLC) tumor challenge; in these mice, tumors grew more slowly than that noted in influenza-naïve controls[56]. Contrarily, B6 mice concomitantly challenged with lymphocytic choriomeningitis virus (LCMV) and B16-F10 melanoma exhibited accelerated tumor growth relative to that observed in uninfected counterparts[57]. Acceleration versus slowing of tumor growth in the presence of infection is context-dependent and may implicate multiple immunological pathways. A mechanism by which infection may contribute to slowing of tumor growth is the induction of cytokines that may promote anti-tumor immune responses. For example, the live, attenuated tuberculosis vaccine Bacillus Calmette-Guérin (BCG) is used as a treatment for bladder cancer; the immune response initiated in response involves upregulation of MHC-II and induction of cytokines such as IFN-γ, TNF-α, GM-CSF, and IL-8, which promote activation of CD8$^+$ T cells and natural killer (NK) cells[58, 59]. Additionally, BCG has been reported to increase the T helper 1 (T cell-centric, Th1): T helper 2 (B cell-centric, Th2) T cell ratio in the tumor, which is considered to be favorable for generating anti-tumor immunity[60]. Taken together, infection may slow tumor growth via production of pro-inflammatory cytokines that modulate the tumor microenvironment such that anti-tumor immune responses can be facilitated. One hypothesis for accelerated growth of tumors in the context of LCMV is the immunosuppressive nature of LCMV infection; LCMV enters CD11c$^+$ and DEC-205$^+$ dendritic cells via binding to the α-dystroglycan (α-DG) receptor, replicates, and consequently dampens antigen presentation and corresponding T cell responses[61]. Global dysfunction of antigen presentation may detrimentally impact anti-tumor T cell responses as well, potentially resulting in tumor growth acceleration[62]. Another possibility is that potent anti-viral immune responses mounted against

immunodominant epitopes might outcompete anti-tumor immune responses, which are weaker due to tumors' similarity to normal self antigens[63]; less vigilant immunological surveillance of tumors could potentially result in acceleration of tumor growth in the context of viral infection.

In 2016, my colleagues and I published a report in which we determined that B6 mice concomitantly challenged with (intranasal) A/PR8/H1N1 influenza and (intradermal) B16-F10 melanoma exhibited accelerated tumor growth and reduced overall survival relative to that observed in influenza-naïve mice (Fig. 1.1)[64]. Interestingly, this finding was not limited to influenza, as other pathogens such as *Staphylococcus aureus* and LCMV also accelerated tumor growth[64]. Further, such pathogens accelerated growth of multiple tumor types beyond B16-F10 melanoma, including MCA205 sarcoma, 4T1 breast cancer, and Braf/Pten inducible melanoma[64]. Mechanistically, acceleration in tumor growth was attributable to egress of tumor-reactive CD8^{+} T cells from the tumor—where they are indispensable for tumor control—to the lungs, the site of infection (Fig 1.1)[64]. Given this finding, it is imperative to ask whether influenza infection can recruit immune cells to the tumor, if the infection and tumor are present at the same anatomical location. These data suggest that, if infection recruits anti-tumor immune cells, that concomitant infection and tumor challenge in a shared anatomical location should result in pro-inflammatory immune infiltration of the tumor microenvironment, and consequently, reduce tumor growth. Similar to that described for the proposed mechanisms of action for Coley's toxin as a cancer treatment, local infection should result in TLR activation, dendritic cell maturation, pro-inflammatory cytokine production, and expansion of CD8^{+} T cells capable of tumor

elimination. It is this hypothesis that is the foundation for the work that is to be described

below.
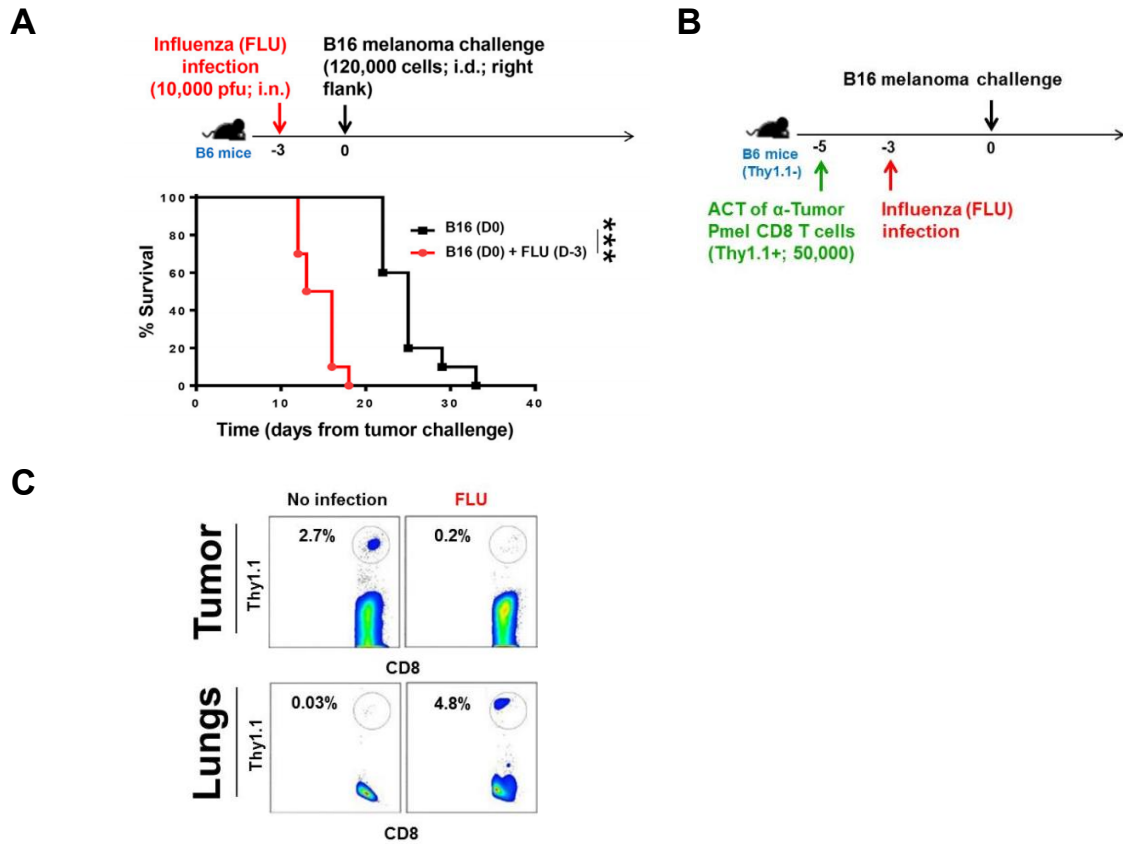
Fig. 1.1 Influenza in the lungs accelerates growth of melanoma in the skin of the flank and promotes egress of anti-tumor CD8$^+$ T cells to the lungs. (A) Experimental design. Survival was defined by tumor size <100 mm^2. ***, P<0.001 [Mantel-Cox logrank test]. (B) Experimental design for studies in which B6 mice received adoptive cell transfer (ACT) of Pmel cells on day −5, were infected with influenza on day −3, and were challenged with B16 melanoma on day 0. (C) Tumors from experiment described in (B) were resected at day 15 and analyzed via flow cytometry. Results depicted by representative flow plots show % of pmel (α-gp100) CD8$^+$ T cells among all CD8$^+$ T cells. Axes on all plots are log scale. All experiments were performed with 5–10 mice per group with at least two independent repeat experiments. i.d., intradermal, i.n., intranasal. Adapted from Kohlhapp *et al.*, 2016[64].

CHAPTER 2: INFLUENZA INFECTION IN THE LUNGS IMPROVES OUTCOMES IN MICE AND PATIENTS WITH CANCER IN THE LUNGS

Previous research in the laboratory indicated that mice concomitantly challenged with influenza in the lungs and melanoma in the skin of the flank exhibit accelerated tumor growth relative to uninfected controls[57]. Mechanistic interrogation revealed that there was shunting of tumor-reactive CD8$^+$ T cells from the tumor to the site of infection[64]. To determine whether immune cells could be recruited to a shared site of an infection and tumor (and thereby inflame the tumor microenvironment with tumor-targeting pro-inflammatory cells), immunocompetent B6 mice were administered B16-F10 melanoma intravenously, for homing of the tumor to the lungs. B16-F10 melanoma is an immunotherapy-resistant (including αPD-1), non-metastatic, transplanted syngeneic model of cancer commonly used in the field of tumor immunology[65, 66]. Concurrently, A/PR8/H1N1 influenza—a widely used Influenza A infection adapted for replication in the mouse respiratory tract[67]–was administered intranasally to create a productive infection in the lung. Indeed, influenza infection in the lungs reduced the number of melanoma foci in the lung, and this effect was augmented in combination with αPD-1 checkpoint blockade (Fig. 2.1, A and B). These data suggest that influenza can promote anti-tumor immunity when present in the same location as the tumor, and that infection can sensitize tumors to αPD-1 treatment.

To assess clinical relevance, the SEER-Medicare Linked Database, which contains medical information of over 30,000 patients with lung cancer, was surveyed for recorded influenza diagnoses. Patients who had one or more diagnoses of influenza infection during their lung cancer course exhibited decreased lung cancer-specific and overall mortality (Fig. 2.1, C and D), in agreement with mouse model observations.

Importantly, the time to lung cancer-specific mortality and overall mortality in 25% of each population was prolonged 12 and 19 months, respectively, for patients with a diagnosis of influenza infection during their lung cancer course (Fig. 2.1, E and F). Altogether, these mouse and human data reveal that infection may be inflaming the tumor microenvironment *in situ* and consequently contributing to the reduced tumor growth observed. This requires further experimentation to understand the mechanisms of action and to optimize treatment for the clinic; these efforts will be discussed in following chapters of this dissertation.
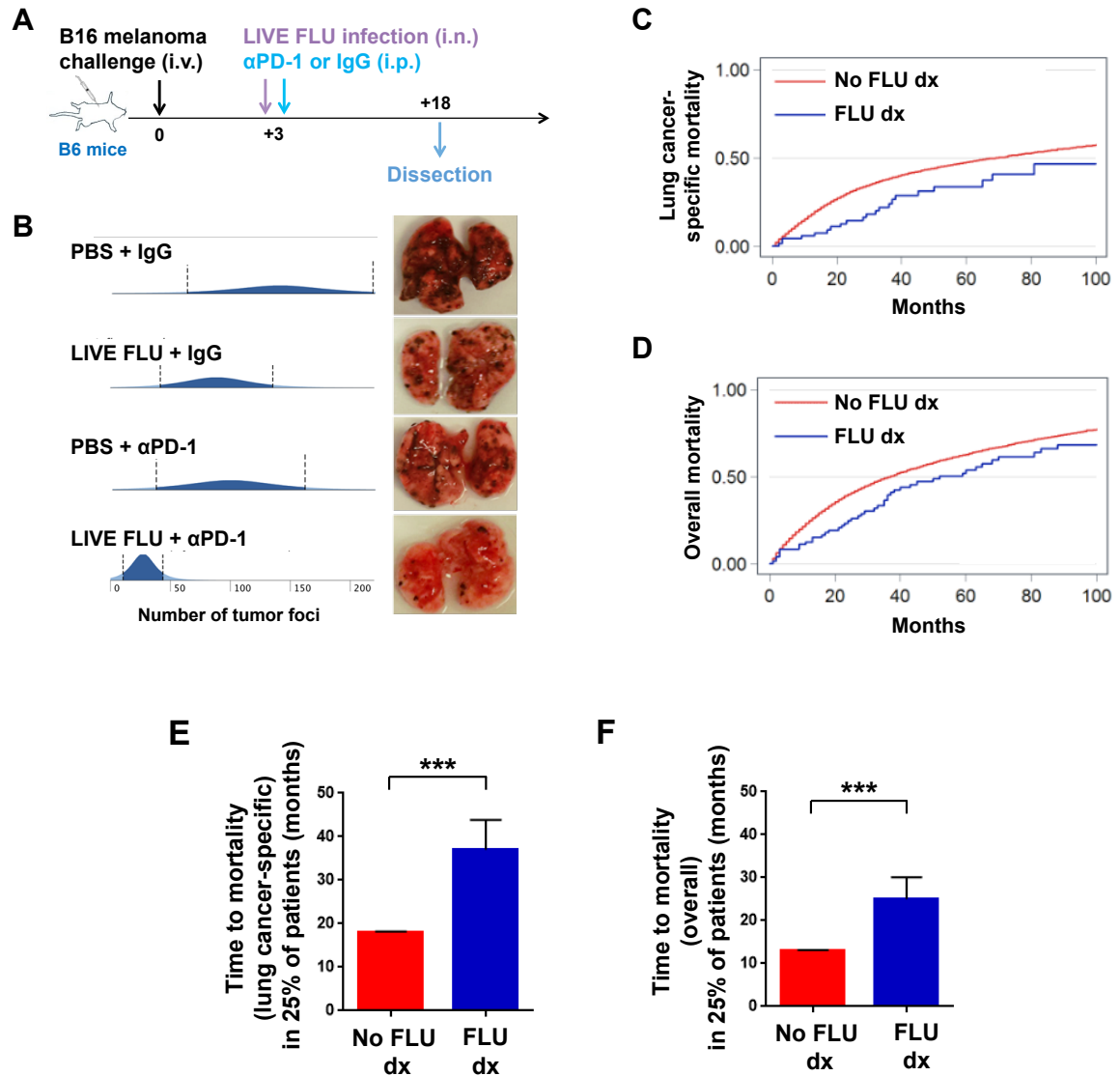
Fig. 2.1 Influenza infection in the lungs improves outcomes in mice and patients with tumors in the lungs (A) Experimental design. Data are representative of at least two independent experiments with similar results. (B) Histograms showing number of melanoma foci per lung surface (left; n = 10 mice/group) and representative lung images (right). P<0.05 for comparisons between all groups except between LIVE FLU + IgG and PBS + αPD-1 [One-way ANOVA with Tukey correction]. (C) Kaplan-Meier curves of lung cancer-specific mortality in patients with lung cancer included in the SEER-Medicare Linked Database and followed for 100 months, who had a recorded diagnosis (FLU dx) or not (No FLU dx) of influenza infection during their cancer course. n=34,277. (D) As in (C), but assessing overall mortality. n=34,529. (E) Bar graphs showing mean time to lung cancer-specific mortality in 25% of patients (P25). (F) As in (E), but for overall mortality. ***P< 0.001 [Two-tailed student t test]. Mean ± s.e.m. i.v., intravenous. i.n., intranasal. i.p., intraperitoneal. LIVE FLU, live influenza virus.

CHAPTER 3: INTRATUMORAL HEAT-INACTIVATED, BUT NOT LIVE, INFLUENZA ADMINISTRATION REDUCES TUMOR GROWTH IN THE SKIN

Intratumoral Heat-inactivated, But Not Live, Influenza Slows Growth of Melanoma in the Skin

Influenza infection reduces growth of B16-F10 melanoma in the lungs; however, since melanomas naturally form in the skin[68], it is imperative to ask whether influenza can slow tumor growth when injected intratumorally into a skin melanoma. Contrary to what was observed when influenza was concomitant with B16-F10 melanoma in the lungs, influenza did not reduce tumor growth of skin melanoma when injected intratumorally (Fig. 3.1, A-C). One potential reason for this difference in results could be the tropism of the influenza virus; the natural target for influenza is pulmonary epithelial cells[69]. Due to its disparate anatomical location and composition, the skin lacks this cell type, meaning that live influenza virus injected into the skin will not establish a productive infection. Further, studies have shown that influenza infection results in infection, death, and dysregulation of dendritic cells; influenza-infected dendritic cells, particularly of the myeloid subset, exhibit reduced capability in presenting antigens on MHC-I, resulting in weak cross-presentation and compromised $CD8^+$ T cell immunity[70]. Collectively, these defects and the lack of infection of cells in the skin may lead to an insufficient immune response that cannot substantially alter the tumor microenvironment. To bypass this requirement for productive infection and antigen processing, influenza was heat-inactivated to kill the virus[71, 72]. Indeed, intratumoral administration of heat-inactivated influenza (heat-inactivated [hiFLU]) reduced tumor growth and prolonged host survival (Fig. 3.1, D-F).
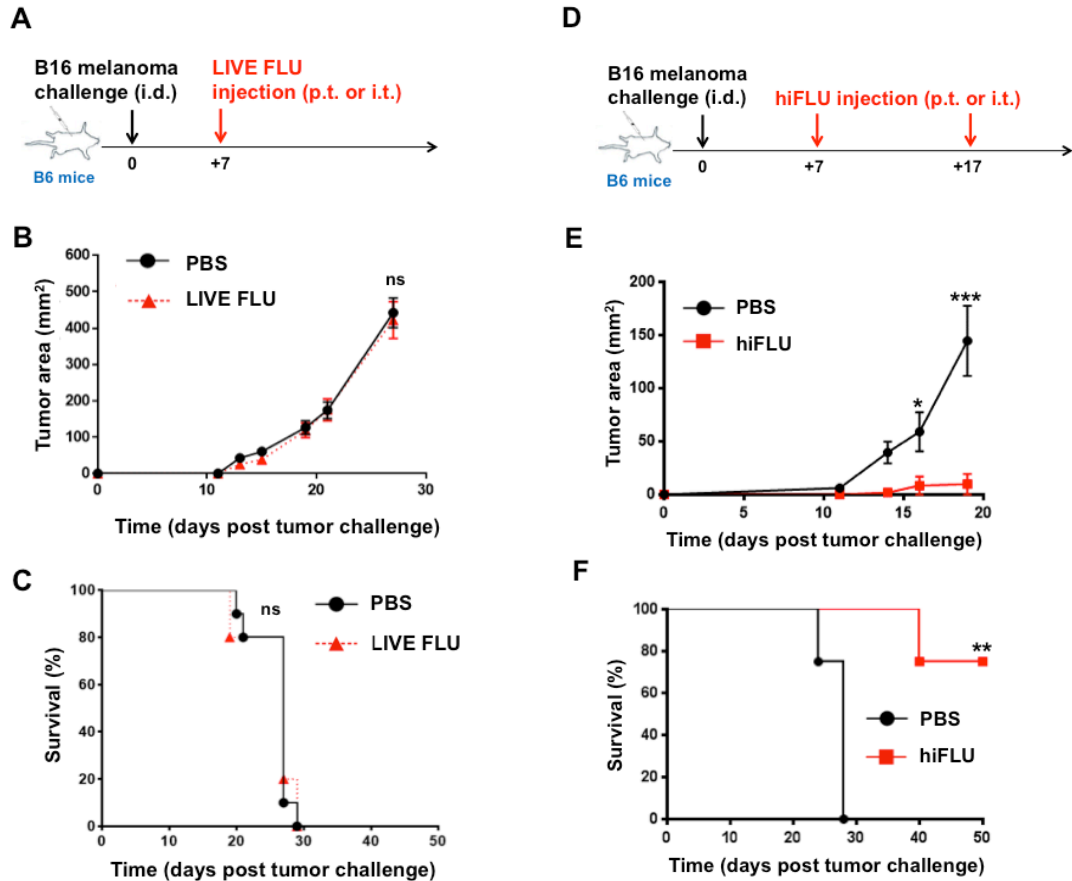
Fig. 3.1 Intratumoral heat-inactivated, but not live, influenza slows growth of melanoma in the skin (A) Experimental design for intradermal (i.d.) and/or peritumoral (p.t.) live influenza virus (LIVE FLU) administration. (B) Tumor growth curves for experiment described in (A). (C) Kaplan-Meier survival curves for experiment described in (A). (D) Experimental design for i.d. and/or p.t. heat-inactivated influenza virus (hiFLU) administration. (E) Tumor growth curves for experiment described in (D). (F) Kaplan-Meier survival curves for experiment described in (D). ns= not statistically significant, **P<0.01, ***P<0.001 [Two-way ANOVA with Bonferroni correction (B, E) and Mantel-Cox logrank test (C, F)]. Mean ± s.e.m. Data are representative of at least two independent experiments with similar results.

Heat-Inactivated Influenza Increases the Proportion of Dendritic Cells and CD8^{+} T Cells in the Tumor

Intratumoral hiFLU administration increased dendritic cells (DCs) among antigen presenting cells (APCs) in the tumor and, specifically, cross-presenting CD8^{+} DCs (Fig. 3.2), relative to that observed in phosphate-buffered saline (PBS)-injected controls and in mice intratumorally administered live influenza. Further, hiFLU (harboring the SIINFEKL peptide of ovalbumin for the purpose of tracking antigen presentation with commonly used laboratory reagents) increased antigen presentation by DCs within the tumor, as indicated by increased expression of an MHC-I-SIINFEKL complex on the cell surface (Fig. 3.3, A and B). Dendritic cells are indispensable for anti-tumor immunity, as they acquire tumor antigens to present to T lymphocytes, and mature to provide co-stimulation to these T cells[73]. Cross-presenting dendritic cells have been shown to be important in anti-tumor and anti-pathogen (including oncolytic virus) immune responses, especially for priming of CD8^{+} T cell responses[74, 75]. In Batf3^{-/-} mice, which lack cross-presenting DCs[74], intratumoral hiFLU had no effect on tumor growth, thus demonstrating their necessity (Fig. 3.3, C and D). Consistent with these findings, intratumoral CD8^{+} T cells, and importantly, anti-tumor CD8^{+} T cells, were increased within the tumor microenvironment after hiFLU influenza administration (Fig. 3.4). These findings demonstrate that heat-inactivated influenza can be employed to augment anti-tumor immune responses in the skin.
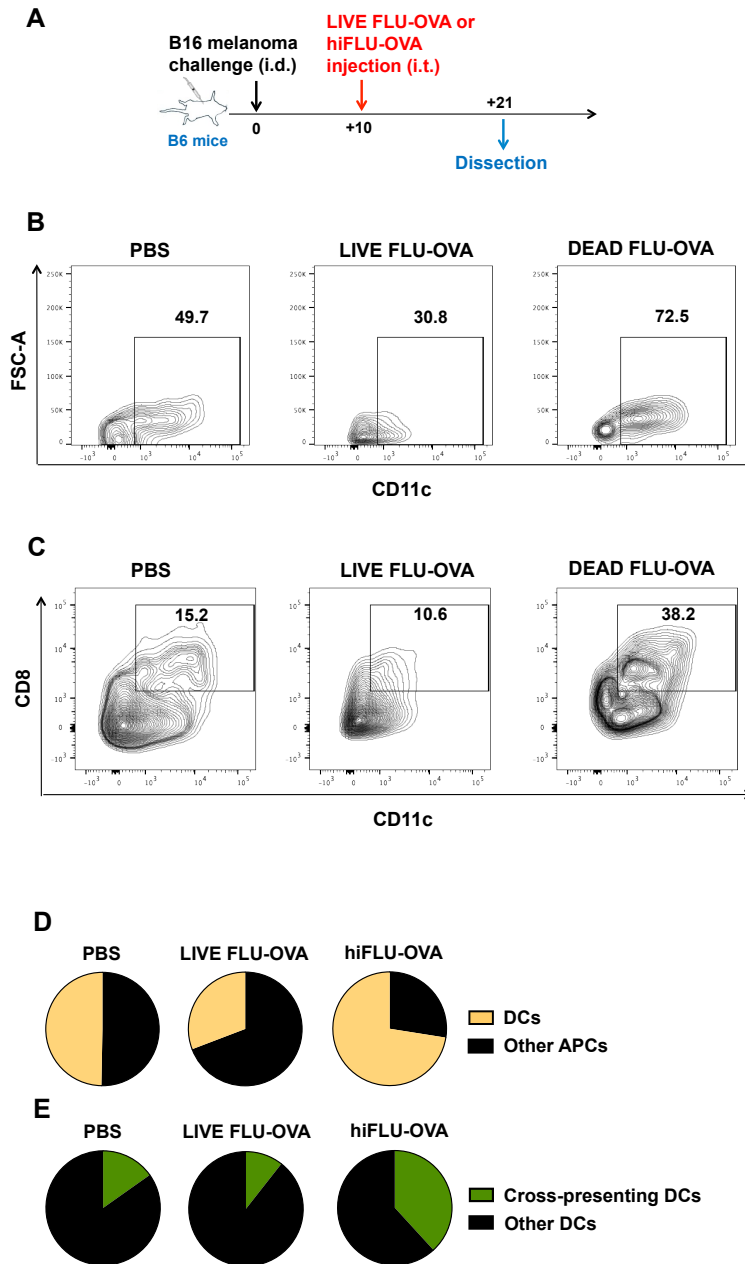
Fig. 3.2 Heat-inactivated influenza increases fraction of intratumoral dendritic cells.
(A) Experimental design. n=3-5 mice pooled/group. (B, D) Flow cytometry plots and corresponding cumulative pie charts, respectively, of DCs (CD11c$^+$) among intratumoral antigen presenting cells (APCs; CD45$^+$MHC-II$^+$) and (C, E) of cross-presenting dendritic cells (CD11c$^+$ CD8a$^+$) among APCs for experiment described in (A). Data are representative of at least two independent experiments with similar results. i.d., intradermal, i.t., intratumoral. FLU-OVA, influenza expressing the SIINFEKL peptide from ovalbumin (OVA). hiFLU-OVA, heat-inactivated influenza-OVA. FSC-A, forward scatter area.
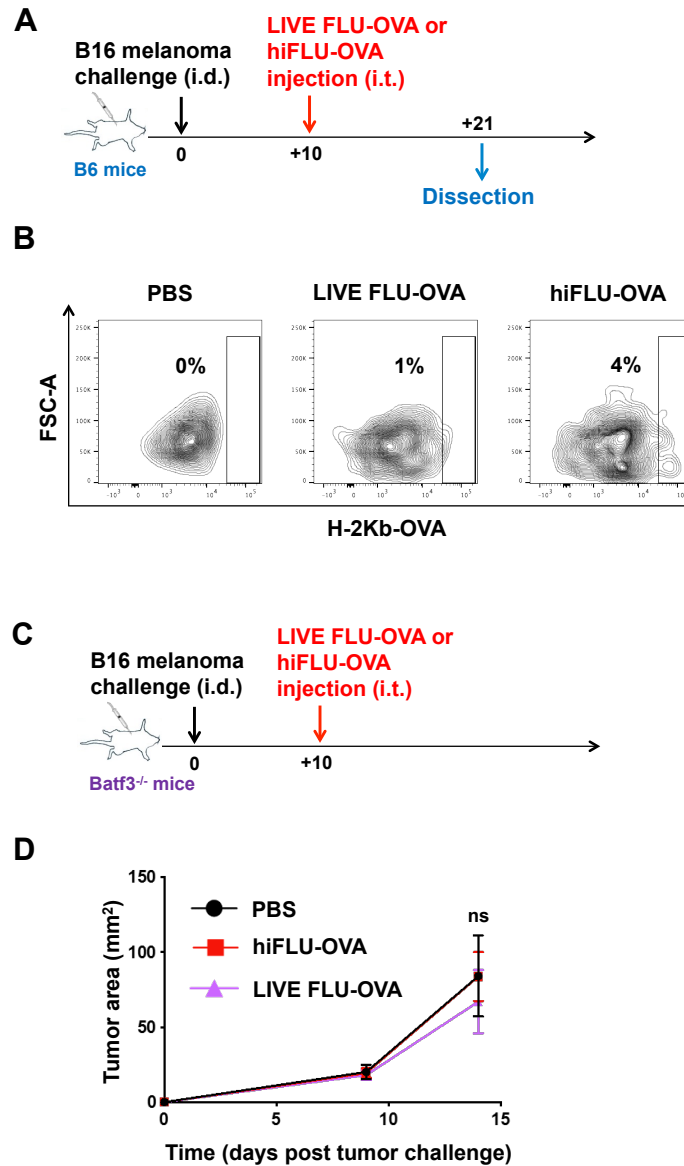
Fig. 3.3 Heat-inactivated influenza increases antigen presentation by dendritic cells (DCs) and requires cross-presenting dendritic cells for tumor reduction. (A) Experimental design for OVA antigen presentation by DCs after intratumoral injection of heat-inactivated (hiFLU-OVA) and live influenza virus (LIVE FLU-OVA) expressing OVA antigen. (B) Flow cytometry plots of OVA antigen (SIINFEKL) presentation within the H-2Kb MHC-I complex (H-2Kb-OVA) by intratumoral CD45^{+}CD11c^{+} DCs for experiment described in (A). n=3-5 mice pooled/group. FSC-A, forward scatter-area. (C) Experimental design utilizing Batf3^{-/-} mice. n=5 mice/group. (D) Tumor growth curves for experiment described in (C). Data are representative of at least two independent experiments with similar results. ns, not significant for all comparisons, including the timepoint labeled [Two-way ANOVA with Tukey correction (D)]. Mean ± s.e.m. i.d., intradermal, i.t., intratumoral.
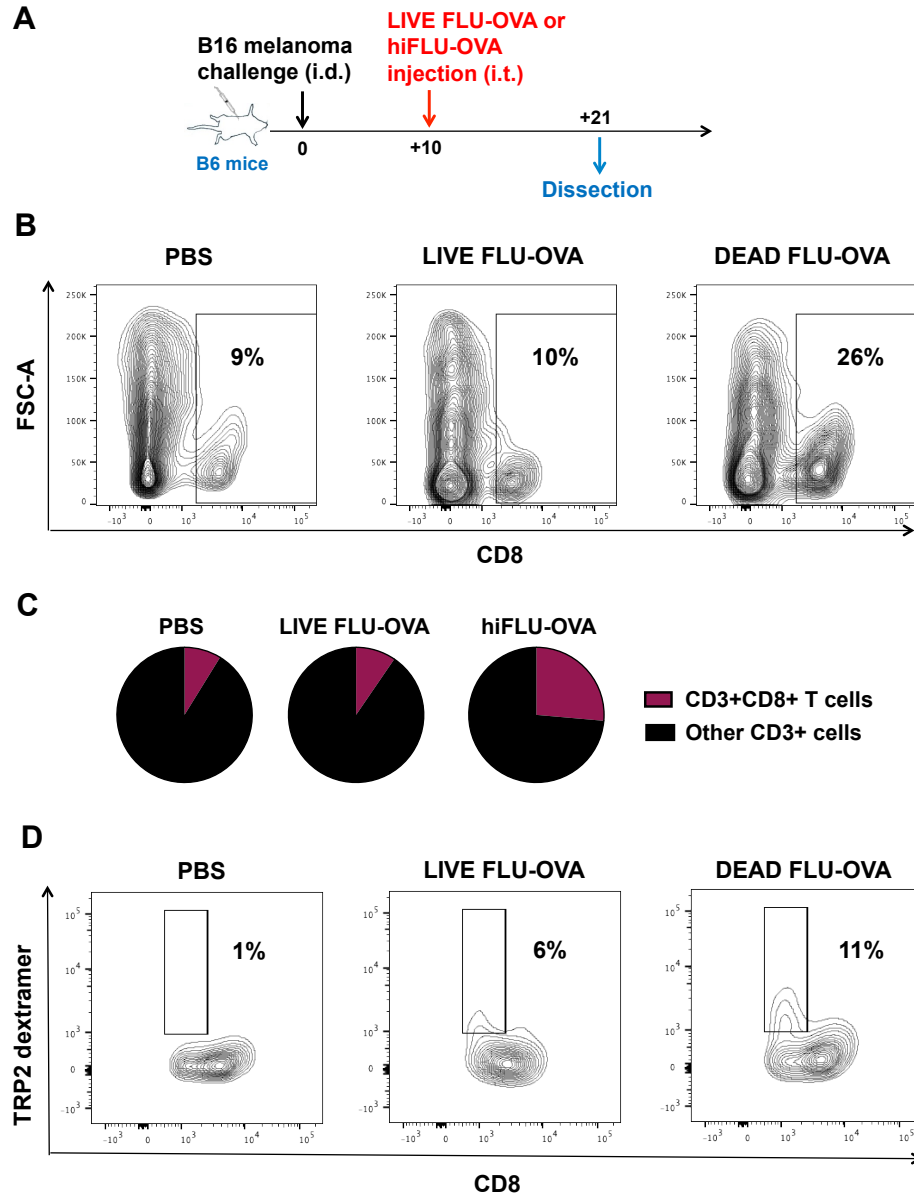
Fig. 3.4 Heat-inactivated influenza induces an increased proportion of overall and tumor-reactive CD8$^+$ T cells in the tumor (A) Experimental design. (B) Flow cytometry plots of CD8$^+$T cells among intratumoral CD45$^+$CD3$^+$cells for experiment described in (A). n=3-5 mice pooled/group. (C) Cumulative pie chart representing data shown in (B). (D) Flow cytometry plots of tumor-reactive (TRP2-dextramer$^+$) CD8$^+$T cells among intratumoral CD8$^+$T cells for experiment described in (A). n=3-5 mice pooled/group. Data are representative of at least two independent experiments with similar results. i.t, intratumoral. i.d, intradermal. LIVE FLU-OVA, live influenza virus expressing the SIINFEKL peptide from ovalbumin (OVA). hiFLU-OVA, heat-inactivated influenza expressing the SIINFEKL peptide from ovalbumin OVA. FSC-A, forward scatter area.

Heat-inactivated Influenza Slows Growth of Tumors Distant from the Injection Site

The long-term success of a treatment for cancer is largely dependent on its ability to reduce not only primary lesions, but also metastases, from which the majority of patients suffer fatality[76]. To determine whether the sum of the mechanistic changes observed with intratumoral hiFLU provides systemic immunity, a bilateral tumor experiment was conducted. In this model, mice were administered B16-F10 melanoma tumors on both the right and left flanks and were subsequently injected with hiFLU in the right tumor only. Both the treated (injected) right and untreated (non-injected) left flank tumors exhibited reduced melanoma growth (Fig. 3.5, A-C), suggesting that local intratumoral hiFLU can provide not only control of tumor growth at the site of injection, but also systemic control of tumor growth. Interestingly, the kinetics of tumor reduction were similar when comparing injected versus non-injected tumors; initially, this was viewed as a surprising result, as the anti-tumor immune response is believed to be primed at the tumor site, with systemic immunity generated at a later timepoint, after migration of cells throughout the lymphatic system[77]. While this is conventional wisdom in the field of immunology, recent clinical data suggest that abscopal response (defined as a response to therapy in a lesion distant from the treatment site) to radiation therapy and immunotherapy can occur[78, 79]. A similar systemic outcome was observed in the 4T1 model of (naturally) metastatic triple-negative breast cancer, in which both primary tumor growth and lung metastases were reduced (Fig. 3.5 D-F), suggesting that intratumoral hiFLU-mediated tumor reduction is not limited to melanoma, to skin cancer, or to non-metastatic tumors.

Intratumoral Heat-Inactivated Influenza Slows Tumor Growth in Influenza-experienced Hosts

Another consideration for the utility of hiFLU as a treatment for cancer is the impact previous exposure of influenza virus has on the effectiveness of intratumoral hiFLU in slowing tumor growth. To test this, influenza was administered 36 days prior to B16-F10 melanoma tumor challenge. Upon the development of a palpable tumor, hiFLU was administered intratumorally. Importantly, intratumoral hiFLU decreased melanoma growth in hosts previously infected with influenza (Fig. 3.6), suggesting that intratumoral hiFLU as a treatment for cancer can be utilized in hosts that have been previously exposed to influenza. It should be noted that the kinetics of tumor reduction in the context of reintroduction of influenza antigen are slightly slower than that observed in influenza-naïve mice receiving intratumoral hiFLU; this merits further investigation, as perhaps a robust anti-viral immune response temporarily overrides anti-tumor immunity. This finding is of importance for potential translation to the clinic, as influenza-experienced patients would not be excluded from receiving hiFLU intratumorally as a treatment for cancer.
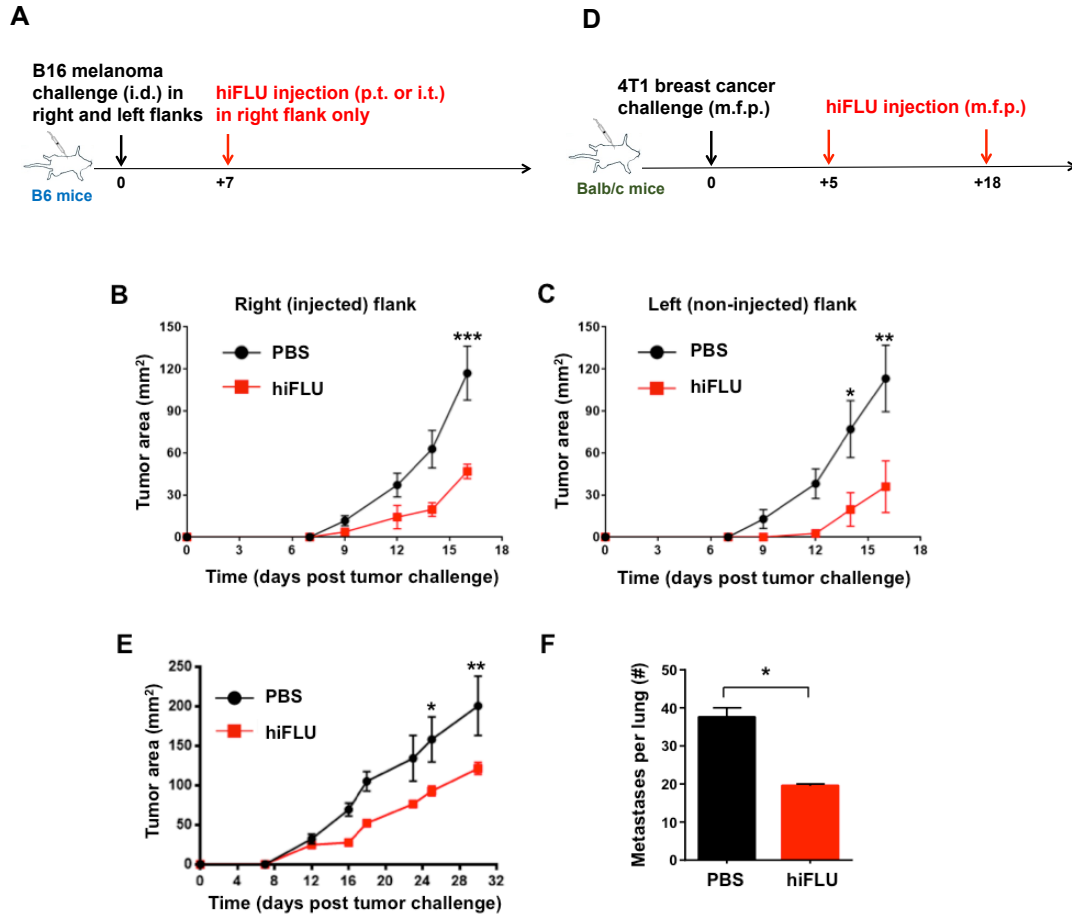
Fig. 3.5 Intratumoral heat-inactivated influenza reduces growth of distant tumors.
(A) Experimental design. (B) Tumor growth curves of right (injected), and (C) left (non-injected) tumor for experiment described in (A). (D) Experimental design for experiment utilizing triple-negative metastatic 4T1 breast cancer. (E) Tumor growth curves for experiment described in (D). (F) Bar graphs showing number of metastases per lung surface. n=3-10 mice/group. Data are representative of at least two independent experiments with similar results. *P< 0.05, **P< 0.01, ***P< 0.001 [Two-way ANOVA with Bonferroni correction (B, C, E) or with two-tailed student t-test (F)] Mean ± s.e.m. hiFLU, heat-inactivated influenza. i.d., intradermal, i.t., intratumoral, m.f.p., mammary fat pad, p.t., peritumoral.

A

LIVE FLU infection (i.n.)

B16 melanoma challenge (i.d.)

hiFLU injection (p.t. or i.t.)

B6 mice

-36   0   +7   +19

B

● LIVE FLU (i.n.) → PBS

■ LIVE FLU (i.n.) → hiFLU

Tumor area (mm^2)

Time (days post tumor challenge)
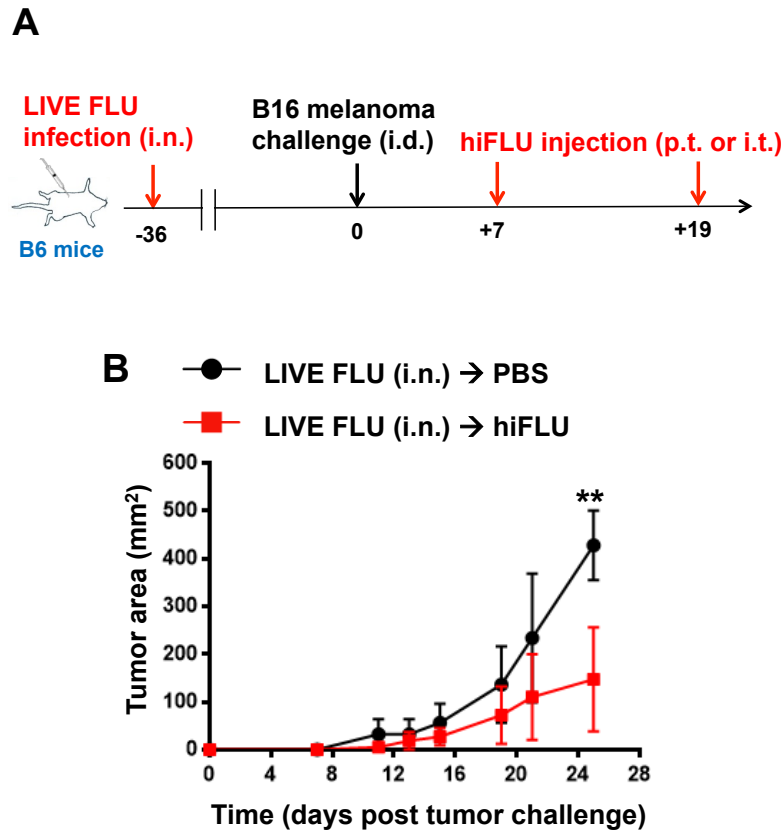
Fig. 3.6 Intratumoral heat-inactivated influenza slows tumor growth in hosts previously infected with influenza. (A) Experimental design of peritumoral (p.t.) or intratumoral (i.t.) heat-inactivated influenza (hiFLU) injection following live influenza intranasal (i.n.) infection and intradermal (i.d.) tumor challenge. (B) Tumor growth curves for mice infected with live influenza and subsequently administered hiFLU at tumor site for experiment described in (A). n=3-10 mice/group. **P< 0.01 [Two-way ANOVA with Bonferroni correction (B)].

Intratumoral Heat-Inactivated Influenza Synergizes with Checkpoint Blockade to Halt Tumor Growth

Currently, 15-40% (varying based on cancer type and several other parameters) of

patients respond to the frontline immunotherapy for cancer: checkpoint blockade[80].

Research has shown that responders often exhibit immune cell infiltration into tumors[8];

this suggests that therapies that inflame the tumor microenvironment –such as hiFLU,

which increases the proportion of intratumoral dendritic cells and CD8$^+$ T cells—might

synergize with checkpoint blockade. To determine whether intratumoral hiFLU could

sensitize tumors to checkpoint blockade immunotherapy, hiFLU and PD-L1 blockade

were administered in combination. Combination treatment with PD-L1 checkpoint

blockade in the melanoma model further reduced tumor growth, compared to that

observed with either hiFLU or PD-L1 blockade alone (Fig. 3.7). This proposes that

patients who respond (even partially) to checkpoint blockade may benefit further from

administration of the intratumoral hiFLU. Here, intratumoral hiFLU was administered at

the start of the treatment regimen, as to infiltrate the tumor with immune cells and

subsequently relieve T cell exhaustion with checkpoint blockade; this combination

timeline has been performed with other inflammatory agents and checkpoint blockade

combination regimens with success[81]. In the future, it will be valuable to determine

whether synergy of hiFLU and checkpoint blockade is achieved when checkpoint

blockade is administered first, as patients will have likely been exposed to this treatment

prior to introduction to other immunotherapies; it is possible that hiFLU will infiltrate the

tumor with (previously absent) immune cells that can subsequently be targeted by

additional doses of checkpoint blockade.

A

B16 melanoma   hiFLU injection (p.t. or i.t.)
challenge (i.d.)   αPD-L1 or IgG (i.p.)

B6 mice   0   +7   +13

B
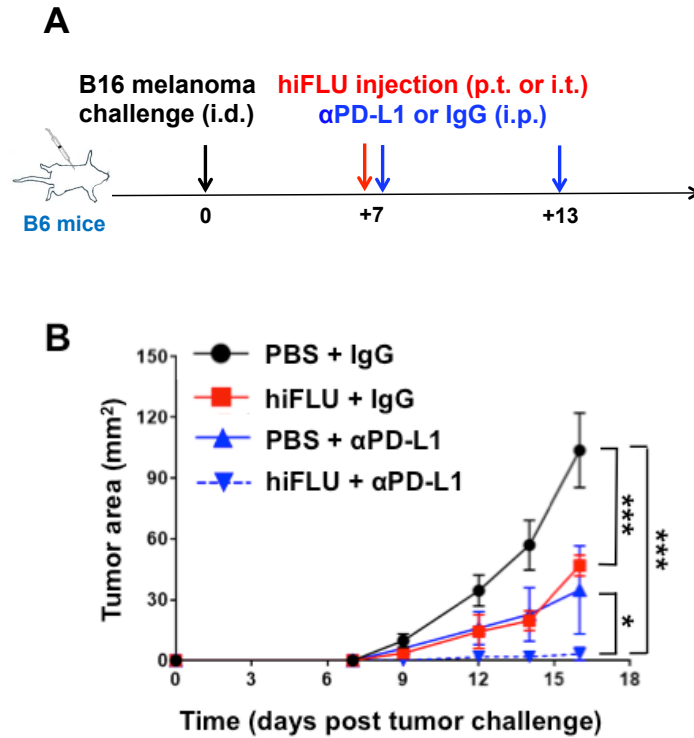
Fig. 3.7 Intratumoral heat-inactivated influenza synergizes with PD-L1 checkpoint blockade to arrest tumor growth (A) Experimental design. (B) Tumor growth curves for experiment described in (A). n=3-10 mice/group. *P< 0.05, ***P< 0.001 [Two-way ANOVA with Tukey correction (B)]. Mean ± s.e.m. hiFLU, heat-inactivated influenza. i.d., intradermal. i.p., intraperitoneal. i.t., intratumoral.

CHAPTER 4: INTRATUMORAL UNADJUVANTED SEASONAL INFLUENZA VACCINE REDUCES GROWTH OF MOUSE AND HUMAN CANCER

Intratumoral Unadjuvanted Influenza Vaccination Slows Growth of B16-F10 Melanoma, Protects Against Influenza Infection, and Synergizes with PD-L1 Blockade

Based on the ability of homemade heat-inactivated influenza to slow tumor growth, commercially available inactivated influenza vaccines were tested to determine whether these (already) FDA-approved formulations could slow tumor growth. Seasonal inactivated influenza vaccines are extensively used and have been lauded for their safety[82]. Inactivated influenza vaccines are comprised of purified hemagglutinin (HA) protein and residual nucleic acids, resuspended in PBS, sodium chloride, or sodium phosphate; such vaccines are reported to induce influenza-specific IgG antibodies, $CD8^+$ T cell, and $CD4^+$ T cell responses[83]. If such vaccines were effective not only in providing immunity against influenza, as intended, but also contributed to anti-tumor immunity, a cost-effective and safe treatment would become available for cancer patients, with little administrative delay.

Indeed, intratumoral, but not intramuscular, injection of the 2017-2018 unadjuvanted influenza vaccine (Table 1)[84-86], hereafter referred to as FluVx, resulted in reduced tumor growth (Figs. 4.1 and 4.2). As with hiFLU, multiple FluVx administrations further reduced tumor growth (Fig. 4.3), suggesting that repeated exposure may enhance the immune response induced. Importantly, intratumoral injection of FluVx afforded hosts protection against subsequent influenza infection (Fig. 4.4), suggesting that administration of the influenza vaccine in the tumor can be used to simultaneously reduce tumor growth and provide vaccination-induced protection against influenza infection. The combination of FluVx with PD-L1 checkpoint blockade further

reduced tumor growth, even in the context in which the tumor was resistant to checkpoint

blockade alone (Fig. 4.5), proposing a role for influenza vaccine intratumoral injection in

patients who lack response to checkpoint blockade alone.

Influenza vaccine[a]	Manufacturer	HA/50 µL dose	Adjuvant	Production vehicle	Method of virus inactivation	Solvent
FLUCELVAX® (FluVx1)	Seqirus	6 µg (1.5 µg per strain)	No	MDCK cells	β-propiolactone and cetyltriammonium bromide	Phosphate buffered saline
FLUVIRIN® (FluVx2)	Seqirus	4.5 µg (1.5 µg per strain)	No	Embryonated chicken eggs	β-propiolactone	Phosphate buffered saline
FLUARIX® (FluVx3)	GlaxoSmithKline	6 µg (1.5 µg per strain)	No	Embryonated chicken eggs	Sodium deoxycholate and formaldehyde	Sodium chloride/sodium phosphate
FLUBLOK® (FluVx4)	Protein Sciences Corporation	18 µg (4.5 µg per strain)	No	Sf9 cells	Live virus never infects cells; antigens extracted using Triton-X 100	Sodium chloride/sodium phosphate
FLUAD® (AdjFluVx)	Seqirus	4.5 µg (1.5 µg per strain)	Yes (MF59®)	Embryonated chicken eggs	Formaldehyde and cetyltriammonium bromide	Oil-water emulsion (MF59®)

Table 1. FDA-approved 2017-2018 seasonal influenza vaccines utilized in the study.
Details regarding vaccine manufacturer, concentration of hemagglutinin (HA) within
each 50 µL dose, adjuvant included in the vaccine (if applicable), vehicle type utilized for
vaccine production, method of virus inactivation, and the vaccine solvent utilized are
provided. More information can be obtained from each vaccine's FDA package insert,
which contains full information regarding vaccine formulation and clinical data[84-86].
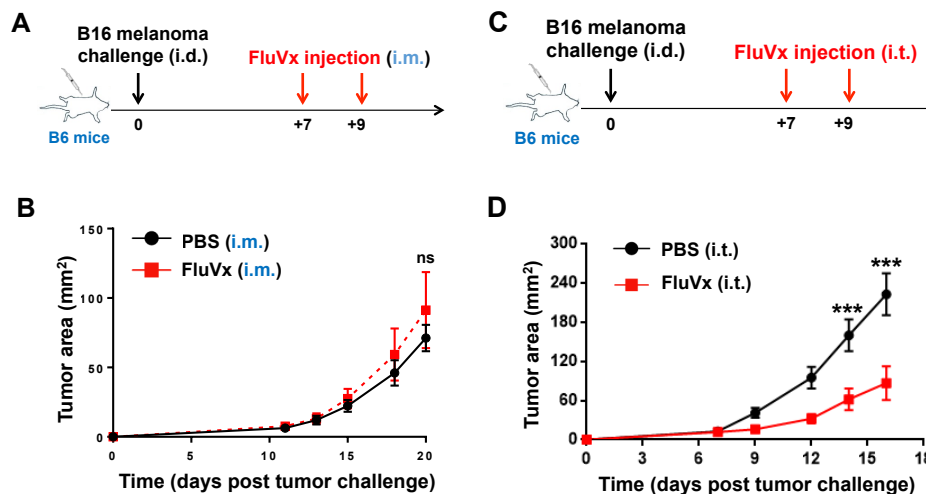
Fig. 4.1 Intratumoral, but not intramuscular, unadjuvanted influenza vaccine slows melanoma growth. (A) Experimental design for intramuscular (i.m.; left lower limb) seasonal influenza vaccine (FluVx), FluVx1 (described in Table 1), administration. (B) Tumor growth curves for experiment described in (A). (C) Experimental design for intratumoral (i.t.) FluVx administration (separate from experiment described in [A]). (D) Tumor growth curves for experiment described in (C). Data are representative of at least two independent experiments with similar results. ns=not significant for all comparisons including the labeled timepoint, ***$P<0.001$ [Two-way ANOVA with Bonferroni correction]. Mean ± s.e.m. n=5 mice/group. i.d., intradermal.
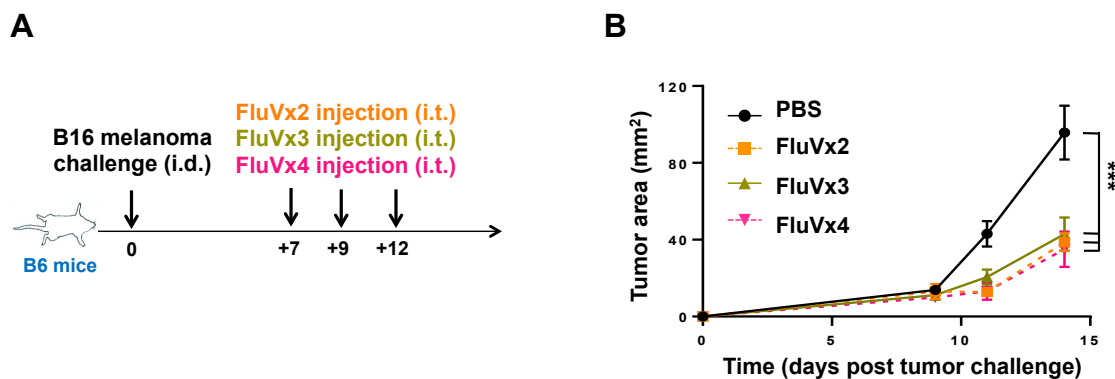
Fig. 4.2 Several varieties of unadjuvanted inactivated seasonal influenza vaccines slow growth of melanoma. (A) Experimental design testing different unadjuvanted formulations of the influenza vaccine (FluVx). FluVx2, FluVx3, and FluVx4 are defined in Table 1. n= 4-5 mice/group. i.d., intradermal., i.t., intratumoral. (B) Tumor growth curves for experiment described in (A). Data are representative of at least two independent experiments with similar results.***$P< 0.001$ [Two-way ANOVA with Tukey correction (B)]. Mean ± s.e.m.
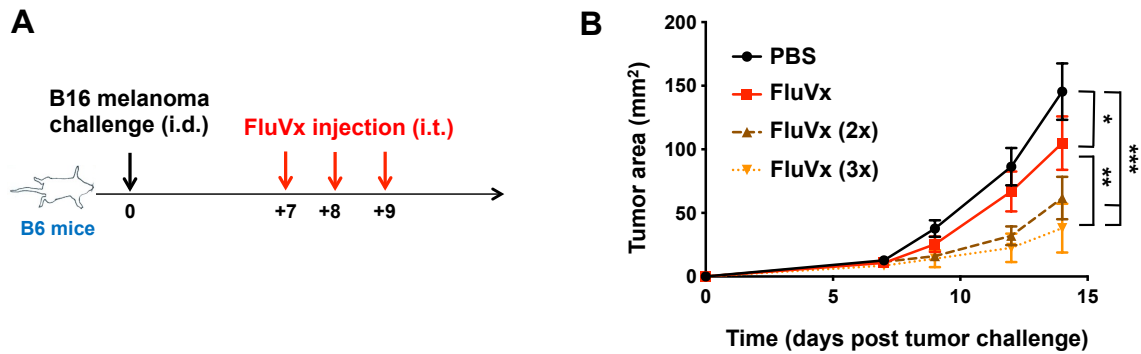
Fig. 4.3 Multiple doses of unadjuvanted inactivated seasonal influenza vaccines enhance efficacy in slowing tumor growth. (A) Experimental design for studies utilizing one [day 7; FluVx1], two [days 7 and 8; FluVx1 (2x)], or three [days 7, 8 and 9; FluVx1 (3x)] injections. n=5-10 mice/group. (B) Tumor growth curves for experiment described in (A). Data are representative of at least two independent experiments with similar results. *P< 0.05, **P< 0.01, ***P< 0.001 [Two-way ANOVA with Tukey correction (B)]. Mean ± s.e.m. i.d., intradermal, i.t., intratumoral.
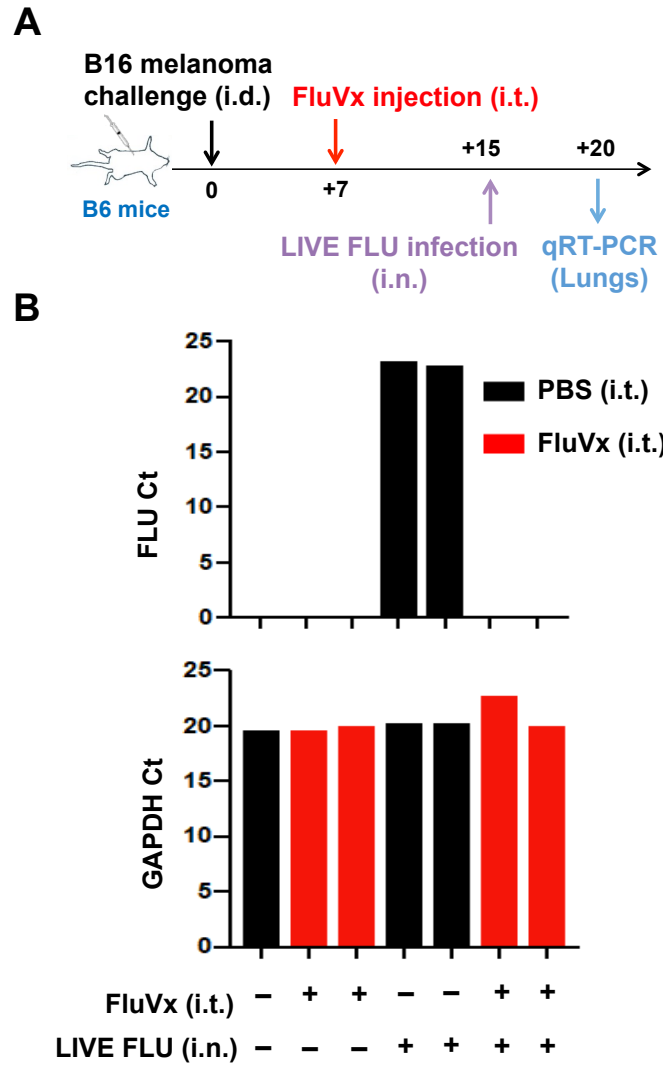
Fig 4.4 Intratumoral influenza vaccination provides protection from subsequent intranasal live influenza challenge. (A) Experimental design for seasonal influenza vaccine FluVx1 administration via intratumoral injection (i.t.) and subsequent A/PR8/H1N1 intranasal (i.n.) influenza infection for Quantitative Reverse Transcription Polymerase Chain Reaction (qRT-PCR) experiments. (B) Bar graphs showing count threshold (Ct) of LIVE FLU or GAPDH control qRT-PCR transcripts for experiment described in (A). i.d., intradermal.

A

B
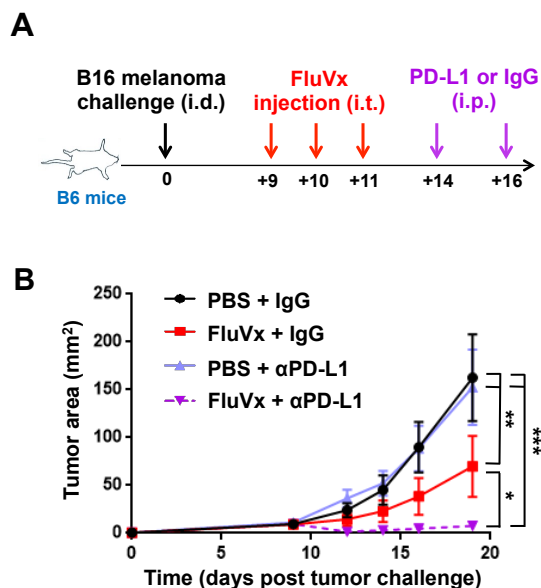
Fig. 4.5 Intratumoral influenza vaccination synergizes with PD-L1 checkpoint blockade to halt tumor growth (A) Experimental design for experiment interrogating combination of unadjuvanted influenza vaccine (FluVx), FluVx1, and checkpoint blockade. (B) Tumor growth curves for experiment described in (A). n=5 mice/group. Data are representative of at least two independent experiments with similar results. *P< 0.05, **P< 0.01, ***P< 0.001 [Two-way ANOVA with Tukey correction (B)]. Mean ± s.e.m. i.d., intradermal, i.p., intraperitoneal, i.t., intratumoral.

Intratumoral Unadjuvanted Influenza Vaccination Slows Growth of Human Tumors

To gauge the effect of intratumoral FluVx administration on patient tumors, an autologous immune-reconstituted patient-derived xenograft (AIR-PDX) mouse model was used. NOD scid gamma (NSG) mice, an immunodeficient strain lacking adaptive immunity (B and T cells) and harboring compromised innate immunity[87], were selected to minimize rejection of human tissue. AIR-PDX mice harbor surgically transplanted patient tumor tissue (maintaining the natural architecture of the patient's tumor) and adoptively transplanted peripheral blood immune cells from the same (autologous) patient (Fig. 4.6A), thus not requiring stem cells and avoiding mismatched immunity in

the tumor versus peripheral blood and tissues. Here, intratumoral FluVx likewise reduced

patient-derived tumor growth (Fig. 4.6B), suggesting the translatability of the findings to

clinical cancer treatment.
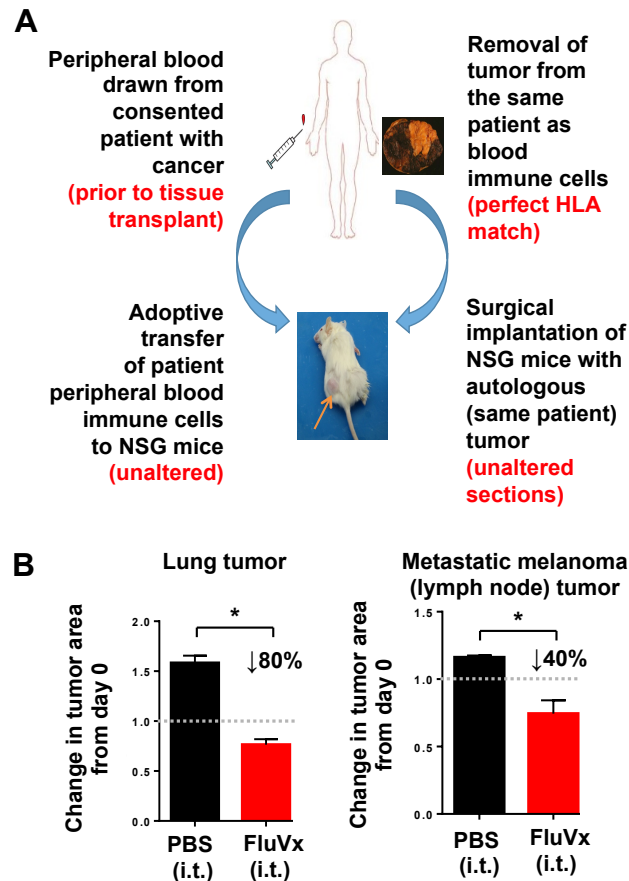
Fig. 4.6 Intratumoral influenza vaccine slows growth of human tumors in an immune-reconstituted humanized mouse model. (A) Schematic describing development of autologous immune-reconstituted patient-derived xenograft (AIR-PDX) mice. NOD scid gamma (NSG) mice were adoptively transferred 0.5×10^6 human peripheral blood mononuclear cells (PBMCs) 12 hours before surgical implantation of 5×5×3 mm tumor sections from the same patient. n = 2-5 mice/group. (B) Bar graphs showing change in tumor size from day 0 (dotted line) in lung tumor 13 days post-treatment with PBS or FluVx (left) or metastatic melanoma tumor from the lymph node (LN) 16 days post-treatment with PBS or FluVx (right) for experiment described in (A). Percentages quantify the difference between tumor growth with PBS and tumor regression with FluVx2. *P< 0.05 [two-tailed t-test (B)] Mean ± s.e.m. i.t., intratumoral.

Intratumoral Unadjuvanted Influenza Vaccination Increases Fraction of Dendritic Cells and CD8^{+} T Cells in the Tumor, Inflaming the Tumor Microenvironment

A central question regarding the mechanism(s) by which FluVx confers reduction in tumor growth is the extent of the contribution of the immune system. The aforementioned heat-inactivated influenza data suggest a strong role for the immune system, as components of both the innate (dendritic cells) and adaptive (CD8^{+} T cells) immune systems were elevated in the context of intratumoral vaccination. To test whether immunity is necessary for reduction in tumor growth mediated by intratumoral influenza vaccination, immunodeficient NSG mice were administered FluVx. Vaccinated mice exhibited tumor growth comparable to that observed in the PBS-injected control group, indicating the necessity of immunity for tumor reduction. However, immune reconstitution of NSG mice via adoptive cell transfer of immune cells from an immunocompetent B6 mouse recovered the anti-tumor effect of FluVx (Fig. 4.7), suggesting that the immune system is sufficient to reduce tumor growth in the context of FluVx.

Towards understanding the specific immunological mechanism(s) by which FluVx reduces tumor growth, flow cytometry of tumor tissue was performed, as done for the aforementioned heat-inactivated influenza experiments. As with hiFLU, intratumoral FluVx increased the proportion of dendritic cells and CD8^{+} T cells within the tumor microenvironment (Fig. 4.8). To determine whether cross-presenting dendritic cells and CD8^{+} T cells are essential for the tumor reduction observed with intratumoral FluVx, mice were administered with a CD8-blocking antibody or isotype-matched control antibody intraperitoneally. Importantly, depletion of CD8-expressing cells completely abrogated the FluVx anti-tumor effect (Fig. 4.9), demonstrating the importance of such

cells in the underlying immune mechanism of FluVx. Among CD8^{+} T cells, an increase in tumor-reactive CD8^{+} T cells was observed (Fig. 4.10A), suggesting that intratumoral anti-pathogen vaccination boosts tumor-specific immunity. Consistent with these findings, and further suggesting that FluVx augments anti-tumor T cell responses, T cell receptor (TCR) sequencing demonstrated an increase in the representation of tumor-associated clones (i.e., increased evenness/clonality) with intratumoral FluVx (Fig. 4.10B), a therapy-induced change previously reported in patients responding to αPD-1 checkpoint blockade[88].

The influx of dendritic cells and CD8^{+} T cells into the tumor upon intratumoral administration of FluVx suggests reversal of the suppressive tumor microenvironment. To further understand how FluVx modulates the tumor microenvironment, RNA was isolated from tumors and was analyzed using the NanoString Pan-Cancer Immune Profiling Panel[89]. A focused analysis of inflammation-related mRNAs previously shown to correlate with clinical response to αPD-1 checkpoint blockade[8] demonstrated high expression of such mRNAs with intratumoral FluVx administration (Fig. 4.11), suggesting conversion of an immunologically "cold" tumor to one that is "hot". The transcripts upregulated in the context of intratumoral FluVx are implicated in antigen presentation, T cell activation and exhaustion, and immune cell migration. The crucial first step of mounting an anti-tumor immune response is presentation of tumor antigen. Qa-1, the protein product of the non-classical MHC I transcript H2-T23 (upregulated in FluVx-treated tumors), can recognize a wide array of peptides and reverse NKG2A inhibition in TAP-deficient cells, leading to the recruitment of CD8^{+} T cells[90]. Also upregulated in the FluVx-treated group were H2-Aa and H2-Eb1, both members of the

MHC Class II pathway associated with reduction of ovarian tumor growth[91], and

Psmb10, which encodes a proteasome subunit with trypsin-like activity implicated in

protein processing as part of the antigen presentation pathway[92]. Additionally as crucial

for mounting an anti-tumor immune response is the ability to recruit immune cells to the

tumor site; in FluVx-treated tumors, an upregulation of transcripts encoding chemokines

CCL5 and CXCL9, and chemokine receptors CXCR6 and CMKLR1, which is associated

with immune cell trafficking that has sometimes been correlated with decreased tumor

burden, was observed[93-96]. Importantly, transcripts encoding molecules implicated in T

cell activation and function, such as costimulatory CD27, antigen recognition co-receptor

CD8a, and IFN signaling-promoting transcription factor STAT1, were also increased in

the context of intratumoral FluVx[97-99]. Further, transcripts associated with T cell

exhaustion (TIGIT, Ido1, Lag3 and PD-L1)—which is a product of prolonged activation

that is easily targetable with checkpoint blockade inhibition—were upregulated in FluVx-

vaccinated tumors[100]. Of particular importance is that FluVx increased expression of

CD274 (PD-L1) transcripts, providing a rationale for synergy of FluVx with αPD-1/αPD-

L1 checkpoint blockade and a mechanistic explanation for reduced tumor growth in

combination, as high PD-L1 levels are associated with response to αPD-1/αPD-L1

therapy[88]. Altogether, intratumoral influenza vaccination leads to upregulation of

transcripts associated with an inflamed tumor microenvironment that is sensitized to

checkpoint blockade.

One supplemental mechanistic question regarding these findings is whether

reduction of tumor growth upon intratumoral injection is exclusive to FluVx, or whether

other immunogenic proteins would provide the same reduction. To test this, the TLR3

agonist poly I:C[101] was injected into tumors in conjunction with either (melanocyte-derived) gp100 (KVPRNQDWL) peptide or (ovalbumin-derived) OVA (SIINFEKL) peptide. Interestingly, tumor growth was reduced only when the poly I:C + OVA combination was administered (Fig. 4.12). This demonstrates that intratumoral administration of poly I:C and a (tolerized) self protein is insufficient to initiate an anti-tumor immune response capable of slowing tumor growth. However, poly I:C in combination with a foreign, immunogenic (yet not viral-derived) peptide, OVA, can slow tumor growth *in vivo* upon intratumoral administration. It should be noted that this data trend was observed, albeit without achieving statistical significance. These data suggest that, perhaps, tumor growth reduction is not limited to intratumoral administration of viral proteins, but rather, other immunogenic, non-self proteins suffice. Also of note is that, within the realm of anti-pathogen vaccines, two bacterial vaccines and another viral vaccine—DTAP, pneumonia, and Hepatitis B vaccine—exhibit a trend of reduced tumor growth upon intratumoral injection (Fig. 4.13). For the remainder of this dissertation, FluVx will be mainly discussed for the purpose of achieving mechanistic focus and its practical ability to serve dually as a tool for influenza prevention and cancer treatment.
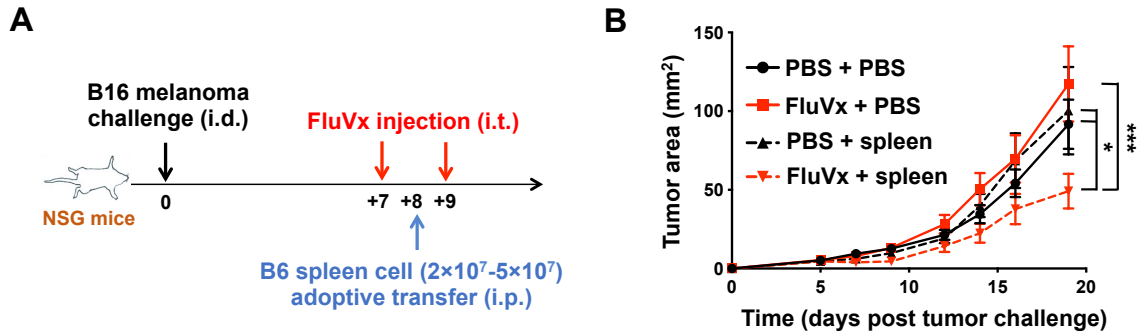
Fig. 4.7 Immunocompetence is necessary for tumor-reduction capability of intratumoral influenza vaccine. (A) Experimental design of seasonal influenza vaccine (FluVx), FluVx1 and FluVx2 (pooled), intratumoral (i.t.) administration in immunocompromised NOD scid gamma (NSG) mice with or without adoptive transfer via intraperitoneal (i.p.) injection of immune cells from C57BL/6 (B6) mouse spleens. n=5-10 mice/group. i.d., intradermal. (B) Cumulative tumor growth curves from two independent experiments described in (A). Data are representative of at least two independent experiments with similar results. *P< 0.05, ***P< 0.001 [Two-way ANOVA with Tukey correction (B)] Mean ± s.e.m.
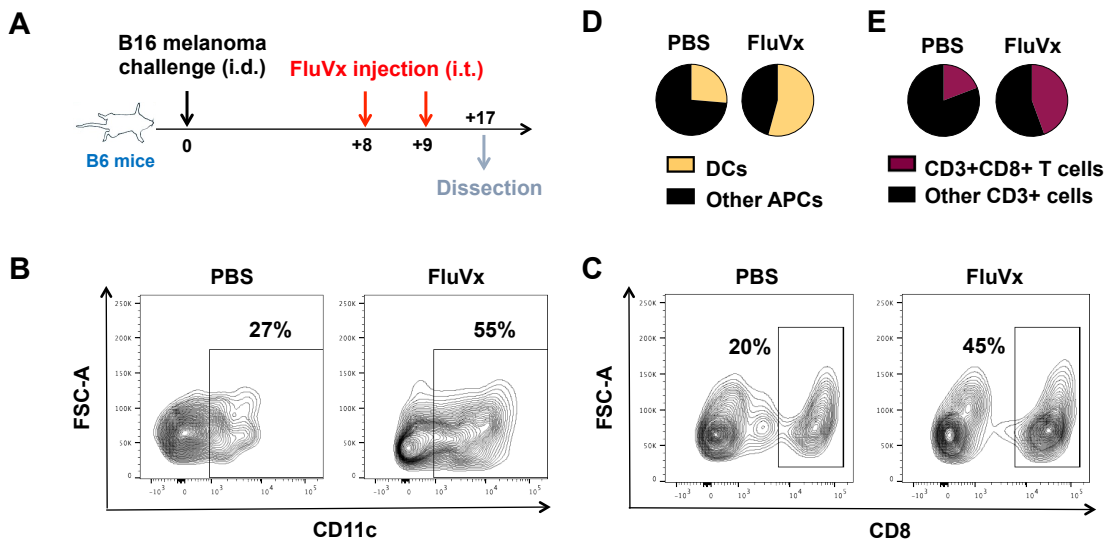
Fig. 4.8 Intratumoral unadjuvanted influenza vaccine increases the proportion of dendritic cells and CD8$^+$ T cells in the tumor. (A) Experimental design. FluVx, (FluVx2) influenza vaccine. (B) Flow cytometry plot showing dendritic cells (DCs, CD11c$^+$), among antigen-presenting cells (APCs; CD45$^+$ MHC-II$^+$) from tumors isolated from mice of the experiment described in (A). n=3-5 tumors pooled/group. (C) Flow cytometry plot showing CD8$^+$ T cells among CD45$^+$ CD3$^+$ cells from tumors isolated from mice of the experiment described in (A). n=3-5 tumors pooled/group. (D) Cumulative pie chart for data shown in (B). (E) Cumulative pie chart for data shown in (C). Data are representative of at least two independent experiments with similar results. i.d., intradermal, i.t., intratumoral. FSC-A, forward scatter area.

Fig. 4.9 Antibody-mediated depletion of CD8 abrogates tumor-reduction ability of intratumoral influenza vaccination. (A) Experimental design for intraperitoneal (i.p.) antibody blockade of CD8 (αCD8) or isotype control antibody IgG in the context of intratumoral (i.t.) influenza vaccination. n=5 mice/group. (B) Tumor growth curves for experiment described in (A). Data are representative of at least two independent experiments with similar results. ***P< 0.001 [Two-way ANOVA with Tukey correction (B)]. Mean ± s.e.m. i.d., intradermal.
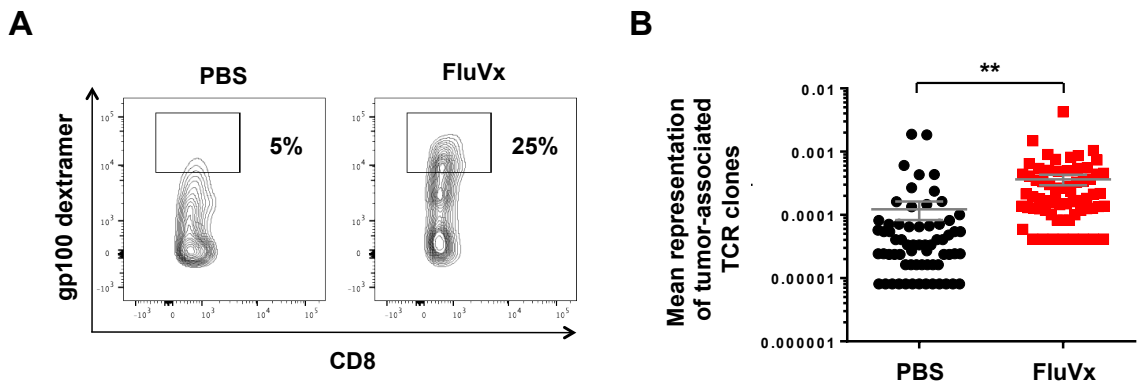
Fig. 4.10. Intratumoral influenza vaccination increases the proportion of tumor-reactive CD8^{+} T cells in the tumor. (A) Tumors were resected on day 17 post tumor challenge from B16-F10 melanoma-bearing mice injected intratumorally with PBS or FluVx on days 8 and 9 post tumor challenge. Flow cytometry plot (n=3-5 tumors pooled/group) of tumor-reactive (gp100 dextramer^{+}) CD8^{+} T cells among intratumoral CD8^{+} T cells (CD45^{+} CD3^{+} CD8^{+}). Data are representative of at least two independent experiments with similar results. (B) Scatter plot from T cell receptor (TCR) sequencing showing increased clonality of TCRs in tumor-residing T cells with FluVx1 administration. **P< 0.01[Two-tailed t-test (B)]. Mean ± s.e.m.
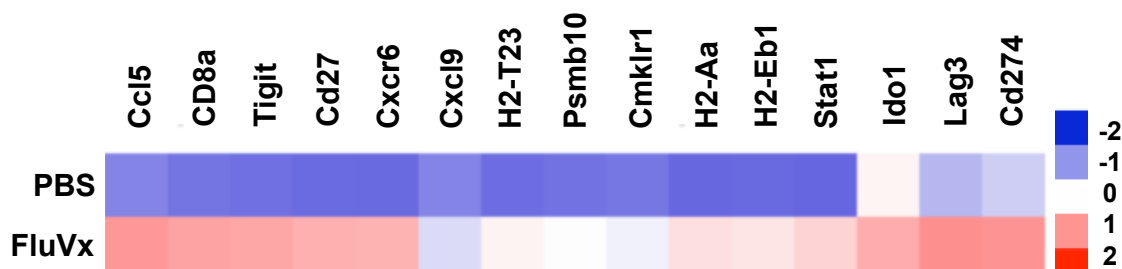
Figure 4.11 Intratumoral influenza vaccination induces upregulation of transcripts implicated in inflammation and response to checkpoint blockade. B16-F10 melanoma-bearing mice were intratumorally injected with PBS or FluVx 7 days post tumor challenge. Tumors were resected on day 14 post tumor challenge and were subject to RNA isolation for Nanostring analysis. Representative heatmap of a focused NanoString PanCancer Immune Profiling panel. Blue color represents downregulation of transcripts and red color represents upregulation of transcripts.
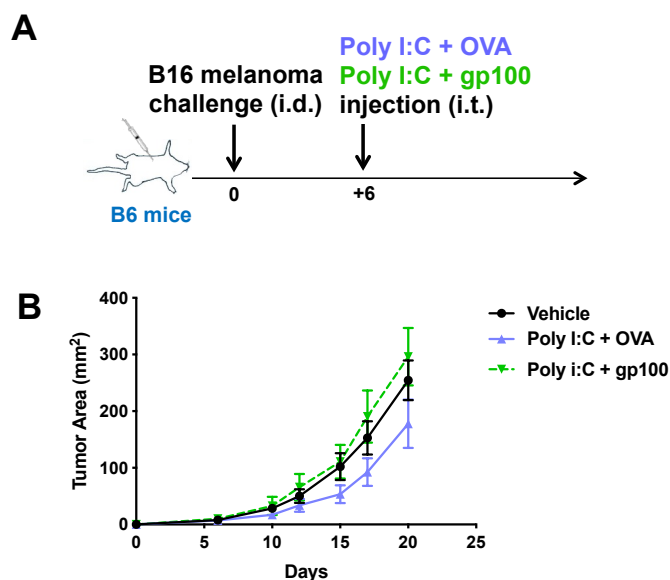
Figure 4.12 Intratumoral administration of TLR3 agonist poly I:C in conjunction with OVA peptide yields slower tumor growth than that of poly I:C + gp100 combination. (A) Experimental design in which 20 µg poly I:C + 0.007 µg peptide was injected in a total volume of 50 µL intratumorally. Vehicle, sterile water or phosphate-buffered saline. Poly I:C, TLR3 agonist. OVA, SIINFEKL peptide from ovalbumin. gp100, KVPRNQDWL melanocyte peptide. i.d., intradermal, i.t., intratumoral. (B) Tumor area growth curve for experiment described in (A). Mean ± s.e.m.
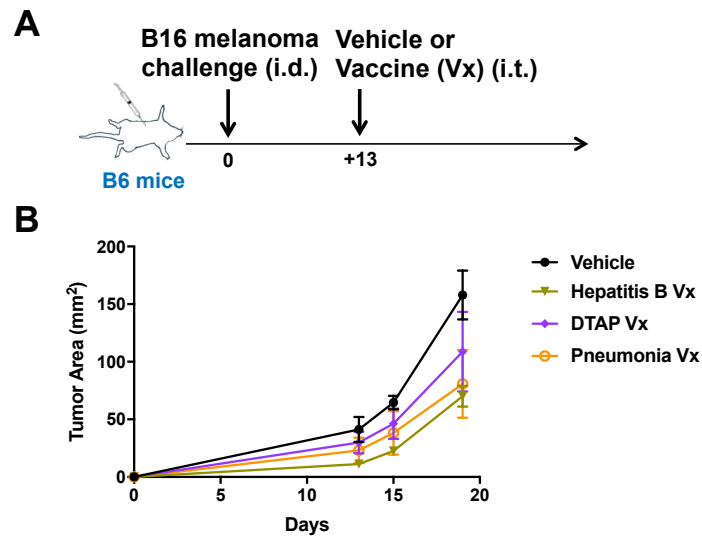
Figure 4.13 Intratumoral administration of other pathogen vaccines reduces tumor growth. (A) Experimental design. i.d., intradermal, i.t., intratumoral. (B) Tumor area growth curve for experiment described in (A). Mean ± s.e.m.

CHAPTER 5: AN ADJUVANTED INFLUENZA VACCINE FAILS TO REDUCE TUMOR GROWTH DUE TO MAINTAINENCE OF REGULATORY B CELLS

Intratumoral Adjuvanted Influenza Vaccine Fails to Slow Growth of Melanoma

With clinical translation as a goal of this research, it is imperative to understand whether all varieties of the seasonal influenza vaccine equally slow tumor growth, and if not, to understand the mechanistic underpinnings underlying any phenotypic differences. All unadjuvanted influenza vaccines tested slowed tumor growth to an equivalent degree (Fig 4.2). Of all influenza vaccinations commercially available, only one formulation, FLUAD[®] (hereafter referred to as AdjFluVx), contained an adjuvant (Table 1). FLUAD[®], designed for elderly and immune-compromised persons, contains a proprietary squalene-based adjuvant, MF59[®], that enhances the anti-influenza humoral immune response relative to that observed for unadjuvanted vaccination[102]. While all tested unadjuvanted influenza vaccines resulted in improved anti-tumor outcomes, AdjFluVx demonstrated no tumor-reduction capabilities (Fig 5.1, A and B). To confirm that the vaccine was fully functional in its intended purpose of providing protection from influenza, mice were vaccinated and subsequently challenged with influenza; AdjFluVx-vaccinated mice did not show an elevation of influenza PR8 transcript, indicating protection from the virus (Fig 5.1, C and D) and thus demonstrating a disconnect between anti-tumor and anti-pathogen responses.

Adjuvant is the Major Determinant of Tumor-Reduction Capability for Intratumoral Influenza Vaccination

Since the major differentiating factor between FluVx and AdjFluVx is the presence of the adjuvant MF59[®] in the latter, it is likely that the presence of this adjuvant detrimentally impacts the ability to control tumor growth. Although intratumoral

injection of the squalene-based adjuvant AddaVax™ (hereafter referred to as Adj) [103-105]

(used in lieu of the proprietary MF59®), alone did not alter tumor growth, the addition of

Adj to (unadjuvanted) FluVx abrogated FluVx's ability to reduce tumor growth (Fig. 5.2,

A and B).
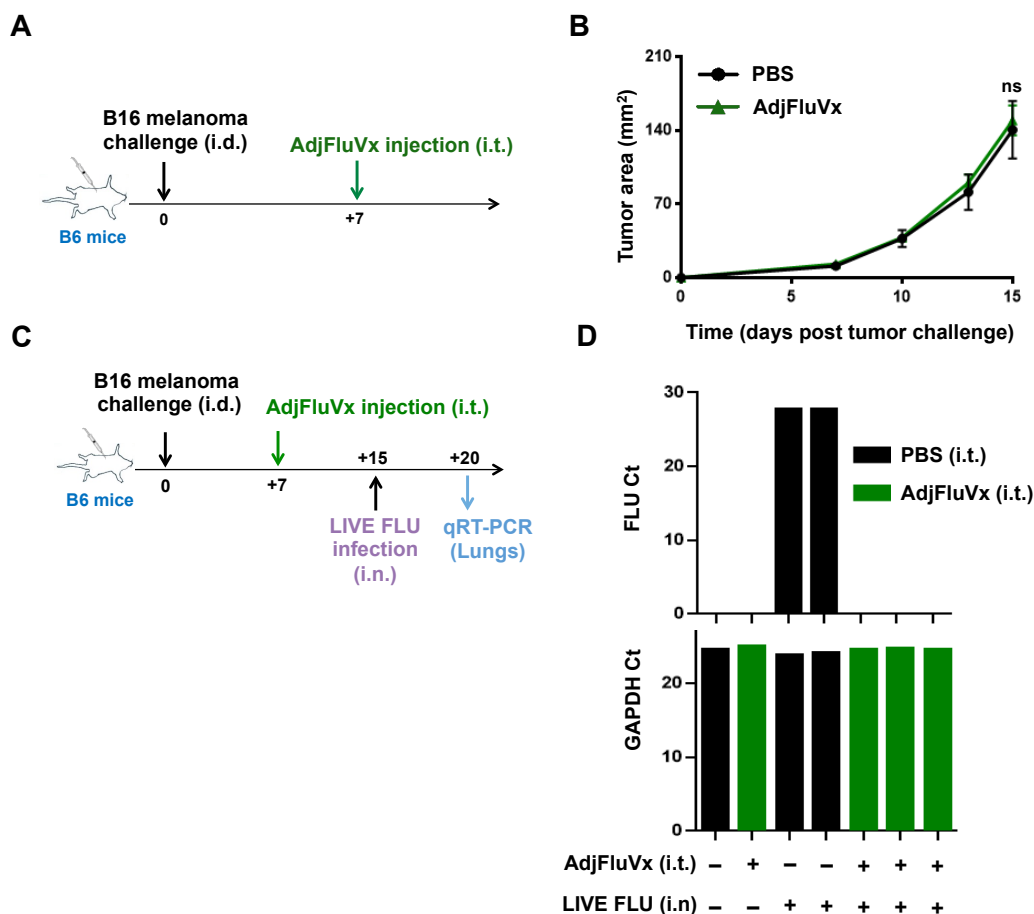
Fig. 5.1 Intratumoral injection of adjuvanted seasonal influenza vaccination fails to slow tumor growth, but provides protection against future influenza infection in the lungs. (A) Experimental design. AdjFluVx, adjuvanted seasonal influenza vaccine. (B) Tumor growth curves for AdjFluVx for experiment described in (A). (C) Experimental design. (D) Bar graphs showing count threshold (Ct) of LIVE FLU or GADPH control Quantitative Reverse Transcription Polymerase Chain Reaction (qRT-PCR) transcripts for experiment described in (C). i.d, intradermal, i.n., intranasal, i.t., intratumoral. ns, not significant [Two-way ANOVA with Bonferroni correction (B)]. Mean ± s.e.m. Data are representative of at least two independent experiments with similar results.

Intratumoral Adjuvanted Influenza Vaccine Does Not Inflame the Tumor Microenvironment and Fails to Reduce Population of Immunosuppressive B Regulatory Cells

Consistent with these tumor growth alterations, analysis of the Nanostring PanCancer Immune Profiling Panel demonstrated a decreased immune signaling transcriptional signature (antigen presentation and processing, T cell activation and exhaustion, innate immune signaling, and chemokines/cytokines) with AdjFluVx (and with Adj added to FluVx [FluVx + Adj]) compared to FluVx (Fig. 5.2C), suggesting that this adjuvant reverses the remodeling of the tumor microenvironment observed with intratumoral FluVx vaccination. Further, removing the adjuvant from AdjFluVx afforded it the ability to reduce tumor growth (Fig 5.3), suggesting that removal of the adjuvant recovers the anti-tumor efficacy of intratumoral influenza vaccination. Although AdjFluVx increased the proportion of DCs among APCs in the tumor, AdjFluVx did not augment CD8$^+$ T, or tumor-reactive CD8$^+$ T cells within the tumor (Fig 5.4). A major observed discrepancy between FluVx and AdjFluVx in the tumor microenvironment was the difference in the T cell: B cell ratio; AdjFluVx skewed the tumor microenvironment towards B cells (Fig 5.5) and correspondingly induced a greater concentration of influenza-specific antibodies in the tumor (Fig 5.6). T cells—particularly CD8$^+$ T cells— are widely acknowledged as the main adaptive immune effectors in the anti-tumor immune response; however, elevation of B cells in the context of cancer is less understood, and has in some studies been associated with tumor progression[106]. Given that MF59® has been documented to increase titers of anti-influenza antibodies[102], B cell skewing in the tumor microenvironment is not surprising, however, here it may come at the expense of anti-tumor immunity.
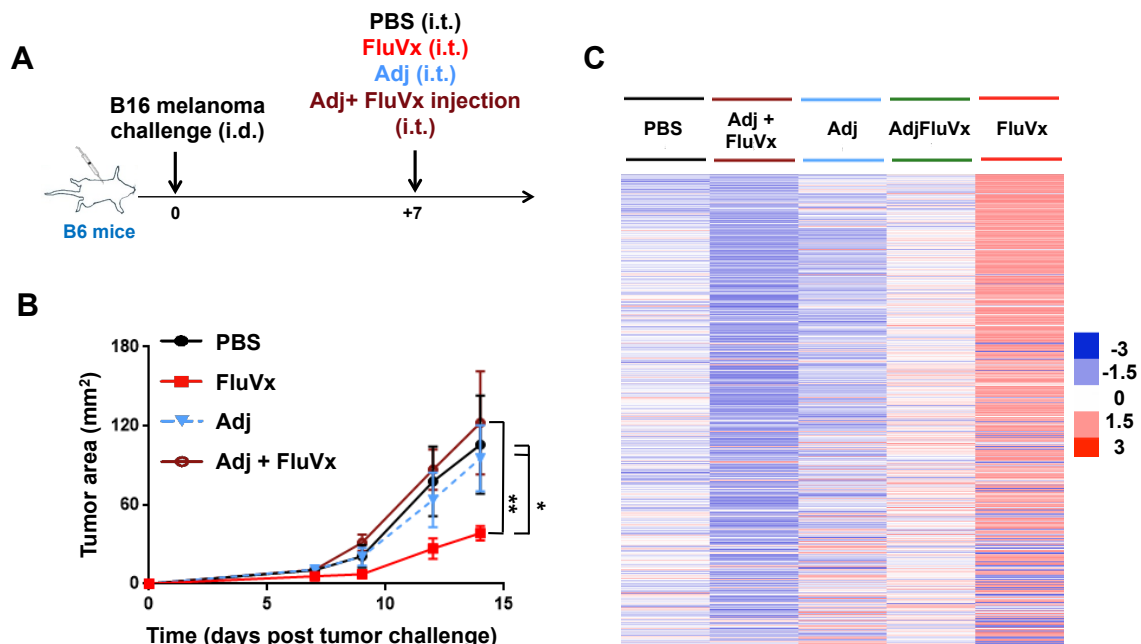
Fig. 5.2 The squalene-based adjuvant in AdjFluVx abrogates tumor-reduction ability and inflammatory transcriptional signature of intratumoral influenza vaccination. (A) Experimental design. (B) Tumor growth curves with the adjuvant (Adj) added to FluVx1. (C) Representative heatmap of the NanoString PanCancer Immune Profiling panel on tumors 14 days post tumor challenge. Blue color indicates downregulation of transcript, and red color indicates upregulation of transcript. n=4 mice/group. *P < 0.05, **P < 0.01 [Two-way ANOVA with Tukey correction (B)]. Mean ± s.e.m. Data are representative of at least two independent experiments with similar results. i.d., intradermal, i.t., intratumoral.
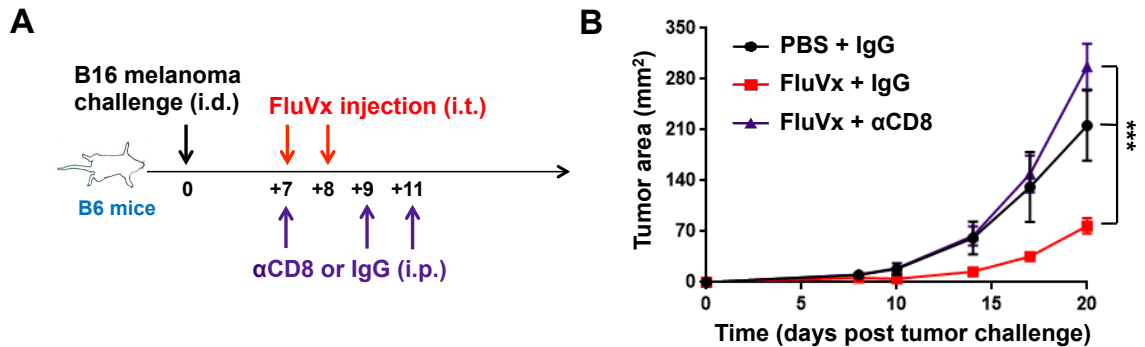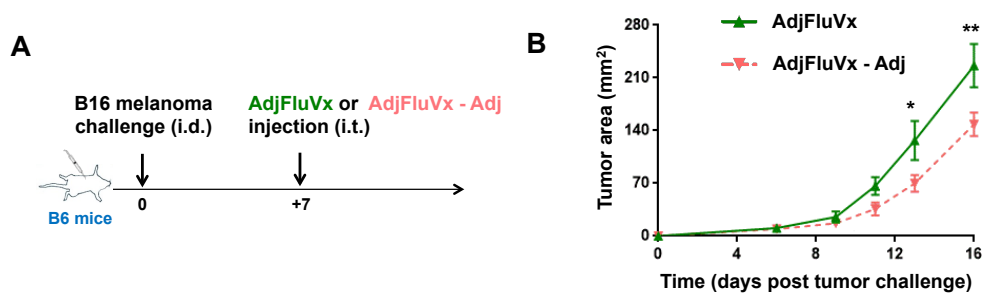

Fig. 5.3 Removal of squalene-based adjuvant from adjuvanted influenza vaccine enables reduction of tumor growth upon intratumoral injection. (A) Experimental design utilizing AdjFluVx in which the Adj has been removed (AdjFluVx -Adj). n=4-5 mice/group. (B) Tumor growth curves for experiment described in (A). *P<0.05, **P<0.01 [Two-way ANOVA with Bonferroni correction (B)]. Mean ± s.e.m. i.d., intradermal, i.t., intratumoral.
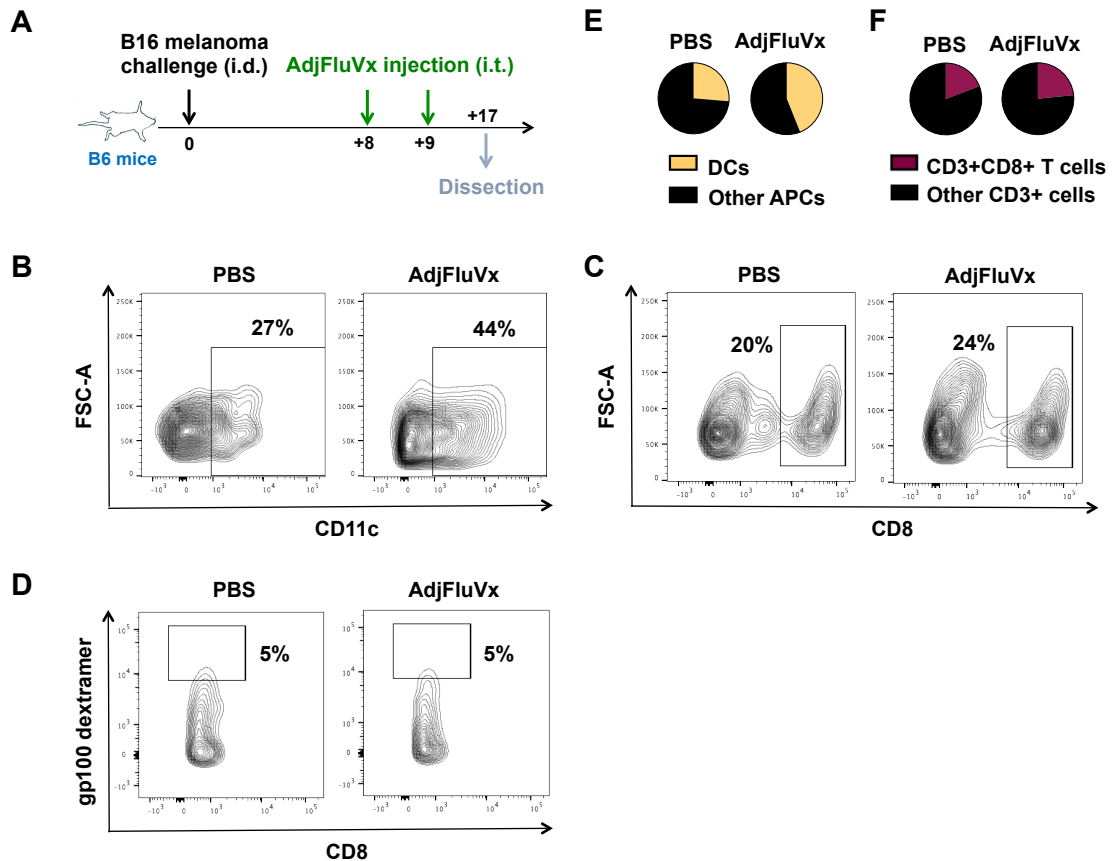
Fig. 5.4 Adjuvanted influenza vaccine increases the proportion of dendritic cells, but not CD8$^+$ T cells, in the tumor upon intratumoral injection. (A) Experimental design. AdjFluVx, adjuvanted influenza vaccine. (B) Flow cytometry plot showing dendritic cells (DCs; CD11c$^+$) among antigen-presenting cells (APCs; CD45$^+$ MHC-II$^+$) from tumors isolated from mice of the experiment described in (A). n=3-5 tumors pooled/group. (C) Flow cytometry plot showing CD8$^+$ T cells among CD45$^+$ CD3$^+$ cells from tumors isolated from mice of the experiment described in (A). n=3-5 tumors pooled/group. (D) Flow cytometry plot showing tumor-reactive (gp100 dextramer$^+$) CD8$^+$ T cells among CD45$^+$ CD3$^+$ cells from tumors isolated from mice of the experiment described in (A). n=3-5 tumors pooled/group. (E) Cumulative pie chart for data shown in (B). (F) Cumulative pie chart for data shown in (C). Data are representative of at least two independent experiments with similar results. i.d., intradermal, i.t., intratumoral. FSC-A, forward scatter area.
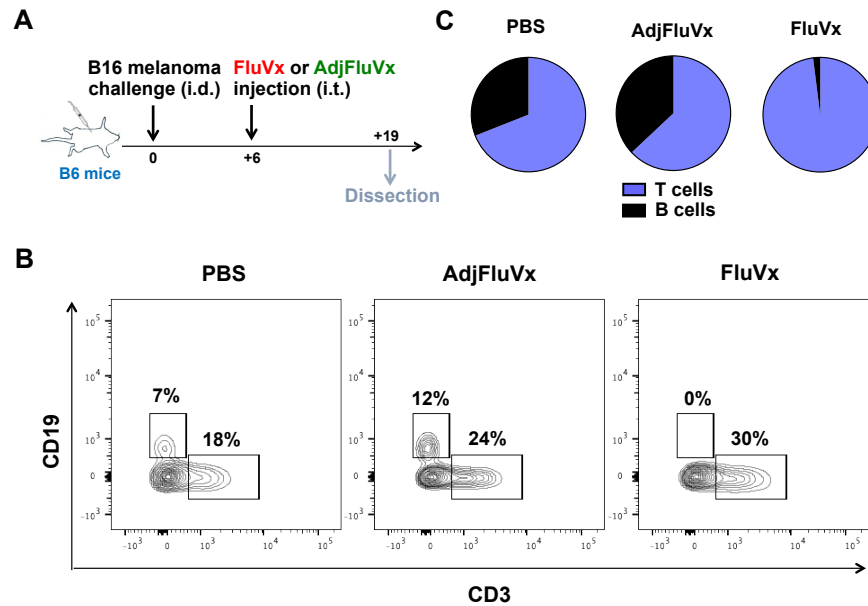
Fig. 5.5 Intratumoral adjuvanted influenza vaccination fails to increase the T:B cell ratio in the tumor. (A) Experimental design. AdjFluVx, adjuvanted seasonal influenza vaccine. FluVx2, unadjuvanted seasonal influenza vaccine. (B) Flow cytometry plot showing the proportion of intratumoral B cells (CD45$^+$ CD19$^+$) to T cells (CD45$^+$ CD3$^+$). n= 3-5 tumors pooled/group. (C) Cumulative pie charts showing ratio of T cells to B cells for data shown in (B). Data are representative of at least two independent experiments with similar results. i.d., intradermal. i.t., intratumoral.
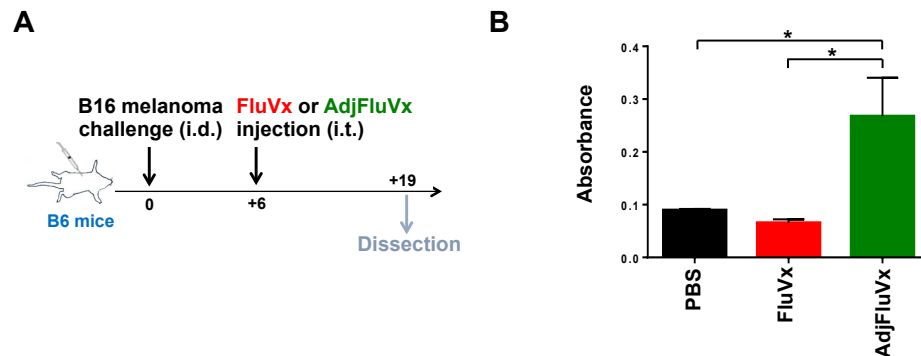
Fig. 5.6 Intratumoral injection of adjuvanted influenza vaccine induces the production of influenza-specific antibodies in the tumor. (A) Experimental design. n= 3-8 mice/group. AdjFluVx, adjuvanted seasonal influenza vaccine. FluVx1, unadjuvanted seasonal influenza vaccine. Tumors were resected and homogenized for use in ELISA assay. (B) Bar graphs showing absorbance measured by ELISA assay for experiment described in (A). *P<0.05 [Kruskal-Wallis with Dunn's Multiple Comparisons comparing all groups to AdjFluVx (A)]. Mean ± s.e.m. Data are representative of at least two independent experiments with similar results. i.t., intratumoral. i.d., intradermal.

Interestingly, analysis of cytokines within the tumor revealed an increase in interleukin-10 (IL-10) with AdjFluVx intratumoral administration (Fig. 5.7). IL-10 is a regulatory cytokine that can be produced by cells of the innate immune system, and some B and T cell subsets[107]; IL-10 can dampen pro-inflammatory immune programs via downregulation of MHC-I and co-stimulatory molecules, ultimately hampering T cell responses[108]. An elevated level of intratumoral regulatory B cells (Bregs; IL-10-producing B cells) with AdjFluVx compared to FluVx administration was observed, without an increase in T regulatory cells (Tregs) (Fig. 5.8). Regulatory B cells have been associated with diminished anti-tumor immunity, and IL-10 produced by regulatory B cells can suppress CD8$^+$ T cell functions, thereby abrogating their ability to mount a cytotoxic anti-tumor immune response[105]. Importantly, intratumoral depletion of either B cells (utilizing αCD20 antibody) or IL-10 rendered AdjFluVx the ability to reduce tumor growth (Fig. 5.9). It should be noted that IL-10 is produced not only by select B and T cell subsets, but also by cells of the innate immune system, such as macrophages[109]; whether there are differences in macrophage populations between AdjFluVx- versus FluVx-vaccinated tumors is of interest for future research. In summation, AdjFluVx fails to reduce tumor growth due to maintenance of suppressive B regulatory cells in the tumor microenvironment.

Due to its role as an immunosuppressive cytokine that potentiates direct effects on T cell lineages, IL-10 was pursued as a key differentiator in phenotype between FluVx and AdjFluVx. However, it should be noted that while most cytokines did not vary in levels in the tumor between the FluVx- and AdjFluVx-treated groups, FluVx-vaccinated mice exhibited the highest levels of intratumoral IL-6, and AdjFluVx-vaccinated mice

exhibited the highest levels of intratumoral IL-9 (Fig. 5.10), albeit these results are not statistically significant. Investigation into further mechanisms involving these cytokines will be meaningful in efforts to understand what differentiates AdjFluVx and FluVx in terms of tumor reduction phenotype. Although research on the role of IL-6 in cancer is conflicting, there is some evidence that is associated with lymphocyte activation, proliferation, and trafficking to the tumor microenvironment in the anti-tumor immune response[110]. IL-9 has also been reported to have both tumor-promoting and anti-tumor attributes[111]. Of interest, IL-9 is mainly produced by Th2 and Th9 helper T cell subsets[111]; given the B cell-skewed microenvironment induced by AdjFluVx, it may be that increased intratumoral IL-9 is a reflection of a Th2-dominant tumor microenvironment that merits further investigation.
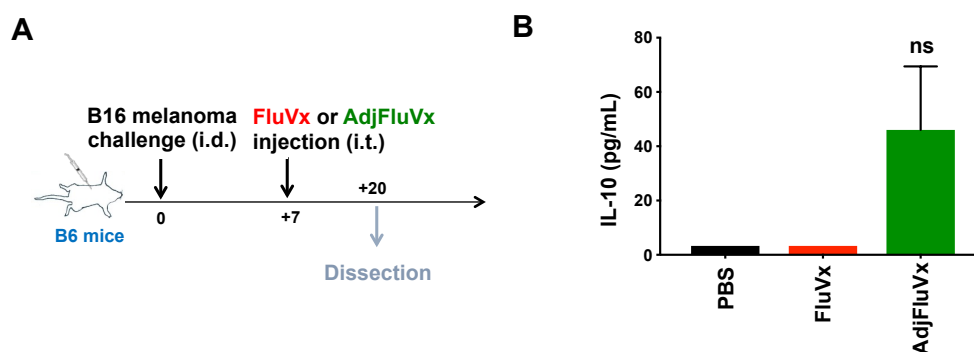
Fig. 5.7 Intratumoral injection of adjuvanted influenza vaccine increases the concentration of IL-10 in the tumor. (A) Experimental design. (B) Bar graphs showing IL-10 levels detected by LEGENDplex assay in the tumors of mice 13 days after treatment for experiment described in (A). n=3-5 mice/group. ns= not significant [Kruskal-Wallis with Dunn's Multiple Comparisons comparing all groups to AdjFluVx (B)]. Mean ± s.e.m. Data are representative of at least two independent experiments with similar results.
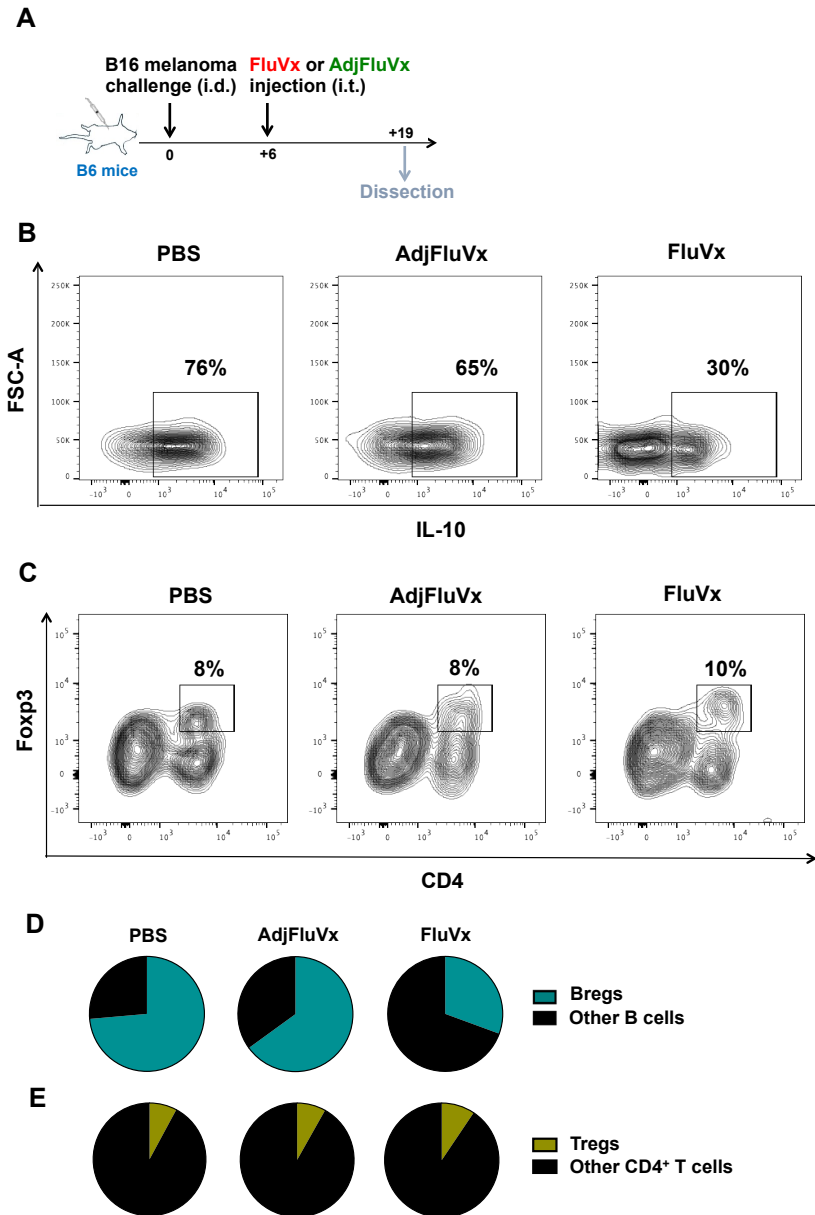
Fig. 5.8 Intratumoral injection of adjuvanted influenza vaccine increases the proportion of B regulatory, but not T regulatory, cells in the tumor relative to that observed with unadjuvanted influenza vaccine. (A) Experimental design. AdjFluVx, adjuvanted seasonal influenza vaccine. FluVx, unadjuvanted seasonal influenza vaccine. i.d., intradermal. i.t., intratumoral. (B) Flow cytometry plot showing the proportion of IL-10^+ cells among $CD45^+$ $CD20^+$ cells in the tumor. n=3-5 tumors pooled/group. (C) Flow cytometry plot showing the proportion of $Foxp3^+$ $CD4^+$ cells among $CD45^+$ $CD3^+$ cells. n=3-5 tumors pooled/group. (D) Cumulative pie chart for data shown in (B). (E) Cumulative pie chart for data shown in (C). Data are representative of at least two independent experiments with similar results.
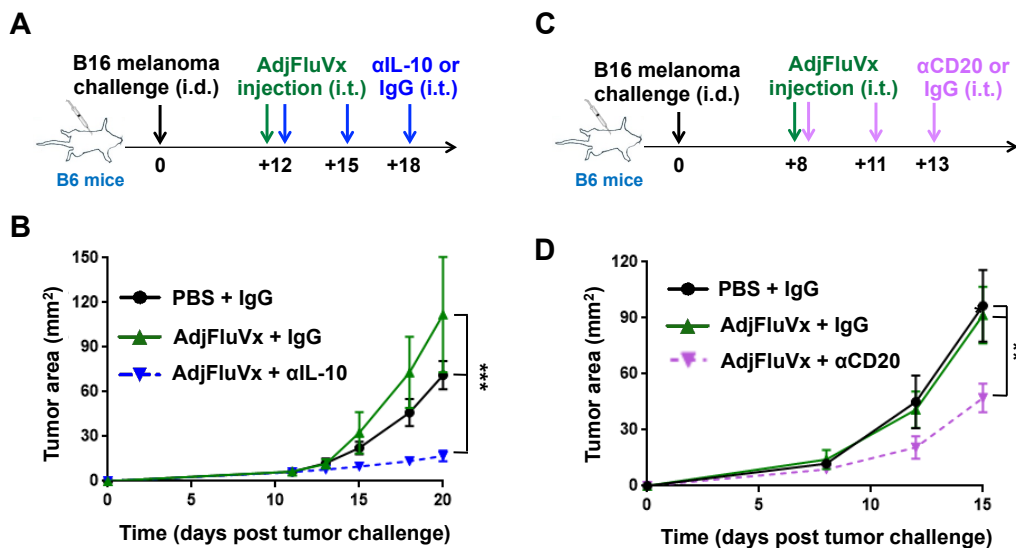
Fig. 5.9 Intratumoral blockade of IL-10 or B cells reverses failure of adjuvanted influenza vaccine to slow tumor growth. (A) Experimental design. (B) Tumor growth curves for experiment described in (A). (C) Experimental design. (D) Tumor growth curves for experiment described in (C). **P<0.01, ***P<0.001 [Two-way ANOVA with Tukey correction (B,D)]. Mean ± s.e.m. n=5-10 mice/group. Data are representative of at least two independent experiments with similar results. i.d., intradermal, i.t., intratumoral.
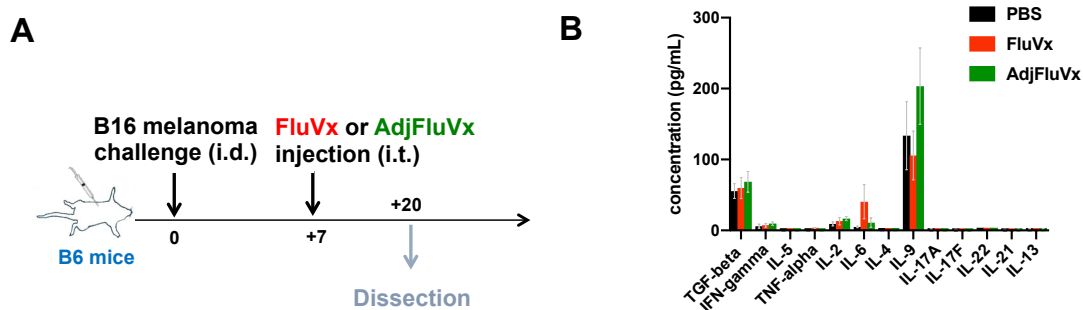
**Fig. 5.10 Cytokine analysis of tumors injected with PBS, FluVx or AdjFluVx.** (A) Experimental design. (B) Bar graphs showing cytokine levels detected by LEGENDplex assay in the tumors of mice 13 days after treatment for experiment described in (A). n=3-5 mice/group. Mean ± s.e.m.

CHAPTER 6: DISCUSSION

Summary of Findings and Clinical Implications

Clinical successes utilizing immunotherapy alone and in combination to improve

and prolong the lives of patients with cancer have demonstrated a vital role for the

immune system in the treatment for cancer. However, thus far, immunotherapies have

been able to produce durable responses only in a limited proportion of patients[3].

Therefore, for the advancement of the field of cancer immunotherapy, novel strategies for

harnessing the immune system to recognize and eliminate cancer need to be pursued.

Here, a new category of viral-based therapy for cancer (non-oncolytic) was tested and

characterized. Influenza virus reduced growth of melanoma in the lungs, and heat-

inactivated influenza (or FDA-approved inactivated influenza vaccines) reduced growth

of melanoma in the skin. In recent years, viral infection has been harnessed as a vehicle

to augment anti-tumor immune responses, and in particular, oncolytic virus therapy has

been employed as a tool in the clinic. Oncolytic viruses preferentially lyse tumor cells

and consequently release tumor antigens and danger-associated molecular patterns

(DAMPs)[2]. However, in the context of oncolytic viruses, productive infection of the

tumor cells themselves is the focus[2]. Here, the overexpression of specific proteins by

tumor cells (but not normal adjacent cells) is hijacked by such viruses, which use these

overexpressed proteins as entry receptors[2]. Normal cells without these receptors or with

less expression do not serve as the major target and are spared, or they utilize interferon

signaling (a pathway that is dysregulated in cancer cells) to limit infection[2]. Thus, a major

focus in this field has centered on the importance of direct infection of the tumor cell as a

prerequisite for generating anti-tumor immunity. However, the idea that tumor cell lysis

by the pathogen is essential for mounting an anti-tumor immune response has been

recently challenged by evidence demonstrating that an inactivated oncolytic virus is capable of initiating anti-tumor immunity via the STING pathway and may support better immunity than its live oncolytic counterpart[112]. It may be that the extent to which an immune response that is mounted against a live pathogen is at the same time immune-suppressing as it is immune-activating, as brakes on the immune response are triggered to limit immune-mediated host destruction[113]. The data presented in this dissertation demonstrate that inactivation of a non-oncolytic virus, such as influenza, can augment an anti-tumor immune response when administered via intratumoral injection, even when the corresponding live virus is incapable of such activity. This indicates that microbial-based cancer therapies are not limited to the oncolytic class of pathogens or even to the use of live pathogens. Further, in terms of clinical translation, just as non-live vaccines are recommended for most cancer patients, inactivated influenza injection is accessible to immunosuppressed cancer patients who are not eligible for live pathogen-based therapies[114] and likewise can be utilized in patients who are not willing to participate in treatments involving live-pathogen infections.

The Role of Innate Immune Signaling in Intratumoral Influenza Vaccination

A priority future direction for this research is interrogation of the role of innate signaling in initiation of anti-tumor immunity. The aforementioned findings reveal that influenza vaccination alters the tumor microenvironment by increasing the proportion of dendritic cells (and notably, increasing representation of the cross-presenting dendritic cell subset) and $CD8^+$ T cells, including those that are tumor-reactive, to overcome immune suppression. This remodeling of the tumor microenvironment is likely to be initiated by TLR activation in innate immune cells upon the encounter with viral-derived

PAMPs[18]. Influenza virus is sensed by TLR3 (dsRNA), TLR7 (ssRNA), TLR8 (ssRNA) and RIG-I (5' triphosphate RNA)[115]. Downstream of TLR3 and TLR7 activation is IRF3/IRF7 and NF-κB activation, which induces production of Type I interferons and proinflammatory cytokines (such as IL-1β and IL-18), respectively[115]. While inactivated influenza vaccination is not a source of live virus, residual viral nucleic acid exists in the formulation as a vestige of the production process that utilizes live virus[85]. Therefore, it is possible that TLR signaling is occurring upon intratumoral influenza vaccination, and that this can be invigorating the immune response observed in the tumor microenvironment; this is a current subject of investigation in the laboratory.

The Role of Viral Antigen and Anti-Viral Immune Responses in the Context of Intratumoral Influenza Vaccination

While innate immune cell signaling would initiate the cascade of events leading to an immune cell population shift in the tumor microenvironment, there may also be a direct role of viral protein and anti-viral CD8$^+$T cell responses contributing to anti-tumor immunity. Firstly, it is possible that the antigenic overlap between viral and tumor peptides may allow anti-pathogen immune cells to subsequently target antigenically similar tumor peptides presented on cancer cells. This type of mimicry[116] proposes that in the context of an anti-pathogen response in the tumor microenvironment, some CD8$^+$ T cells produced against the pathogen may be able to respond against tumor cells harboring an overlapping tumor-derived antigen. At the same time, tumor-reactive CD8$^+$ T cells may be enhanced by the recognition of an overlapping pathogen-derived antigen. Indeed, patients whose tumors harbor the tetrapeptide ESSA, a sequence shared by cytomegalovirus (CMV), have been shown to exhibit increased survival in the context of CTLA-4 checkpoint blockade therapy[117]. Further, studies have reported that pathogen-

specific (CMV, influenza, EBV, etc.) CD8^{+}T cells infiltrate mouse and human tumors and comprise a significant fraction of intratumoral CD8^{+}T cells[118-122]. Recently, in mouse models, virus-specific memory T cells have shown to halt tumor growth when their cognate antigens are injected within the tumor to create a bystander immune-"alarming" effect[118]. In contrast to this strategy, which requires previous immunity against a specific pathogen, the influenza vaccination data discussed suggest that viral antigen-related therapies can be harnessed for anti-tumor immune responses independent of previous exposure, as in the majority of the aforementioned experiments, the hosts had no previous exposure to influenza. Yet, even in such cases, intratumoral administration of inactivated influenza increases dendritic cells and anti-tumor CD8^{+} T cells, and consequently, the reduction of tumor growth, without any prerequisite immunity. This may be particularly important for repurposing the seasonal influenza vaccine for cancer immunotherapy and translating it to clinical care, as the seasonal influenza vaccine includes antigens that are altered yearly to match the anticipated predominant strains of the upcoming season. In this context, the lack of need for previous exposure to the same pathogen and strain is a major advantage. However, it is important to note that previous infection, followed by recovery, to a particular strain of influenza did not prohibit subsequent tumor reduction with an intratumoral influenza vaccine of the exact same strain. This suggests that patients with or without previous immunity to the influenza strain contained within the vaccine may benefit from intratumoral administration of the vaccine. With multiple strains included within each trivalent and quadrivalent influenza vaccine, it may be that optimal response is achieved when a combination of new and previously experienced antigens are utilized, especially in the context of the finding that anti-viral CD8^{+} memory

T cells infiltrate human tumors and can be activated to produce IFN-γ and granzyme B and remodel the tumor microenvironment to slow tumor growth upon (re)-introduction of viral peptides[118]. In this scenario, previously experienced antigens quickly raise inflammatory immune responses, which are quickly quenched with the elimination of the recognized antigen[118]. At the same time, new antigens raise slower responses, but have potential to diversify the arsenal of anti-pathogen T cell responses that can be employed for tumor control. Future studies will address whether CD8^{+} T cells reactive against shared viral/tumor peptides influence anti-tumor immunity, and ultimately, tumor growth. Further, studies will be conducted to determine whether tumor-residing anti-viral CD8^{+} T cells can supplement the inflammatory immune response mounted with intratumoral influenza vaccination upon introduction of viral peptide in influenza-experienced hosts.

The Role of Adjuvants and Other Considerations for Clinical Application

The research presented in this dissertation proposes that intratumoral administration of the influenza vaccine decreases tumor growth by increasing dendritic cells (and their ability to present antigens) and augmenting anti-tumor CD8^{+}T cells within the tumor microenvironment. Further, vaccination at the tumor site converts immunologically "cold" tumors to ones that are immune-infiltrated ("hot") and that enable the initiation of tumor-killing CD8^{+}T cell responses. This conversion of the tumor microenvironment has important implications for the role of intratumoral influenza vaccination in priming patients to respond to existing immunotherapies (including PD-1/PD-L1 blocking antibodies); synergy of influenza vaccine and checkpoint blockade in mice provides clinical rationale for testing this combination in the clinic. A clinical trial

testing intratumoral (unadjuvanted) influenza vaccine in conjunction with PD-1 blockade in patients with non-melanoma skin cancer is currently in preparation.

Important attention must be paid to the formulation of the vaccine, as squalene-based adjuvant provides improved anti-pathogen protection, while limiting the ability of the vaccine to improve anti-tumor outcomes due to maintenance of suppressive B regulatory cells in the tumor microenvironment. The adjuvanted influenza vaccine utilized in this study has been demonstrated to provide enhanced influenza immunity in its intended population (namely, patients over 65 years of age) who may be more immunosuppressed[102,123], and more likely to receive a cancer diagnosis[124]. MF59® is designed for optimal mounting of a B cell response that can lead to production of virus-neutralizing antibodies[125]. Mechanistically, MF59® initiates a strong B cell response as it increases production of lymph node-directing chemokines at the injection site and induces dendritic cell maturation, allowing for more efficient antigen uptake[125]. Further, this adjuvant promotes proliferation and long-term maintenance of antigen-specific CD73$^+$ CD80$^-$ germinal center B cells, and production of high affinity and neutralizing antibodies[125]. While ideal for control of viral infection, the presence of B cells in the tumor microenvironment upon intratumoral administration of AdjFluVx affords the opportunity for conversion to suppressive B regulatory cells. Research has indicated that B cells an increase in IL-27β and IL-12a in response to TLR crosslinking and CD40 activation, resulting in dimerization of these two proteins to form the suppressive cytokine IL-35, which promotes conversion of the B cell to the suppressive B regulatory cell phenotype[126]. In the context of virus-detecting TLR activation, this is likely to occur[126]. More broadly, IL-10 produced by B cells is thought to maintain the skew in the

immune response towards Th2 by actively suppressing Th1 responses[126]; in the context of

MF59®-adjuvanted influenza vaccine, this may represent a double-edged sword in which

B cells are being nurtured in the tumor microenvironment at the expense of pro-

inflammatory T cell populations capable of targeting tumor cells for death. Further,

detrimental effects on anti-tumor immunity are directly incurred via B regulatory cell-

derived IL-10, which has been shown to inhibit T helper cell and $CD8^+$ T cell

functionality[106, 126]. In an effort to avoid induction of a B cell/B regulatory cell centric

immune response, AdjFluVx may be avoided in the clinic via substitution with an

unadjuvanted high antigen dose vaccine that is designed for generating robust anti-viral

immunity in elderly and immunocompromised patients (upon confirmation that anti-

tumor immune responses are not hampered in the context of intratumoral injection)[127].

Future experiments will determine if high-dose influenza vaccine can generate anti-tumor

immune responses similar to that observed for tested unadjuvanted vaccines, while

providing optimal protection from influenza infection.

Adjuvants play an important role in boosting immune responses, and likely within

"unadjuvanted" influenza vaccines inherent adjuvants (i.e., host cell proteins and DNA,

residual single-stranded influenza RNA, etc.) resulting from the process of manufacturing

the inactivated vaccine (rather than influenza peptides alone) improve immunity by

interacting with multiple danger-sensing mechanisms (i.e., RNA-sensing toll-like

receptor 8), previously shown to improve anti-tumor immune responses[128]. These

inherent adjuvants—which here comprise those that are viral-derived—will result in

active TLR3, TLR7 and TLR8 signaling, which induces production of type I interferons,

dendritic cell maturation, and pro-inflammatory cytokine production upon encounter with

viral nucleic acid in the endosomes[129]. Consequently, the (T cell-centric) immune response mounted is designed to eliminate virally-infected cells[129]. Similarly, mounting of a T cell response, particularly a CD8$^+$ T cell response, is of paramount importance for tumor elimination[130]. Given the shared goal of cell elimination by T cells (whether it be of virally-infected cells or abnormal-self [tumor] cells), a vaccine harboring virus-inherent adjuvants without addition of manufactured adjuvants is well suited for repurposing of vaccination as an intratumoral therapy for cancer. Since the majority of seasonal influenza vaccines currently on the market are inactivated, do not contain manufactured adjuvants, have a high safety profile, and are FDA-approved[84], the translatability of these vaccines as innovative immunotherapies for cancer is high and the barrier to reaching many patients with cancer is low.

Although influenza is a major public health concern, with more tens of thousands of deaths annually in the United States[131], the Centers for Disease Control and Prevention (CDC) has reported that in the 2017-18 season, only 37.1% of adults received the influenza vaccine[132]. Importantly, beyond demonstrating that influenza vaccination administered via intratumoral injection can reduce tumor growth, it was shown that protection against future influenza infection is provided via intratumoral (rather than intramuscular) administration. This suggests that patients receiving intratumoral influenza vaccination may experience multiple clinical benefits and that influenza vaccination is a crucial public health tool that can be utilized as both a preventive measure for infection and an immunotherapy for cancer.

Beyond Intratumoral Influenza Vaccination: Future Directions

Beyond intratumoral influenza vaccination for cancer is the prospect of utilizing other pathogen (or other immunogenic protein) vaccines intratumorally for cancer therapy. Preliminary research presented in this dissertation suggests that other commercially available inactivated vaccines (DTAP, pneumonia and Hepatitis B) can slow growth of tumors when injected intratumorally. Two main questions stem forth from the potential translatability of these vaccines as cancer treatments: 1) do the natural adjuvants in other vaccines elicit immunologically pathways mutually favorable to pathogen elimination and tumor destruction, as observed for inactivated influenza vaccine?, and 2) are the supplemental, manufactured adjuvants present in other vaccines detrimental for repurposing as an intratumoral therapy for cancer, as MF59® is? With respect to the question regarding the role of natural adjuvants in the ability of a pathogen vaccine to be repurposed for cancer therapy, there are differences across vaccines in the TLR pathways that will be activated upon vaccination. For instance, the bacteria that cause diphtheria and tetanus are both Gram-positive[133, 134], which are recognized by TLR1, TLR2, and TLR6[135]. Signaling through TLRs 1,2 and 6 occurs via TIRAP and MyD88 adapters to ultimately result in pro-inflammatory cytokine production, but crucially, without induction of the aforementioned type I interferon response[135]. The type I interferon pathway is critical, for induction of anti-viral and anti-tumor immune responses, as it results in dendritic cell maturation and robust CD8$^+$ T cell functionality (production of granzymes and perforin, for example)[136]. Therefore, whether a vaccine solely containing Gram-positive bacteria, for instance, result in robust anti-tumor immunity upon intratumoral injection is questionable and should be investigated.

Interestingly, the aforementioned experiment involving use of intratumoral DTAP vaccine (which immunizes against the bacteria causing diphtheria, tetanus and pertussis)[137], contains one (inactivated) type of Gram-negative bacterium, *Bordetella pertussis*[138], which should activate TLR4, and consequently, a type I IFN response[135], potentially explaining its anti-tumor efficacy in the intratumoral context. Further, the question of whether additional, manufactured adjuvants in pathogen vaccines can influence anti-tumor efficacy is of interest, particularly in the case of the DTAP vaccine, which is adjuvanted with aluminum hydroxide, commonly referred to in the field of immunology as "alum"[139]. Alum induces a potent Th2-skewed immune response, resulting in the predominance of B cells (and resultant antibodies), at the expense of a Th1-dominant response[140]. As with MF59®, high antibody titers are observed upon vaccination with an alum-containing pathogen vaccine[140]; this raises the question of why DTAP may slow tumor growth, while AdjFluVx does not. Interestingly, some adjuvants—including alum, but not MF59® -are considered to be antigen depots, meaning that they act to contain antigen at the injection site for a prolonged period of time and reduce the kinetics of antigen release from this site[140]. The attribute of serving as an antigen depot has been correlated with elevated antibody production, and is therefore a desired feature in pathogen vaccination[140]. While research has suggested that alum's status as an adjuvant is not directly due to its role as an antigen depot, it is possible that the feature of antigen depot is desirable in the context of intratumoral pathogen vaccination. Tumors are naturally poor antigen presenting cells[141], meaning that any therapy that can both reverse immune suppression at the tumor site to stimulate dendritic cells and sustain antigen release for extended periods of time could in theory enhance

anti-tumor immunity. It is possible that an alum-containing vaccine such as DTAP, despite its induction of a strong antibody response, can nevertheless slow tumor growth upon intratumoral injection due to its activation of multiple TLR pathways and its ability to serve as an antigen depot; this hypothesis will be tested in future work in the laboratory.

Future research will be focused on understanding the mechanisms and clinical translatability of pathogen vaccines as intratumoral therapies for cancer. Utilizing FDA-approved pathogen vaccines as a modern-day Coley's toxin may be a safe and cost-effective form of immunotherapy. Towards optimization of this approach for the best possible induction of anti-tumor immunity, different vaccines should be tested (bacterial-based, viral-based, combinations of vaccines) and fine-tuned with appropriate natural and manufactured adjuvants. Clinical trials are currently in preparation to test whether intratumoral influenza vaccination can reduce tumor burden in patients with non-melanoma skin cancer; future research will address whether intratumoral pathogen vaccination can be applied more broadly in a variety of cancers, and with a variety of pathogen vaccines.

CHAPTER 7: MATERIALS AND METHODS

Mice

Mice were housed in specific-pathogen free (SPF) facilities and all experiments were
conducted in accordance with procedures approved by the Institutional Animal Care and
Use Committee (IACUC) and Institutional Biosafety Committee (IBC) at Rutgers, The
State University of New Jersey and Rush University Medical Center, and the Institutional
Review Board (IRB) at Rutgers, The State University of New Jersey. B6 (C57BL/6J),
Batf3-/-(B6.129S(C)-Batf3tm1Kmm/J), NSG (NOD.Cg-PrkdcscidIl2rgtm1Wjl/SzJ; NOD
scid gamma), and Balb/c mice were purchased from Jackson Laboratory at 6-10 weeks of
age.

**Autologous immune-reconstituted patient-derived xenograft (AIR-PDX) mouse
model**

Immune-deficient NSG mice were purchased from Jackson Laboratory and bred in-
house. Patient-derived tumor tissue and peripheral blood were obtained through the
Rutgers Cancer Institute of New Jersey Biospecimen Repository and Histopathology
Service with patient consent. To create AIR-PDX mice, NSG mice were surgically
implanted with ~5 x 5 x 3 mm tumor sections (thus maintaining the natural architecture
of the tumors) into a 5-mm incision in the right flank and closed with a 6-0 proline
horizontal mattress suture (Henry Schein). Mice recovered from this minor survival
surgery in warming cages and were monitored for assurance of a minimum respiratory
rate of 30 breaths/minute. Additionally, these NSG mice were adoptively transferred
500,000 peripheral blood mononuclear cells (PBMCs) obtained by Ficoll gradient
centrifugation in 100 μL sterile PBS via retro-orbital injection at least 12 hours before
tumor implantation. Mice were surveyed for successful tumor implantation (defined as

two successive tumor measurements without regression at one and two weeks after surgery) and for immune reconstitution (minimum standard of 10% human CD45: mouse CD45 cells in peripheral blood) by flow cytometry of PBMCs obtained via a cheek bleed two weeks after the PBMC adoptive cell transfer.

SEER-Medicare linked database subjects

Study subjects were identified from the SEER-Medicare Linked Database. All cases of primary stage I to II non-small cell lung cancer (NSCLC; tumor site codes 34.0-34.9 and ICD-O-2 morphology codes 8010-8040, 8050-8076, 8140, 8143, 8250-8260, 8310, 8320, 8323, 8470-8490, and 8550-8573), age > 65 years, treated with either surgery or chemo-radiation during the span of 100 months between 2001 and 2011 were included. Samples were limited to patients with histologically confirmed cancers and excluded cases diagnosed at autopsy or death certificate. Survival was determined as the interval from the date of cancer diagnosis to the Medicare date of death. These data are updated daily by Medicare and thus are current as of the day that data were extracted for linkage with SEER. For analyses involving lung-cancer specific survival, SEER survival data were used as Medicare does not provide information regarding the cause of death. Data on the cause of death in SEER were obtained from state death certificates and included in the PEDSF file using ICD-9 codes. Presence of influenza infection was considered 'yes' (FLU dx) based on codes obtained from MEDPAR files for hospitalization for influenza. Since lung cancer-specific mortality did not reach 50% for the FLU dx group, time to mortality (lung cancer-specific and overall) in 25% of the patients (P25) was calculated.

Live and heat-inactivated influenza

For experiments utilizing live influenza (LIVE FLU) infections, mice were administered

1×10^6 plaque-forming units (pfu) of A/PR8/1934/H1N1 (FLU) [142] or OVA257-

264SIINFEKL-expressing A/PR8/1934/H1N1 (FLU-OVA) [143] by intranasal,

intratumoral, or peritumoral injection (25-50 µL). Control mice were administered an

equal volume of PBS via the same route. Whole body weights were recorded serially to

assess health of influenza-infected mice. For experiments utilizing heat-inactivated

influenza (hiFLU) or hiFLU-OVA, virus was heat-inactivated by incubation at 90°C for 5

minutes on an IncuBlock™ Plus heat block (Denville Scientific) prior to peritumoral or

intratumoral injection into mice.

Vaccines and adjuvants

FDA-approved 2017-2018 seasonal influenza vaccines were purchased from their

respective manufacturers: FLUCELVAX®[FluVx1] (Seqirus), FLUVIRIN®[FluVx2]

(Seqirus), FLUARIX® QUADRIVALENT [FluVx3] (GlaxoSmithKline),

FLUBLOK®[FluVx4] (Protein Sciences Corporation), and FLUAD®[AdjFluVx]

(Seqirus). Vaccine details are provided in Table 1. These vaccines were administrated via

intratumoral or intramuscular injection (50 µL). To mimic adjuvant MF59® (Novartis),

AddaVax™ (InvivoGen) was administered via intratumoral injection (50 µL). Control

mice were administered PBS at the same volume via the same route. In experiments in

which the adjuvant and vaccine were jointly delivered, 50 µL adjuvant + 50 µL vaccine

were mixed and delivered in a total volume of 100 µL via intratumoral injection. In some

experiments, MF59®, which is primarily composed of squalene, was removed by

centrifugal filtration using Amicon Ultra Centrifugal Filter Units with regenerated

cellulose filters (with a 30 kDa molecular weight cut-off). MF59®-containing AdjFluVx (500 μL) was added to the unit and washed with acetone (250 μL three times) followed by PBS (250 μL three times). The protein component of the vaccine was collected using a pipette, freeze dried, and reconstituted to the original volume using PBS. In the experiment utilizing poly I:C + peptide, 20 μg poly I:C + 0.007 μg of either gp100 peptide (KVPRNQDWL) or OVA peptide (SIINFEKL) was injected intratumorally. Other vaccines tested in the context of 50 μL intratumoral injection were the DTAP vaccine Infanrix, Hepatitis B vaccine Engerix-B, and pneumonia vaccine Pneumovax®23.

Tumor challenge

For tumor challenge experiments, C57BL/6 and NSG mice were anesthetized with isoflurane and administered 100,000-150,000 B16-F10 melanoma cells (ATCC) via intravenous or intradermal injection and BALB/c mice were anesthetized with isoflurane and administered 100,000-150,000 4T1 triple-negative breast cancer cells (ATCC) in the mammary fat pad. B16-F10 and 4T1 cancer cell lines were cultured in DMEM (Gibco), 10% fatal bovine serum (Sigma Aldrich), 100 units/mL penicillin (Gibco), 100 mg/mL streptomycin (Gibco), and 0.29 mg/mL glutamine (Gibco) prior to harvesting for tumor injection. Primary tumor growth was monitored by Vernier caliper measurements in two perpendicular directions serially after tumor challenge. Mice harboring tumors were euthanized when the tutor area reached 20 mm in any direction or met other health-related endpoints, as per institutional IACUC policies. To quantify 4T1 lung metastases, 5% India ink (Fisher Scientific) diluted in distilled water was injected into the trachea after euthanasia. Lungs were dissected and transferred to Fekete's solution [40 mL glacial acetic acid, 32 mL (37%) formalin, 700 mL 100% ethanol, and 228 mL double-distilled

water] and washed 3-4 times in this solution and once in phosphate buffered saline (PBS). 4T1 lung surface metastases (white in appearance) and B16-F10 lung surface foci (black in appearance) were manually counted with the use of a magnifying glass. All experiments were conducted with mice 8-to 12-weeks-old at the initiation of the study and with 5-10 mice in each experimental group, unless noted otherwise.

Depletions, blockades, and adoptive cell transfer

In vivo antibody-mediated depletions and blockades were performed using the following antibodies: αCD20 (BioLegend, clone SA271G2), αCD8 (BioXCell, clone 2.43), αIL-10 (BioXCell, clone JES5-2A5), and αPD-L1 (BioXCell, clone 10F.9G2), or their respective isotype control antibodies. Antibodies were diluted to desired concentrations in InVivoPure pH 6.5 Dilution Buffer (BioXCell) and administered at either 250 μg via intraperitoneal injection or 50 μg via intratumoral injection. In experiments requiring transfer of splenic cells from donor to recipient, spleens were mechanically dissociated through a 70-μm filter and red blood cells were removed using 1 mL of Ack Lysing Buffer (Gibco) per spleen under sterile conditions. Cells were washed and re-suspended in PBS and adoptively transferred to recipient mice via intravenous injection (i.v., retro-orbital sinus) in a total volume of 100 μL.

Tissue processing and flow cytometry

For optimal staining of IL-10, 500 μg of monesin (Sigma-Aldrich) dissolved in dimethyl sulfoxide (DMSO) (Sigma Aldrich) was administered via i.v. injection (retro-orbital sinus) in mice six hours prior to euthanasia and dissection. Resected tumors were mechanically dissociated using a gentleMACS™ Octo Dissociator utilizing program Tumor 01_01 (Miltenyi Biotec) in HBSS, enzymatically digested in HBSS containing 1

mg/mL type IV collagenase from *Clostridium histolyticum* (Sigma-Aldrich) and 40

μg/mL DNAse I from bovine pancreas (Sigma-Aldrich) at 37°C for 30 minutes with

constant rocking, and then mechanically dissociated using Dissociator program Tumor

02_01. Dissociated cells were applied to a 70-μm filter and subsequently washed with

PBS to yield a single-cell suspension. Spleens were mechanically dissociated through a

70-μm filter and red blood cells were removed using 1 mL of Ack Lysing Buffer per

spleen. Cells were washed with PBS prior to staining for flow cytometry. H-2Db gp100

dextramer, KVPRNQDWL (Immudex) or H-2Kb TRP2 dextramer, SVYDFFVWL

(Immudex) were applied to cell pellets at a concentration of 5 μL/tetramer or dextramer

in a total volume of 50 μL PBS for 20 minutes at room temperature to quantify $CD8^+$ T

cell populations that recognize the aforementioned peptides. Extracellular staining was

subsequently performed using antibodies specific to CD3, CD4, CD8, CD11c, CD19,

CD20, CD45, H-2Kb-SIINFEKL (OVA) and MHC-II, purchased from either BioLegend

or eBiosciences/ThermoFisher Scientific, using 1-5 μL/test in a total volume of 100 μL

PBS for 30 minutes at room temperature. The LIVE/DEAD Fixable Aqua Dead Cell

Stain Kit for 450 nm excitation (ThermoFisher Scientific) at 0.25 μL/test was added to

each sample. Cells were washed with PBS before proceeding to intracellular staining

steps. Intracellular staining was performed using the True-Nuclear™ Transcription

Buffer Set (BioLegend), in accordance with the protocol published by the manufacturer.

Antibodies selective for Foxp3 and IL-10 (eBiosciences/ThermoFisher Scientific) were

used at 1-5 μL/test in a total of 100 μL of 1X Perm Buffer (BioLegend). Cells were

washed three times in Perm Buffer and fixed using BD™ Stabilizing Fixative (Becton

Dickinson). Flow cytometry was performed using a BD LSR II cytometer. Analysis of

flow cytometry was performed using Flow Jo (TreeStar). Gating was performed on live

singlet lymphocytes utilizing forward scatter (FSC) and side scatter (SSC) width, height,

and area as well as LIVE/DEAD, as previously described[144].

LEGENDPlex™ analysis

Resected tumor tissue (0.1 g/tumor) was homogenized using the gentleMACS™ Octo

Dissociator RNA_01_01 setting (Miltenyi Biotec) in 1 mL of PBS. Then 12.5 µL of each

homogenate was diluted 2x for use in the LEGENDPlex™ T helper cytokine panel kit

(BioLegend), in accordance with the manufacturer's protocol. Data acquisition was

performed using a BD LSR II flow cytometer. LEGENDPlex™ Data Analysis Software

was used to determine the concentration of cytokines in the tumor homogenates.

Quantitative PCR and NanoString analysis

Dissected tissues (tumors and lungs) were placed in 1mL of TRIzol™ (Invitrogen) and

stored at -80°C until RNA extraction was performed. Subsequently, tissues were

homogenized using Benchmark's BEADBUG™ 6 Microtube Homogenizer. RNA was

isolated using the Qiagen RNeasy Plus Mini Kit. The purity of the resulting RNA was

then measured using a NanoDrop™ spectrophotometer (Thermo Fisher Scientific).

Quantitative reverse transcription polymerase chain reaction (qRT-PCR) for influenza

was performed using the primers 5' CATGGAATGGCTAAAGACAAGACC (forward),

5' CCATTAAGGGCATTTTGGACA (reverse), and the TaqMan® probe FAM-5′

TTTGTGTTCACGCTCACCGTGCCCATAMRA (ThermoFisher Scientific). GAPDH

was used as a housekeeping gene control. qRT-PCR was conducted using a StepOnePlus

Real-Time PCR System (Applied Biosystems). Profiling of transcripts implicated in the

anti-tumor immune response was assessed via the NanoString PanCancer Immune

Profiling Panel using an nCounter Digital Analyzer (NanoString Technologies). Total RNA (100 ng) was used for each sample analyzed. Analysis of NanoString data was performed using nSolver Analysis software.

T cell receptor (TCR) sequencing and analysis

Tumors were frozen at -80ºC upon dissection. Samples were analyzed by Adaptive Biotechnologies utilizing the immunoSEQ®assay, which assesses diversity and clonality of the CDR3 region of the TCR of T cells. Sequences were characterized by utilizing a multiplex PCR strategy followed by Illumina sequencing[145-149]. Data were analyzed using immunoSEQ® Analyzer software and Excel (Microsoft). To determine whether TCR clones within the tumor microenvironment of a control (PBS-injected) tumor are expanded with FluVx treatment (i.e., demonstrate increased clonality/evenness), the mean representation of tumor-associated TCR clones was analyzed. Productive TCR clones were derived from FluVx1-treated and control tumors and compared. TCR clones from control tumors were considered "tumor-associated." Tumor-associated TCR clones represented in at least one control tumor (n) and detected in a greater number of FluVx1-treated tumors (at least n + 1) were further considered. Among these TCR clones, average clonality within control tumors was compared to FluVx1-treated tumors and a graph was generated.

Statistical analyses

Prism versions 6.0 -8.0 (Graph Pad) were used for generation of all graphs and performance of statistical analyses, except for Extended Data Fig. 1 where Numbers (Apple) was used to generate the histograms. Two-tailed student t test (for two groups) or one-way ANOVA with Tukey correction (for more than two groups) was used to

determine statistical significance for data comparisons at a single timepoint. Two-way

ANOVA with Bonferroni (for two groups) or Tukey (for more than two groups)

correction was used to determine statistical significance for data comparisons of tumor

growth curves with multiple timepoints. For survival experiments, Kaplan-Meier curves

were generated, and the Mantel-Cox log rank test was performed to determine statistical

significance across treatment groups. Kruskal-Wallis with Dunn's Multiple Comparisons

test was performed for focused comparisons of one group to all other groups at a single

timepoint. Statistical significance is denoted as $*P < 0.05$, $**P < 0.01$, and $***P < 0.001$.

Comparisons with significance at $P < 0.001$ or $P < 0.0001$ are listed as $***P < 0.001$.

REFERENCES

1. Zhang H and Chen J (2018) Current status and future directions of cancer immunotherapy. *Journal of Cancer* 9(10): 1773-1781.
2. Kaufman HL, Kohlhapp FJ, and Zloza A (2015) Oncolytic viruses: a new class of immunotherapy drugs. *Nature Reviews Drug Discovery* 14(9): 642-62.
3. Archard C, *et al*. (2018) Lighting a Fire in the Tumor Microenvironment Using Oncolytic Immunotherapy. *EBioMedicine* 32; 17-24.
4. Galon J and Bruni D (2019) Approaches to treat immune hot, altered and cold tumours with combination immunotherapies. *Nature Reviews Drug Discovery* 18(3): 197-218.
5. Binnewies M, *et al*. (2018) Understanding the tumor immune microenvironment (TIME) for effective therapy. *Nature Medicine* 24(5): 541-550.
6. Cristescu R, *et al*. (2018) Pan-tumor genomic biomarkers for PD-1 checkpoint blockade-based immunotherapy. *Science* 362(6411).
7. Gajewski TF, *et al*. (2017) Cancer Immunotherapy Targets Based on Understanding the T Cell-Inflamed Versus Non-T Cell-Inflamed Tumor Microenvironment. *Advances in experimental medicine and biology* 1036:19-31.
8. Ayers M, *et al*. (2017) IFN-gamma-related mRNA profile predicts clinical response to PD-1 blockade. *The Journal of Clinical Investigation* 127(8): 2930-2940.
9. Martínez-Lostao L, Anel A, & Pardo J (2015) How Do Cytotoxic Lymphocytes Kill Cancer Cells? *Clinical Cancer Research* 21(22): 5047-5056.
10. Sharpe A (2017) Introduction to Checkpoint Inhibitors and Cancer Immunotherapy *Immunology Reviews* 276(1): 5-8.
11. Wilkinson RW and Leishman AJ (2018) Further Advances in Cancer Immunotherapy: Going Beyond Checkpoint Blockade. *Frontiers in immunology* 9:1082-1082.
12. Newman JH and Zloza A (2017) Infection: a Cause of and Cure for Cancer. *Current Pharmacology Reports* 3(6): 315-320.
13. Jessy T (2011) Immunity over inability: The spontaneous regression of cancer. *Journal of Natural Science, Biology and Medicine* 2(1): 43-49.
14. Kucerova P and Cervinkova M (2016) Spontaneous regression of tumour and the role of microbial infection—possibilities for cancer treatment. *Anticancer Drugs* 27(4): 269-277.
15. Ebbell B (1937) The Papyrus Ebers: the greatest Egyptian medical document. Levin and Munksgaard
16. Coley WB (1891) Contribution to the Knowledge of Sarcoma. *Annals of Surgery* 14(3): 199-220.
17. Coley WB (1894) Treatment of Inoperable Malignant Tumors with Toxines of Erysipelas and the Bacillus Prodigiosis. *The American Journal of the Medical Sciences* 108,1.
18. Orange M, Reuter U and Hobohm U (2016) Coley's Lessons Remembered. *Integrative Cancer Therapies* 15(4): 502-511.
19. Rous P (1911) A sarcoma of the fowl transmissible by an agent separable from the tumor cells. *Journal of Experimental Medicine* 13(4):397–411.

20. Javier RT and Butel JS (2008) The history of tumor virology. *Cancer Research* 68(19):7693–7706.
21. Temin HM and Rubin H (1958) Characteristics of an assay for Rous sarcoma virus and Rous sarcoma cells in tissue culture. *Virology* 1958;6(3):669–688.
22. Baltimore D (1970) Viral RNA-dependent DNA polymerase: RNA-dependent DNA polymerase in virions of RNA tumour viruses. *Nature* 226:1209–1211.
23. Temin HM and Mizutani S (1970) Viral RNA-dependent DNA polymerase: RNA-dependent DNA polymerase in virions of Rous sarcoma virus. *Nature* 226:1211–1213.
24. Donehower LA and Varmus HE (1984) A mutant murine leukemia virus with a single missense codon in pol is defective in a function affecting integration. *Proceedings of the National Academy of Sciences* 81(20): 6461–6465.
25. Stehelin D, Varmus HE, Bishop JM, and Vogt PK (1976) DNA related to the transforming gene(s) of avian sarcoma viruses is present in normal avian DNA. *Nature* 260:170–173.
26. Martin GS (2004) The road to Src. *Oncogene* 23:7910–7917.
27. Lodish H *et al.* (2000) Molecular cell biology. 4th ed. New York: W. H. Freeman.
28. Karidis NP, Delladetsima I, and Theocharis S (2015) Hepatocyte turnover in chronic HCV-induced liver injury and cirrhosis. *Gastroenterology Research and Practice* 2015:654105.
29. Bartosch B (2010) Hepatitis B and C viruses and hepatocellular carcinoma *Viruses* 2(8): 1504–1509.
30. El-Serag HB (2012) Epidemiology of viral hepatitis and hepatocellular carcinoma. *Gastroenterology* 142(6): 1264–1273.
31. Schmidt-Arras D and Rose-John S (2016) IL-6 pathway in the liver: from physiopathology to therapy. *Journal of Hepatology* 64(6): 1403–1415.
32. Wong VW *et al.* (2009) High serum interleukin-6 level predicts future hepatocellular carcinoma development in patients with chronic hepatitis B. *International Journal of Cancer* 124(12):2766–2770.
33. Benn J, Su F, Doria M, and Schneider RJ (1996) Hepatitis B virus HBx protein induces transcription factor AP-1 by activation of extracellular signal-regulated and c-Jun N-terminal mitogen-activated protein kinases. *Journal of Virology* 70(8): 4978–4985.
34. Freeman HJ (2008) Colorectal cancer risk in Crohn's disease. *World Journal of Gastroenterology* 14(12):1810–1811.
35. Wroblewski LE, Peek RM, Jr, and Wilson KT (2010) Helicobacter pylori and gastric cancer: factors that modulate disease risk. *Clinical Microbiology Reviews* 23(4):713–739.
36. Saha A and Robertson ES (2011) Epstein-Barr virus-associated B-cell lymphomas: pathogenesis and clinical outcomes. *Clinical Cancer Research* 17(10): 3056–3063.
37. Shuda M *et al.* (2015) Merkel cell polyomavirus small T antigen induces cancer and embryonic Merkel cell proliferation in a transgenic mouse model. *PLoS One* 10(11): e0142329.
38. Dahl J, You J and Benjamin TL (2005) Induction and utilization of an ATM signaling pathway by polyomavirus. *Journal of Virology* 79(20): 13007–13017.

39. Zheng Z and Baker CC (2006) Papillomavirus genome structure, expression, and post-transcriptional regulation. *Frontiers in Bioscience* 11:2286–2302.
40. Howie HL, Katzenellenbogen RA and Galloway DA (2009) Papillomavirus E6 proteins. *Virology* 384(2): 324–334.
41. Rubinstein PG, Aboulafia DM and Zloza A (2014) Malignancies in HIV/AIDS: from epidemiology to therapeutic challenges. *AIDS* 28(4): 453–465.
42. Corthay A (2014) Does the immune system naturally protect against cancer? *Frontiers in Immunology* 10.3389/fimmu.2014.00197.
43. Kohlhapp FJ and Kaufman HL (2016) Molecular pathways: mechanism of action for talimogene laherparepvec, a new oncolytic virus immunotherapy. *Clinical Cancer Research* 22(5): 1048–1054.
44. "FDA approves first-of-its-kind product for the treatment of melanoma." U.S. Food & Drug Administration; October 2015. Accessed 14 Jun 2017.
45. Rehman H, Silk AW, Kane MP and Kaufman HL (2016) Into the clinic: talimogene laherparepvec (T-VEC), a first-in-class intratumoral oncolytic viral therapy. *Journal of Immunotherapy for Cancer* 4:53.
46. Tomazin R, Hill AB, Jugovic P, York I, van Endert P, Ploegh HL, Andrews DW, and Johnson DC (1996) Stable binding of the herpes simplex virus ICP47 protein to the peptide binding site of TAP. *EMBO Journal* 15(13): 3256-3266.
47. Andtbacka RH *et al.* (2015) Talimogene laherparepvec improves durable response rate in patients with advanced melanoma. *Journal of Clinical Oncology* 33(25): 2780–2788.
48. Chiocca EA and Rabkin SD (2014) Oncolytic viruses and their application to cancer immunotherapy. *Cancer Immunology Research* 2(4): 295–300.
49. Malhotra A, Sendilnathan A, Old MO and Wise-Draper TM (2015) Oncolytic virotherapy for head and neck cancer: current research and future developments. *Oncolytic Virotherapy* 4:83–93.
50. Andtbacka RHI *et al*. (2015) Final data from CALM: a phase II study of Coxsackievirus A21 (CVA21) oncolytic virus immunotherapy in patients with advanced melanoma. Journal of Clinical Oncology. 33:9030.
51. Holl EK *et al*. (2016) Recombinant oncolytic poliovirus, PVSRIPO, has potent cytotoxic and innate inflammatory effects, mediating therapy in human breast and prostate cancer xenograft models. *Oncotarget* 7(48): 79828–79841.
52. Wollmann G, Ozduman K and van den Pol AN (2012) Oncolytic virus therapy of glioblastoma multiforme—concepts and candidates. *Cancer Journal* 18(1):69–81.
53. Jhawar SR, *et al.* (2017) Oncolytic Viruses—Natural and Genetically Engineered Cancer Immunotherapies. *Frontiers in Oncology* 7:202.
54. Hamid O, Hoffner B, Gasal E, Hong J and Carvajal RD (2017) Oncolytic immunotherapy: unlocking the potential of viruses to help target cancer. *Cancer Immunology Immunotherapy* 10.1007/s00262-017-2025-8.
55. Fukuhara H, Ino Y, and Todo T (2016) Oncolytic virus therapy: A new era of cancer treatment at dawn. *Cancer Science* 107(10): 1373-1379.
56. Iheagwara UK *et al.* (2014) Influenza virus infection elicits protective antibodies and T cells specific for host cell antigens also expressed as tumor-associated antigens: a new view of cancer immunosurveillance. *Cancer Immunology Research* 2(3): 263-273.

57. Kohler M Ruttner B, Cooper S, Hengartner H, & Zinkernagel RM (1990) Enhanced tumor susceptibility of immunocompetent mice infected with lymphocytic choriomeningitis virus. *Cancer Immunology, Immunotherapy*: CII32 (2): 117-124.

58. Bevers RFM, Kurth K-H and Schamhart DHJ (2004) Role of urothelial cells in BCG immunotherapy for superficial bladder cancer. *British Journal of Cancer* 91(4): 607-612.

59. Ibarra C, *et al.* (2019) BCG-induced cytokine release in bladder cancer cells is regulated by Ca^{2+} signaling. *Molecular Oncology* 13(2): 202-211.

60. Pichler R, *et al.* (2016) Tumor-infiltrating immune cell subpopulations influence the oncologic outcome after intravesical Bacillus Calmette-Guérin therapy in bladder cancer. *Oncotarget* 7(26): 39916-39930.

61. Sevilla N, Kunz S, McGavern D, and Oldstone MBA (2003) Infection of Dendritic Cells by Lymphocytic Choriomeningitis Virus. *Current Topics in Microbiology and Immunology* 276: 125-144.

62. de Charette M, Marabelle A, and Houot R (2016) Turning tumour cells into antigen presenting cells: The next step to improve cancer immunotherapy? *European Journal of Cancer* 68: 134-147.

63. Cassady KA *et al.* (2016) To Infection and Beyond: The Multi-Pronged Anti-Cancer Mechanisms of Oncolytic Viruses. *Viruses* 8(2): 43.

64. Kohlhapp FJ, *et al.* (2016) Non-oncogenic Acute Viral Infections Disrupt Anti-cancer Responses and Lead to Accelerated Cancer-Specific Host Death. *Cell Reports* 17(4): 957-965.

65. Lechner MG, *et al.* (2013) Immunogenicity of murine solid tumor models as a defining feature of in vivo behavior and response to immunotherapy. *Journal of Immunotherapy.* 36(9): 477-489.

66. Pan D, *et al.* (2018) A major chromatin regulator determines resistance of tumor cells to T cell–mediated killing. *Science.* 359(6377): 770-775.

67. Radigan KA, Misharin AV, Chi M, and Scott Budinger GR (2015) Modeling human influenza infection in the laboratory. *Infection and Drug Resistance.* 8: 311-320.

68. Apalla Z *et al.* (2017) Epidemiological trends in skin cancer. *Dermatology Practical and Conceptual* 7(2): 1-6.

69. Fiege JK and Langlois RA (2015) Investigating Influenza A Virus Infection: Tools To Track Infection and Limit Tropism. *Journal of Virology* 89(12): 6167-6170.

70. Smed-Sorensen A, *et al.* (2012) Influenza A virus infection of human primary dendritic cells impairs their ability to cross-present antigen to CD8 T cells. *PLoS Pathogens* 8(3): e1002572.

71. Thomas C, King DJ, and Swayne DE (2008) Thermal inactivation of avian influenza and Newcastle disease viruses in chicken meat. *Journal of Food Protection* 71: 1214-1222.

72. Jonges M, *et al.* (2010) Influenza Virus Inactivation for Studies of Antigenicity and Phenotypic Neuraminidase Inhibitor Resistance Profiling. *Journal of Clinical Microbiology* 48(3): 928-940.

73. Fu C and Jiang A (2018) Dendritic Cells and CD8 T Cell Immunity in the Tumor Microenvironment. *Frontiers in Immunology* 9: 3059.
74. Hildner K, *et al.* (2008) Batf3 deficiency reveals a critical role for CD8alpha+ dendritic cells in cytotoxic T cell immunity. *Science* 322(5904): 1097-1100.
75. Dai P, *et al.* (2017) Intratumoral delivery of inactivated modified vaccinia virus Ankara (iMVA) induces systemic antitumor immunity via STING and Batf3-dependent dendritic cells. *Science Immunology* 2(11).
76. Seyfried TN and Huysentruyt (2013) On the Origin of Cancer Metastasis. *Critical Reviews in Oncogenesis* 18(1-2): 43-73.
77. Aznar MA *et al.* (2017) Intratumoral Delivery of Immunotherapy- Act Locally, Think Globally. *Journal of Immunology* 198(1): 31-39.
78. Dagoglu N, Karaman S, Caglar HB and Oral EN (2019) Abscopal Effect of Radiotherapy in the Immunotherapy Era: Systematic Review of Reported Cases. *Cureus* 11(2): e4103.
79. Zhang H, Hyrien O, Pandya KJ, Keng PC and Chen Y (2008) Tumor response kinetics after schedule-dependent paclitaxel chemoradiation treatment for inoperable non-small cell lung cancer: a model for low-dose chemotherapy radiosensitization. *Journal of Thoracic Oncology* 3(6): 563-8.
80. Onyshchenko M (2018) The Puzzle of Predicting Response to Immune Checkpoint Blockade. *EBioMedicine* 33: 18-19.
81. Hu-Lieskovan S and Ribas A (2017) New Combination Strategies Using Programmed Cell Death 1/Programmed Cell Death Ligand 1 Checkpoint Inhibitors as a Backbone. *Cancer Journal* 23(1): 10-22.
82. Trombetta CM, Gianchecchi E, and Montomoli E (2018) Influenza vaccines: Evaluation of safety profile. *Human Vaccines and Immunotherapeutics* 14(3): 657-670.
83. Sridhar S, Brokstad KA, and Cox RJ (2015) Influenza Vaccination Strategies: Comparing Inactivated and Live Attenuated Influenza Vaccines. *Vaccines (Basel)* 3(2): 373-389.
84. Influenza vaccines—United States, 2018-19 influenza season (2019). *Centers for Disease Control and Prevention* https://www.cdc.gov/flu/professionals/vaccines.htm#anchor-star. Accessed 28 Jun 2019.
85. FDA Package Insert- Fluvirin (2017). *Seqirus Inc.* https://www.fda.gov/media/75156/download. Accessed 28 Jun 2019.
86. Rondy M, *et al.* (2018) Interim 2017/18 influenza seasonal vaccine effectiveness: combined results from five European studies. *Eurosurveillance* 23(9): 18-00086.
87. Shultz LD, *et al.* (2005) Human lymphoid and myeloid cell development in NOD/LtSz-scid IL2R gamma null mice engrafted with mobilized human hemopoietic stem cells. *Journal of Immunology* 174(10): 6477-89.
88. Tumeh PC, *et al.* (2014) PD-1 blockade induces responses by inhibiting adaptive immune resistance. *Nature* 515(7528): 568-571.
89. Cesano A (2015) nCounter® PanCancer Immune Profiling Panel (NanoString Technologies, Inc., Seattle, WA). *Journal for ImmunoTherapy of Cancer* 3:42.

90. Oliveira CC *et al.* (2010) The nonpolymorphic MHC Qa-1b mediates CD8+ T cell surveillance of antigen-processing defects. *Journal of Experimental Medicine* 207(1): 207-221.

91. Turner TB *et al.* (2017) Epigenetic modifiers upregulate MHC II and impede ovarian cancer tumor growth. *Oncotarget* 8: 44159-44170.

92. Ferrington DA and Gregerson DS (2012) Immunoproteasomes: Structure, Function, and Antigen Presentation. *Progress in Molecular Biology and Translational Science* 109: 75-112.

93. Araujo JM *et al.* (2018) Effect of CCL5 expression in the recruitment of immune cells in triple negative breast cancer. *Scientific Reports* 8: 4899.

94. Heesch K *et al.* (2014) The function of the chemokine receptor CXCR6 in the T cell response of mice against Listeria monocytogenes. *PLoS One* 9(5): e97701.

95. Ding Q *et al.* (2016) CXCL9: evidence and contradictions for its role in tumor progression. *Cancer Medicine* 5(11): 3246-3259.

96. Song Y *et al.* (2019) Chemerin partly mediates tumor-inhibitory effect of all-trans retinoic acid via CMKLR1-dependent natural killer cell recruitment. *Immunology* 157(3): 248-256.

97. Song DG *et al.* (2012) CD27 costimulation augments the survival and antitumor activity of redirected human T cells in vivo. *Blood* 119(3): 696-706.

98. Cole DK *et al*. (2012) The molecular determinants of CD8 co-receptor function. *Immunology* 137(2): 139-148.

99. Quigley M, Huang X, and Yang Y (2008) STAT1 signaling in CD8 T cells is required for their clonal expansion and memory formation following viral infection in vivo. *Journal of Immunology* 180(4): 2158-64.

100. Marin-Acevedo JA *et al.* (2018) Next generation of immune checkpoint therapy in cancer: new developments and challenges. *Journal of Hematology and Oncology* 11:39.

101. Kumar A, Zhang J and Yu FX (2006) Toll-like receptor 3 agonist poly(I:C)-induced antiviral response in human corneal epithelial cells. *Immunology* 117(1): 11-21.

102. Tsai TF (2013) Fluad(R)-MF59(R)-Adjuvanted Influenza Vaccine in Older Adults. *Infection & chemotherapy* 45(2): 159-174.

103. Tegenge MA, *et al*. (2016) Pharmacokinetics and biodistribution of squalene-containing emulsion adjuvant following intramuscular injection of H5N1 influenza vaccine in mice. *Regulatory toxicology and pharmacology*: RTP81: 113-119.

104. Goff PH, *et al*. (2013) Adjuvants and immunization strategies to induce influenza virus hemagglutinin stalk antibodies. *PloS one* 8(11): e79194.

105. Sasaki E, *et al*. (2018) Modeling for influenza vaccines and adjuvants profile for safety prediction system using gene expression profiling and statistical tools. *PloS one* 13(2): e0191896.

106. Yuen GJ, Demissie E and Pillai S (2016) B lymphocytes and cancer: a love-hate relationship. *Trends Cancer* 2(12): 747-757.

107. Ng, THS *et al.* (2013) Regulation of Adaptive Immunity; The Role of Interleukin-10. *Frontiers in Immunology* 4:129.

108.   Maynard CL and Weaver CT (2008) Diversity in the contribution of IL-10 to T-cell-mediated immune regulation. *Immunology Reviews* 226: 219-233.

109.   Shouval DS, *et al.* (2014) Interleukin 10 Receptor Signaling: Master Regulator of Intestinal Mucosal Homeostasis in Mice and Humans. *Advances in Immunology* 122: 177-210.

110.   Fisher DT, Appenheimer MM and Evans SS (2014) The two faces of IL-6 in the tumor microenvironment. *Seminars in Immunology* 26(1): 38-47.

111.   Lee JE*, et al.* (2019) The Role of Interleukin-9 in Cancer. *Pathology Oncology Research* doi: 10.1007/s12253-019-00665-6.

112.   Dai P, *et al.* (2017) Intratumoral delivery of inactivated modified vaccinia virus Ankara (iMVA) induces systemic antitumor immunity via STING and Batf3-dependent dendritic cells. *Science Immunology* 2(11).

113.   Zajac AJ, *et al.* (1998) Viral Immune Evasion Due to Persistence of Activated T Cells Without Effector Function. *Journal of Experimental Medicine* 188(12): 2205-2213.

114.   Ariza-Heredia EJ, and Chemaly RF (2015) Practical review of immunizations in adult patients with cancer. *Human Vaccines and Immunotherapeutics* 11(11): 2606-2614.

115.   Iwasaki A and Pillai PS (2014) Innate immunity to influenza virus infection. *Nature Reviews Immunology* 14(5): 315-28.

116.   Fujinami *et al.* (1983) Molecular mimicry in virus infection: Crossreaction of measles virus phosphoprotein or of herpes simplex virus protein with human intermediate filaments. *Proceedings of the National Academy of Sciences* 80: 2346-2350.

117.   Snyder A, *et al.* (2014) Genetic basis for clinical response to CTLA-4 blockade in melanoma. *The New England Journal of Medicine* 371(23): 2189-2199.

118.   Rosato PC, *et al.* (2019) Virus-specific memory T cells populate tumors and can be repurposed for tumor immunotherapy. *Nature Communications* 10(1): 567.

119.   Simoni Y, *et al.* (2018) Bystander CD8(+) T cells are abundant and phenotypically distinct in human tumour infiltrates. *Nature* 557(7706): 575-579.

120.   Kvistborg P, *et al.* (2012) TIL therapy broadens the tumor-reactive CD8(+) T cell compartment in melanoma patients. *Oncoimmunology* 1(4): 409-418.

121.   Andersen RS, *et al.* (2012) Dissection of T-cell antigen specificity in human melanoma. *Cancer Research* 72(7): 1642-1650.

122.   Erkes DA, *et al.* (2017) Virus-Specific CD8(+) T Cells Infiltrate Melanoma Lesions and Retain Function Independently of PD-1 Expression. *Journal of Immunology* 198(7): 2979-2988.

123.   Khurana S, *et al.* (2011) MF59 adjuvant enhances diversity and affinity of antibody-mediated immune response to pandemic influenza vaccines. *Science Translational Medicine* 3(85): 85ra48.

124.   White MC, *et al.* (2014) Age and Cancer Risk. *American Journal of Preventive Medicine* 46(301): S7-15.

125. 　　　Lofano G, *et al.* (2015) Oil-in-Water Emulsion MF59 Increases Germinal Center B Cell Differentiation and Persistence in Response to Vaccination. *Journal of Immunology* 195(4): 1617-1627.

126. 　　　Dai Y, Zhong J and Xu J (2017) Regulatory B cells in infectious disease. *Molecular Medicine Reports* 16(1): 3-10.

127. 　　　Wilkinson K, *et al.* (2017) Efficacy and safety of high-dose influenza vaccine in elderly adults: A systematic review and meta-analysis. *Vaccine* 35(21): 2775-2780.

128. 　　　Shayan G, *et al.* (2018) Phase Ib Study of Immune Biomarker Modulation with Neoadjuvant Cetuximab and TLR8 Stimulation in Head and Neck Cancer to Overcome Suppressive Myeloid Signals. *Clinical Cancer Research* 24(1): 62-72.

129. 　　　Xagorari A and Chlichlia K (2008) Toll-Like Receptors and Viruses: Induction of Innate Antiviral Immune Responses. *The Open Microbiology Journal* 2: 49-59.

130. 　　　Farhood B, Najafi M and Mortezaee K (2019) CD8+ cytotoxic T lymphocytes in cancer immunotherapy: A review. *Journal of Cellular Physiology* 234(6): 8509-8521.

131. 　　　Young-Xu Y, van Aalst R, Russo E, Lee JKH, & Chit A (2017) The Annual Burden of Seasonal Influenza in the US Veterans Affairs Population. *PloS one* 12(1): e0169344-e0169344.

132. 　　　Estimates of Influenza Vaccination Coverage Among Adults—United States, 2017-18 Flu Season. October 25, 2018. *Centers for Disease Control and Prevention.* https://www.cdc.gov/flu/fluvaxview/coverage-1718estimates.htm. Accessed 29 Jun 2019.

133. 　　　Murphy JR. Corynebacterium Diphtheriae. In: Baron S, editor. Medical Microbiology. 4th edition. Galveston (TX): University of Texas Medical Branch at Galveston; 1996. Chapter 32. Available from: https://www.ncbi.nlm.nih.gov/books/NBK7971/

134. 　　　Hanif H, *et al.* (2015) Isolation and Antibiogram of Clostridium tetani from Clinically Diagnosed Tetanus Patients. *American Journal of Tropical Medicine and Hygiene* 93(4): 752-756.

135. 　　　Kawai T and Akira S (2006) TLR signaling. *Cell Death and Differentiation* 13(5): 816-25.

136. 　　　Budhwani M, Mazzieri R, and Dolcetti R (2018) Plasticity of Type I Interferon-Mediated Responses in Cancer Therapy: From Anti-tumor Immunity to Resistance. *Frontiers in Oncology* 8:322.

137. 　　　Liang JL, *et al.* (2018) Prevention of Pertussis, Tetanus, and Diphtheria with Vaccines in the United States: Recommendations of the Advisory Committee on Immunization Practices (ACIP). *MMWR Recommendations and Reports* 67(2): 1-44.

138. 　　　Finger H, von Koenig CHW. Bordetella. In: Baron S, editor. Medical Microbiology. 4th edition. Galveston (TX): University of Texas Medical Branch at Galveston; 1996. Chapter 31. Available from: https://www.ncbi.nlm.nih.gov/books/NBK7813/

139. 　　　Terhune TD and Deth RC (2018) Aluminum Adjuvant-Containing Vaccines in the Context of the Hygiene Hypothesis: A Risk Factor for

Eosinophilia and Allergy in a Genetically Susceptible Subpopulation? *International Journal of Environmental Research and Public Health* 15(5).

140.　　Awate S, Babiuk LA, and Mutwiri G (2013) Mechanisms of Action of Adjuvants. *Frontiers in Immunology* 4:114.

141.　　Petersen TR, Dickgreber N and Hermans IF (2010) Tumor antigen presentation by dendritic cells. *Critical reviews in immunology* 30(4): 345-86.

142.　　Rutigliano JA, *et al.* (2014) Highly pathological influenza A virus infection is associated with augmented expression of PD-1 by functionally compromised virus-specific CD8$^+$ T cells. *Journal of Virology* 88(3): 1636-1651.

143.　　Jenkins MR, Webby R, Doherty PC, & Turner SJ (2006) Addition of a prominent epitope affects influenza A virus-specific CD8$^+$ T cell immunodominance hierarchies when antigen is limiting. *Journal of Immunology* 177(5): 2917-2925.

144.　　Zloza A, *et al.* (2012) NKG2D signaling on CD8(+) T cells represses T-bet and rescues CD4-unhelped CD8(+) T cell memory recall but not effector responses. *Nature Medicine* 18(3): 422-428.

145.　　Carlson CS, *et al.* (2013) Using synthetic templates to design an unbiased multiplex PCR assay. *Nature Communications* 4: 2680.

146.　　Robins HS, *et al.* (2009) Comprehensive assessment of T-cell receptor beta-chain diversity in alphabeta T cells. *Blood* 114(19): 4099-4107.

147.　　Yousfi Monod M, Giudicelli V, Chaume D, & Lefranc MP (2004) IMGT/JunctionAnalysis: the first tool for the analysis of the immunoglobulin and T cell receptor complex V-J and V-D-J JUNCTIONs. *Bioinformatics* 20 Suppl 1:i379-385.

148.　　Emerson RO, *et al.* (2013) High-throughput sequencing of T-cell receptors reveals a homogeneous repertoire of tumour-infiltrating lymphocytes in ovarian cancer. *The Journal of Pathology* 231(4): 433-440.

149.　　Wu D, *et al.* (2012) High-throughput sequencing detects minimal residual disease in acute T lymphoblastic leukemia. *Science Translational Medicine* 4(134): 134ra163.

ADDENDUM

[This addendum was directly obtained from Newman JH *et al.* (2018) Novel bone morphogenetic protein receptor inhibitor JL5 suppresses tumor cell survival signaling and induces regression of human lung cancer *Oncogene* 37: 3672-3685.]

INTRODUCTION

An estimated 170,000 people this year in the U.S. will die from lung cancer. More people will die from lung cancer then prostate, colon, breast, and kidney cancer combined. Despite advances in targeted therapy 85% of patients diagnosed with lung cancer will succumb to the disease. It is clear that better treatment options are needed for the treatment of lung cancers.

Bone morphogenetic proteins (BMPs) are members of the transforming growth factor beta (TGFβ) superfamily that are phytogenetically conserved morphogens required for embryonic development across species from insects to humans[1,2]. BMP2 and BMP4 regulate a plethora of activities during embryogenesis, including the development of the lung. Following the development of the lungs there is little expression of BMP signaling in normal adult lung tissue[1]. The BMP signaling cascade is reactivated in lung cancer and inflammation[1,3]. Studies have reported that the bone morphogenetic signaling cascade has a significant role in promoting tumorigenesis in lung and other cancers. The BMP2 ligand is overexpressed in 98% of non-small cell lung cancers but not in benign lung tumors[4]. BMP signaling is reported to enhance tumorigenesis in many other cancers including prostate[5], breast[6,7], pancreas[8], melanoma[9], and sarcoma[10]. Aberrant BMP signaling has been reported to enhance cell migration, invasion, metastasis, proliferation, and angiogenesis, and is associated with a worse prognosis[3, 11-14].

There are ~20 BMP ligands that signal through transmembrane serine/threonine kinases composed of type I and type II receptors. The type I receptors are ALK2 (ActR-1), ALK3 (BMPR-IA), and ALK6 (BMPR-IB)[15] and the type II receptors are BMPR-II and activin type II receptors ActR-II and AcR-IIB[15]. There are different affinities of the BMP ligands to each type I receptors[15]. Ligand binding to the type I receptor leads to phosphorylation by the constitutively active type II receptor. The BMPRI/BMPRII receptor complex phosphorylates Smad-1/5[16], which then translocates to the nucleus leading to the transcription activation of downstream target genes including inhibitor of differentiation proteins (Id1, Id2, and Id3)[17-21].

Recently, we reported that the BMP signaling cascade regulates several antiapoptotic proteins in lung cancer cells through evolutionarily conserved signaling pathways, which include X-linked inhibitor of apoptosis protein (XIAP), TGFβ activated kinase 1 (TAK1), and inhibitor of differentiation proteins (Id1-Id3)[22]. During embryonic development, XIAP binds to the BMP type I and type II receptors preventing its ubiquitination and subsequent degradation via proteasomes, thus increasing its expression[23]. XIAP binds to TAB1, leading to the activation of TAK1[24]. XIAP is the most potent of the inhibitor of apoptosis proteins and is the only antiapoptotic protein that inactivates caspases[25]. XIAP binds and inactivates effector caspase-3 and caspase-7 and initiator caspase-9[26]. XIAP has been shown to block apoptosis induced by many pro-apoptotic agents. TAK1 also potently inhibits apoptotic cell death through the activation of NF-kappa B (NF-κB)[27] and prevention of reactive oxygen species (ROS) production[28]. NF-κB inhibition of apoptotic cell death involves the induction of cellular FLICE-like

protein (c-FLIP), XIAP, cellular inhibitor of apoptosis protein 1 (c-IAP-1), and c-IAP-2 [27].

Dorsomorphin was identified in a zebrafish library screen to be a small molecule inhibitor of the BMP receptors[29]. Several generations of BMP inhibitors have been synthesized based on substitutions to this pyrazolo[1,5-*a*]pyrimidine core with varying affinities to the kinase domain of the BMP type I and type II receptors[30,31]. The BMP analog, DMH1 has been shown in tumors in mice to suppress metastatic growth without tumor regression or downregulation of Id1, TAK1, or XIAP[7,32]. Our in vitro studies showed that the BMP analog DMH2 is significantly more potent in downregulating XIAP, pTAK1, and Id1 expression and inducing death of lung cancer cells than LDN-193189 and DMH1[22]. However, DMH2 does not downregulate XIAP, ID1, or pTAK1 in tumor xenografts, likely because of its poor pharmacokinetic profile in mice[22]. The development of stable BMP inhibitors that have potent inhibition of BMP-regulated antiapoptotic proteins Id1, pTAK1, and/or XIAP in tumor xenografts is needed to better evaluate the role of BMP inhibitors as a cancer therapeutic. The BMP signaling pathway is also known to regulate the activation and development of dendritic cells[33], T cells[34], and natural killer cells[35]. However, the effects of BMP inhibitors on immune cells within the tumor microenvironment are not known. Since BMP signaling regulates immune cells it essential to understand how BMP inhibitors affect the immune cells within the tumor microenvironment and to determine whether BMP inhibition in the context of an immune system enhances or attenuates tumor growth.

In our study, genetic profiling indicates that mutations that could cause resistance to a BMP receptor inhibitor are infrequent in non-small cell lung cancer (NSCLC). We

have identified the chemical instability of DMH2 and designed a compound, JL5, to circumvent the chemical hydrolysis of the morpholine side-chain. JL5 inhibits BMP type I and type II receptors at similar concentrations, induces in vitro cancer cell death, and downregulates Id1, XIAP, and pTAK1 with similar potency as DMH2. Importantly, JL5 is more metabolically stable than DMH2, and downregulates Id1 and pTAK1 and induces tumor regression in lung tumor xenografts. JL5 demonstrates a positive effect on immune cells within the tumor microenvironment by increasing immune cell infiltration within the tumor. JL5 maintains suppression of tumor growth even in the presence of adoptively transferred immune cells. These data demonstrate that BMP signaling is targetable in NSCLC and propose that targeted suppression of BMP receptors can be developed as a therapeutic drug to treat lung and other cancers.

RESULTS

BMP ligands are frequently overexpressed in NSCLC

In a prior study, we have shown that BMP2 protein is highly overexpressed in 98% of lung cancers (independent of cell type) with little expression in normal lung tissue[4]. However, genetic alteration could cause resistance to a target-specific therapeutic, by alterations that inactivate the signaling pathway, mutations of the receptor that affect its interaction with the small molecule, and amplifications of essential downstream signaling events. Therefore, to determine whether the BMP signaling cascade is a targetable pathway (i.e., it exhibits low mutation frequency), we queried The Cancer Genome Atlas (TCGA) to examine the genetic alterations effecting BMP ligands, receptors, transcription factors, and downstream targets in NSCLC. Only 2 of the 117 lung

adenocarcinomas had a deep deletion, missense mutation, or truncating mutation of the BMP2 ligand (Fig. 1A). Sixty-eight percent of lung adenocarcinomas had upregulation of mRNA and 26% had amplification of one or more BMP ligands (Fig. 1A).

Genetic alterations of the BMP signaling cascade are infrequent in NSCLC

Deep deletions, truncating mutations, or missense mutations were present in 8 (6%) of the BMP type I and 4 (3%) of the BMP type II receptors among 135 lung adenocarcinomas examined (Fig. 1B). None of the tumors had mutations in all three of the type I or type II receptors (Fig. 1B) Mutations of Smad-1/5/9 were also infrequent (5%) and never occurred in all three transcription factors (Fig. 1B). Amplification of the downstream BMP targets XIAP, TAK1, and Id1 has the potential to cause resistance to a BMP inhibitor if it upregulates expression. Amplification of XIAP occurred in 0.7%, of TAK1/MAP3K7 in 0%, of Id1 in 6%, of Id2 in 0%, and of Id3 in 2% of lung adenocarcinomas (Fig. 1B).
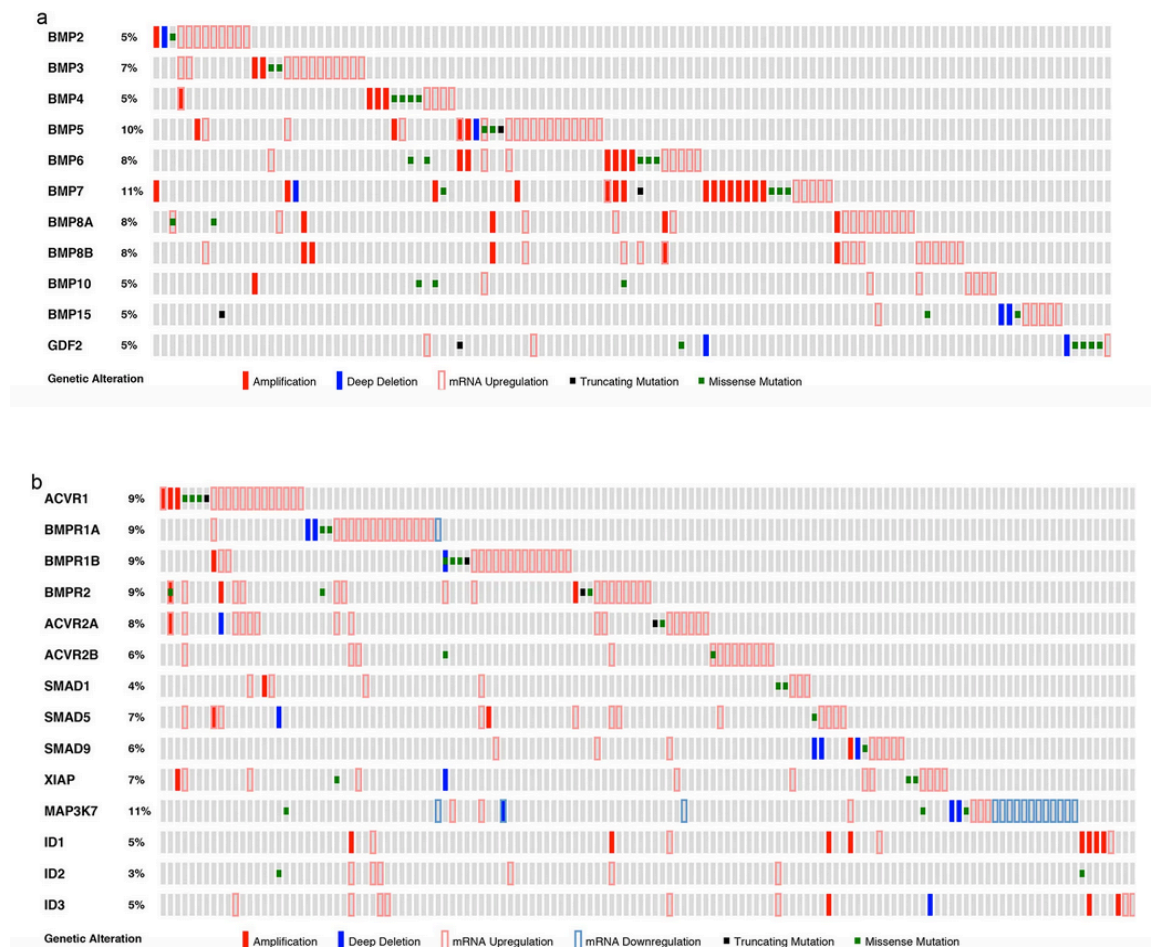
Fig. 1 Genetic alterations of the BMP signaling cascade are infrequent in lung adenocarcinomas. (A) The TCGA database was queried for DNA amplifications, deep deletions, truncating mutations, missense mutations, and mRNA expression of BMP ligands in lung adenocarcinomas (n = 117) and (B) BMP receptors, BMP transcription factors (Smad-1/5/9), and BMP downstream targets (XIAP, MAP3K7/TAK1, ID1, ID2, ID3) in lung adenocarcinomas (n = 135). Gray boxes indicate gene expression without alteration.

Similar levels of genetic alterations were identified in squamous carcinoma of the lung and adenocarcinoma lung cancer cell lines (Fig. 2 and Fig. 3). The low rate of mutations and the redundancy of the BMP signaling cascades suggest that resistance to BMP receptor inhibitors in lung cancer because of genetic alterations is likely to be a rare event.
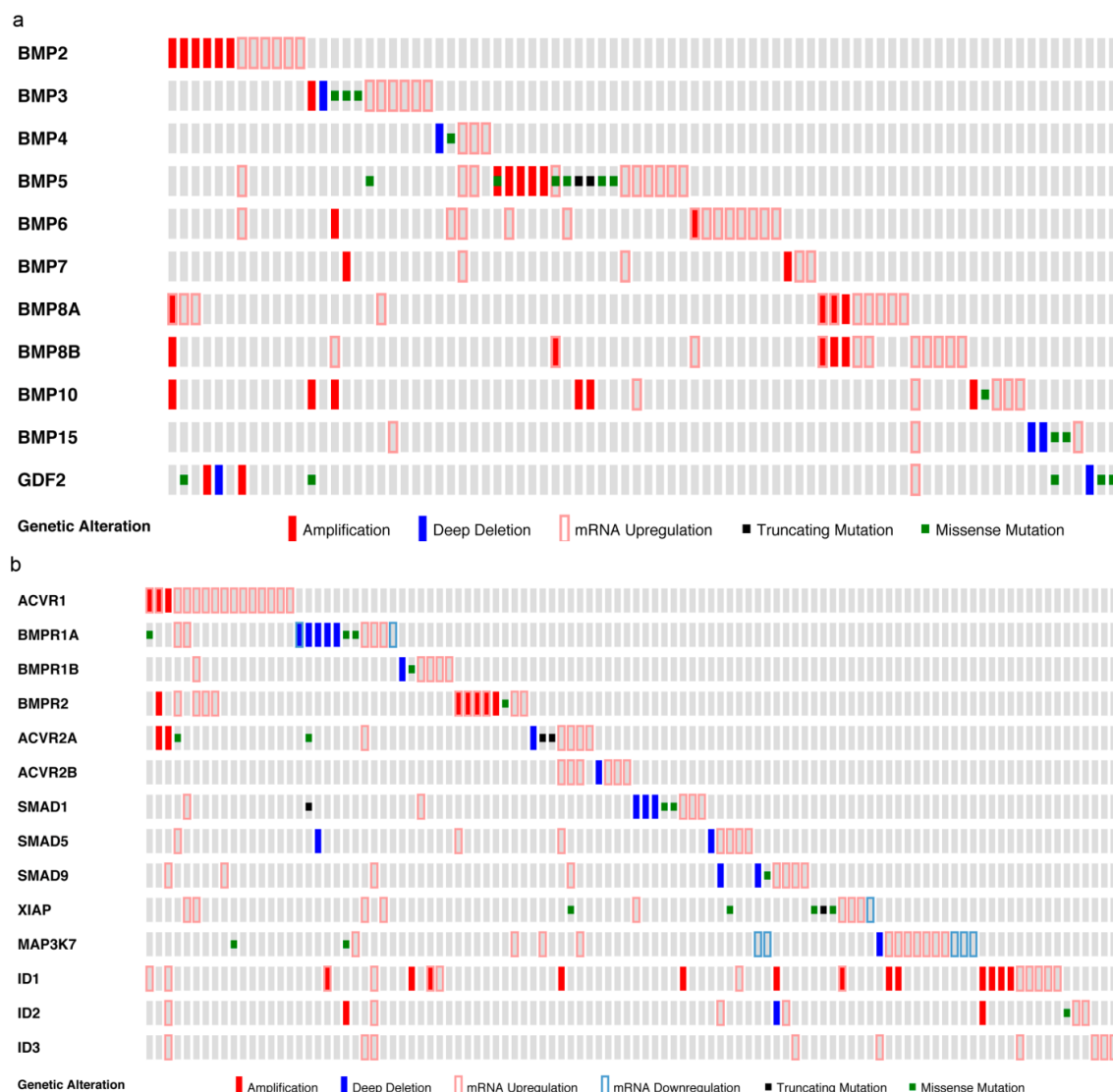
Fig. 2 Genetic alterations of the BMP signaling cascade are infrequent in lung squamous cell carcinomas. (A) The TCGA database was queried for DNA amplifications, deep deletions, truncating mutations, missense mutations, and mRNA expression of BMP ligands in lung squamous cell carcinomas (n=82) and (B) BMP receptors, BMP transcription factors (Smad-1/5/9), and BMP downstream targets (XIAP, MAP3K7/TAK1, ID1, ID2, ID3 in lung squamous cell carcinomas (n=104). Gray boxes indicate expression without alteration. The percent indicates the frequency of any mutation for that gene.
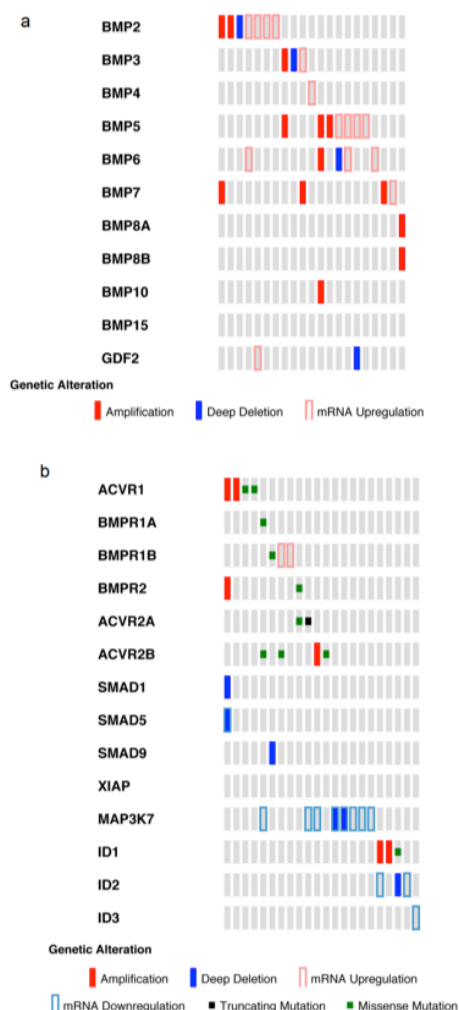
Fig. 3 Genetic alterations of the BMP signaling cascade are infrequent in lung adenocarcinoma cell lines. (A) Genetic alterations and mRNA expression were queried in the TCGA data base for BMP ligands on lung adenocarcinoma cancer cell lines (n=21) and (B) BMP receptors, BMP transcription factors, and BMP downstream targets on lung adenocarcinoma cancer cell lines (n=22). Gray boxes indicate expression without alteration.

Design of JL5 improves on the pharmacokinetic profile of DHM2

Based on the inability of DMH2 to downregulate XIAP, ID1, or pTAK1 in vivo
[22], we designed a series of DMH2 analogs. The pyrazolo [1,5-*a*] pyrimidine core of the

BMP dorsomorphin (Fig. 4A) has been utilized as a heterocyclic core to synthesize BMP

inhibitors[36]. Analogs of Dorsomorphin, DMH1, DMH2[30], and LDN-193189 (LDN)[37]

differ in the substitutions made at the R-position of the pyrazolo [1,5-*a*] pyrimidine core

(Fig. 4A). We found that after four months, aliquoted samples of DMH2 have decreased

potency to downregulate Id1 expression and induce death of lung cancer cells in vitro

(personal observation). Analysis using liquid chromatography-mass spectrometry

(LCMS) of a sample of DMH2 stored as a solid in a desiccator for 4 months revealed a

phenolic byproduct due to morpholine side-chain hydrolysis (Fig. 4B).

This observation led us to design a compound devoid of an oxygen by

replacement with a carbon atom to generate JL5 (Fig. 4C). JL5 was synthesized in simple

and convergent fashion by palladium-catalyzed coupling using microwave reactor to

couple the brominated pyrazolo[1,5-a]pyrimidine '2' to the borate ester of the morpholine

side-chain '3' to generate '1' in 48% yield as a white crystalline solid (Scheme 1). An

additional substitution of JL5 was made at the R2 position of the core with an

imidapyrazole creating JL12 (Fig. 4C).
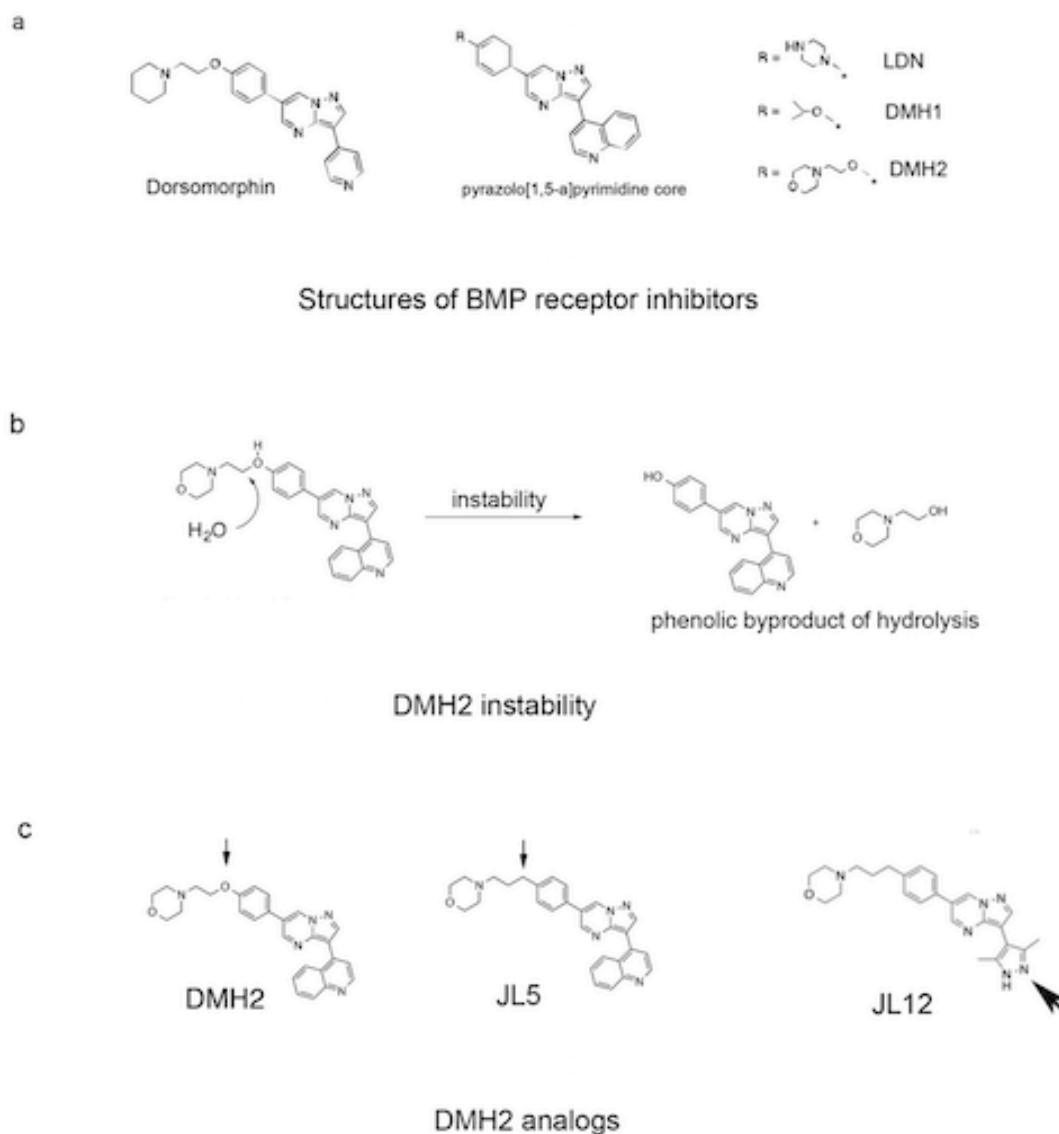
Fig. 4 A carbon for oxygen substitution to DMH2 results in the formation of JL5.
(A) Structures of Dorsomorphin analogs which were derived from the same pyrazolo[1,5-a]pyrimidine core. BMP inhibitors DMH2, DMH1, and LDN differ in the substitutions made at the R position of the pyrazolo[1,5-a]pyrimidine core. (B) DMH2 was found to be chemically and metabolically unstable. LCMS of a sample of stored DMH2 for 4 months revealed the phenolic byproduct due to morpholine side-chain hydrolysis. (C) Structure of DMH2 analogs JL5 and the inactive analog JL12. The small arrowhead shows the carbon substitution for oxygen in the DMH2 side chain to create JL5. The large arrowhead shows the imidapyrazole substitution made to JL5 to create JL12.
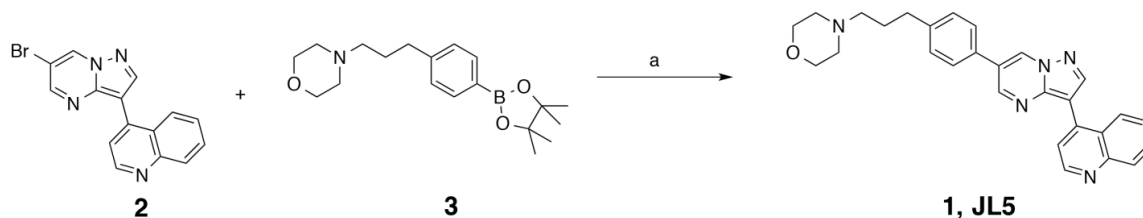
Scheme 1. Chemistry used to synthesize JL5.

Using mouse liver microsomes, we demonstrated that the intrinsic clearance of JL5 is 48% lower than that of DMH2 (Table 1). Both JL5 and DMH2 demonstrated high binding to mouse plasma proteins (Table 1). Following a single intravenous administration of JL5 to male BALB/c mice at 2 mg/kg dose, JL5 showed very high plasma clearance (194 mL/min/kg) exceeding normal hepatic clearance, likely due to a high volume of distribution (Vss) of 8.78 L/kg and an elimination half-life of 0.57 h, indicative of high tissue penetration (Table 2). The area under the curve (AUC) was determined to be 1605 h×ng/mL with a C_0/C_{max} of 1282 ng/mL (Table 2). The Vss of DMH2 (0.95 L/kg) was lower than that of JL5 (8.78 L/kg) so its distribution into the tissue is significantly lower than that of JL5 (Table 2). Since the pharmacokinetic properties of JL5 were improved over DMH2, we proceeded with further in vitro and in vivo xenograft studies.

Parameter	DMH2	JL5
Clearance$_{INT}$ (mL/min/kg)	250	129
Plasma protein binding	98.60%	98.30%

Table 1. *In vitro* PK parameters. Intrinsic clearance (Clearance$_{INT}$) and plasma protein binding for DMH2 and JL5.

Compound	Route	C$_0$/C$_{max}$ (ng/mL)	AUC$_{last}$ (hr*ng/mL)	AUC$_{inf}$ (hr*ng/mL)	T$_{1/2}$ (hr)	CL (mL/min/kg)	Vss (L/kg)
DMH2	i.v.	3,035	485	487	0.95	68	0.95
	p.o.	684	707	729	-	-	-
JL5	i.v.	568	349	381	0.57	194	8.78
	p.o.	1,282	1,605	1,645	-	-	-

Table 2. Pharmacokinetics for DMH2 and JL5. Pharmacokinetic data for DMH2 and JL5 compounds. i.v., intravenous, p.o., per os (oral route).

JL5 potently inhibits BMP receptors without inducing toxicity

Towards determining the functional capability of JL5, we determined its half maximal inhibitory concentration (IC$_{50}$) for inhibiting BMP type I and type II receptors. JL5 demonstrated a single digit nanomolar (nM) IC$_{50}$ for the BMP type I receptors alk2, alk3, and alk6, which is lower than previously reported for DMH2 (Table 3). Although JL5 only had an approximately 8 µM IC$_{50}$ for the BMP type II receptor BMPR2, it was similar to that of DMH2 (Table 3). JL12 demonstrated very little inhibition of the BMP type I and type II receptors, and therefore, was used as a negative control in our subsequent studies (Table 3). These studies show that the inhibition of the BMP type I and type II receptors by JL5 is very similar to that of DMH2.

Compound	IC50 (nM)					
	ALK2/ACVR1	ALK3/BMPR1A	ALK6/BMPR1B	BMPR2	ALK5/TGFβR1	TGFβR2
DMH2	23	92	43	7,950	1,690	193
JL5	1	<5	2	8,510	440	40
JL12	2,690	8,690	9,310	>10,000	-	3,670

Table 3. Receptor kinase inhibition for DMH2, JL5 and JL12. Half maximal inhibitory concentration (IC$_{50}$) for inhibition of receptor kinases by DMH2, JL5 and JL12 is provided, expressed in nanomolar concentrations (nM).

To determine whether JL5 causes toxicity, NSG mice were injected intraperitoneally (IP) with 0, 3 mg/kg, 10 mg/kg of JL5 twice daily for 4 days. Mice showed no evidence of systemic toxicity such as loss of appetite, anorexia, and lethargy. Histological examination of the livers, lungs, and kidneys by a veterinary pathologist did not reveal any evidence of toxicity (Fig. 5) or weight loss (Fig. 6). Further, a blood chemistry screen revealed no significant difference between mice treated with JL5 or DMSO (Table 4). In addition, in our 21-day studies (10 mg/kg of intraperitoneal JL5 twice daily) mice had no signs of toxicity as demonstrated by the lack of anorexia, lethargy, or loss of weight.
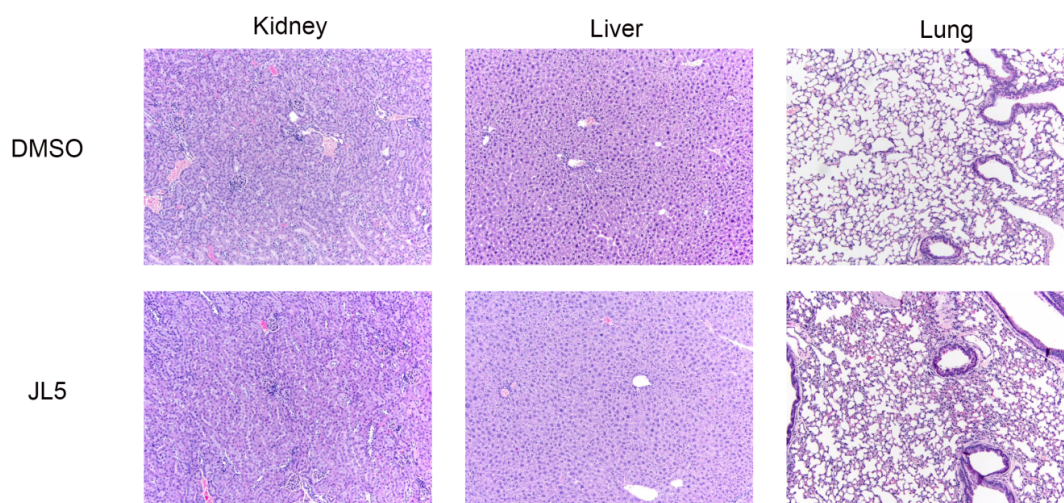
Fig. 5 JL5 administration to mice in vivo does not lead to toxicity in mice. NSG mice without immune cells were treated with DMSO or JL5 10 mg/kg (twice daily) for 4 days. The lungs, kidneys, and lungs were placed in formalin and sectioned, and H&E staining was performed. A veterinarian pathologist examined organs for changes indicative of toxicity. No evidence of toxicity to organs was observed in mice treated with DMSO or JL5.
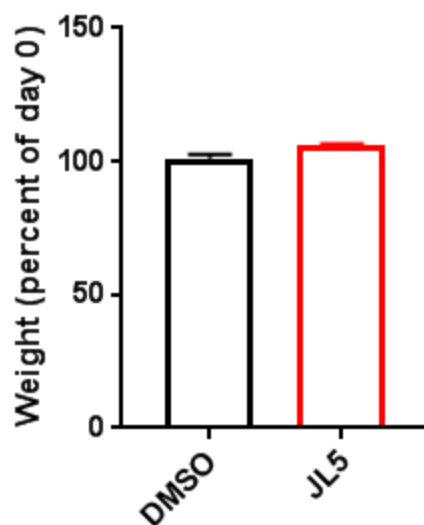
Fig. 6 JL5 administration to mice in vivo does not lead to changes in weight. NSG mice without immune cells were treated with DMSO or JL5 10 mg/kg (twice daily) for 4 days. Mouse weights on day 4 were compared to day 0. No evidence of weight differences were observed in mice treated with DMSO versus JL5.

	DMSO	JL5
Glucose (mg/dL)	206.7	231.7
Sodium (mmol/L)	151.7	151.7
Potassium (mmol/L)	5.2	4.2
Chloride (mmol/L)	107.7	105.7
CO2 (mmol/L)	16.1	15.7
Anion Gap	28.0	30.3
BUN (mg/dL)	19.0	18.7
Creatinine (mg/dL)	0.5	0.5
Total Protein (g/dL)	4.9	5.1
Albumin (g/dL)	3.1	3.1
Alkaline Phosphatase (U/L)	100.7	101.0
Calcium (mg/dL)	10.3	10.4
ALT (U/L)	18.3	25.3
AST (U/L)	81.3	61.3
Total Bilirubin (mg/dL)	0.2	0.3

Table 4. Blood Chemistry Screen. Blood chemistry results obtained from mice treated with either JL5 or DMSO.

JL5 inhibits BMP signaling and induces death of lung cancer cells

To determine whether JL5 inhibition of BMP receptors leads to inhibition of downstream BMP signaling mediators, H1299 lung cancer cells were treated with JL5, JL12 (inactive derivative of JL5), and/or DMSO. JL5 treatment caused a decrease in the expression of Id1 and XIAP (Fig. 7A) in a similar manner as previously reported for DMH2[22]. Like DMH2, JL5 at lower concentrations caused an increase in the expression of pTAK1, which became undetectable at the highest concentration (Fig. 7A)[22]. JL12 had no effect on the expression of Id1, XIAP, or pTAK1 (Fig. 7B). Since BMP signaling is a direct transcriptional regulator of the Id1 promoter, we examined whether JL5 regulates the Id1 promoter. H1299 cells stably expressing the Id1 promoter regulating the luciferase reporter were treated with JL5. JL5 caused a dose-related decrease in the expression of the Id1-luciferase reporter, while JL12 had no effect (Fig. 7C). Three-day treatment with JL5 induced a significant dose-dependent increase in cell death (Fig. 7D) and a decrease in the number of live H1229 cells (Fig. 7E). JL12 had no effect on either cell death or cell growth of the H1299 cells (Fig. 7D, E). JL5 and DMH2 caused the same amount of cell death at 2.5 μM after 3 days (Fig. 7D). After 7 days, the majority of the H1299 cells treated with JL5 were dead with few live cells remaining in comparison to the DMSO control (Fig. 7F, G). JL5 also suppressed growth of A549 cells, an adenocarcinoma cell line harboring an activating K-Ras mutation (Fig. 8). JL5 induced the activation of caspase-3 and cleavage of PARP, suggesting like DMH2, it induces apoptotic cell death (Fig. 7H)[22]. Annexin V staining is frequently used to detect early and late stages of apoptosis. Cells that stain for 7-AAD but not Annexin V are considered to have undergone cell death by necrosis. H1299 cells treated with JL5 for 48 h showed a

significant increase in the percentage of cells in late stages of apoptosis as well as

necrosis (Fig. 7I) in comparison to the DMSO control. The TUNEL assay demonstrated

that JL5 induces DNA double-stranded breaks (DSBs) of H1299 cells (Fig. 7J). The

caspase inhibitor Z-VAD-FMK (VAD) partially inhibited JL5-induced cell death, while

the RIPI kinase inhibitor necrostatin-1 (Necro) had no effect (Fig. 7K). These data

demonstrate that cell death caused by JL5 occurs in part by inducing apoptosis.
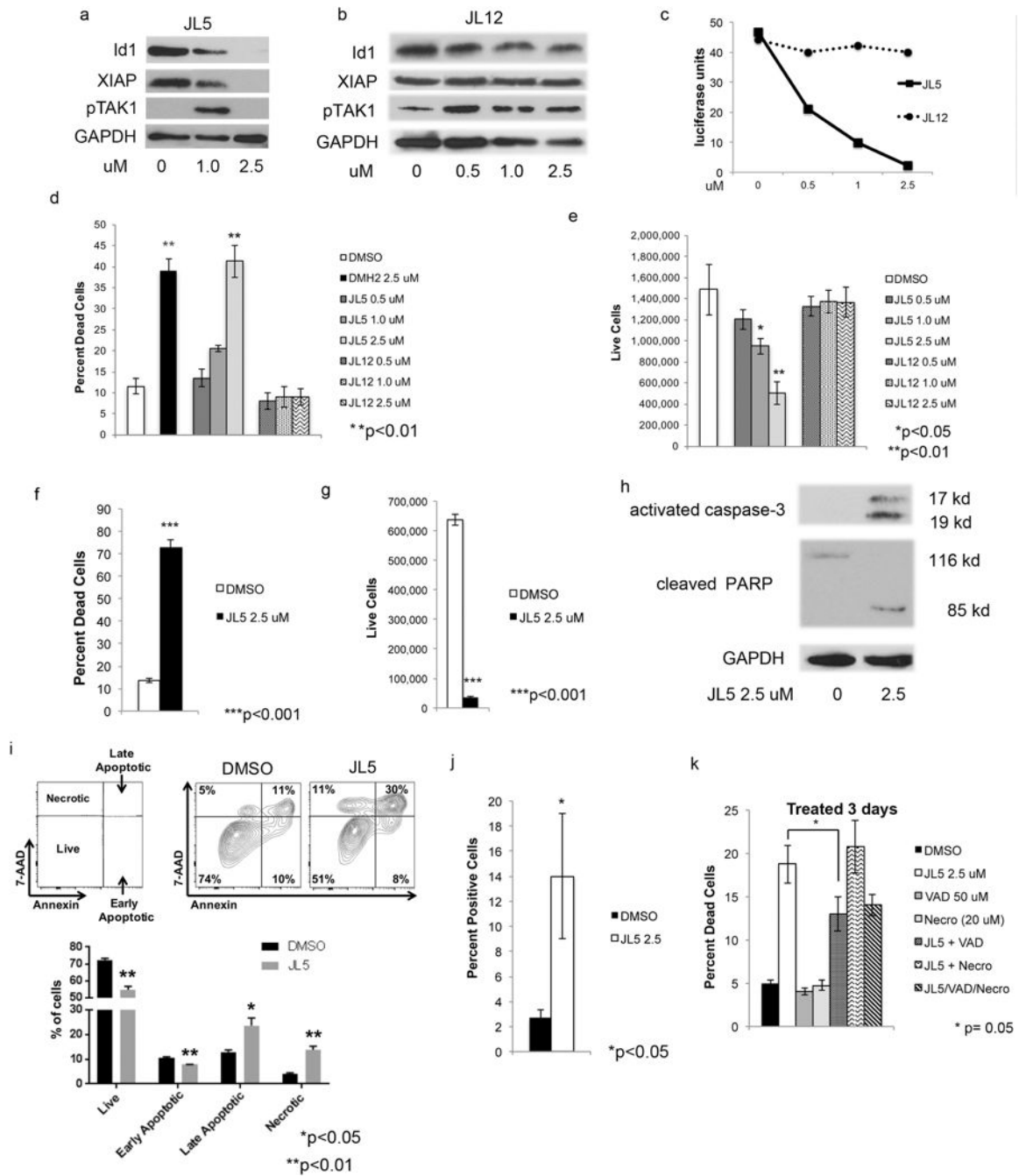
Fig. 7 JL5 but not JL12 regulates BMP signaling and induces cell death. (A,
B) Western blot analyses of H1299 cells treated with JL5 or JL12 for 72 h showing
that JL5 but not JL12 decreases expression of Id1, XIAP, and pTAK1. (C) H1299 cells
stably expressing the Id1-luciferase reporter were treated with JL5 and JL12 for 48 h.
JL5 but not JL12 decreases the activity of the Id1 promoter. (D, E) H1299 cells were
treated with JL5 or JL12 for 72 h and (D) the percent dead and (E) the number of live
cells determined. (F,G) H1299 cells were treated with JL5 for 7 days and the percent
dead and number of live cells determined. (H) Western blot analysis of H1299 cells

treated with JL5 for 3 days demonstrating that JL5 activates caspase-3 and cleaves PARP. (I) H1299 cells were treated with JL5 2.5 µM for 48 h. Cells were stained were then stained with fluorescently labeled Annexin V and 7-AAD and analyzed by flow cytometry. JL5 induced both late stage apoptosis and necrotic cell death. (J) TUNEL assay of H1299 cells treated with JL5 for 24 h demonstrating an increase in DNA double-stranded breaks. (K) H1299 cells were pretreated with Z-VAD-FMK (VAD) or necrostatin for 1 h then treated with DMSO or JL5 for 3 days and percent death cells determined. VAD but not necrostatin partially inhibited cell death induced by JL5. All experiments were performed at least 3 times with similar results except (C), which was performed twice with similar results.
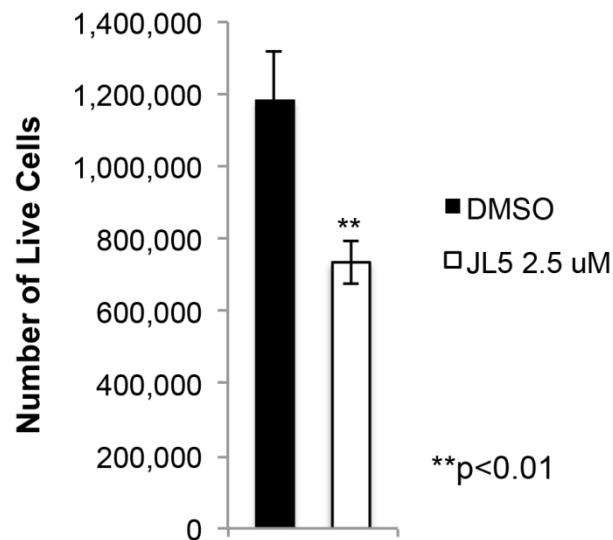
Fig. 8 JL5 suppresses growth of A549 cells. A549 cells were treated with DMSO or JL5 for three days and the number of live cells determined. Data represent the mean of four experiments.

JL5 inhibits tumor growth and induces tumor regression in NSG mice without immune cells

Towards determining whether JL5 exhibits anti-tumor effects in vivo, we first examined whether JL5 downregulates BMP downstream targets in established H1299 tumors in NOD-*scid* IL2Rgamma[null] (NSG) mice that do not have immune cells. Similar to what was reported for DMH2, JL5 at a lower concentration (3 mg/mL) caused a feedback increase in the expression of Id1 after 4 days (Fig. 9A)[22]. After 4 days, JL5-treated tumors (10 mg/kg) had a decreased protein expression of Id1 and TAK1 but not XIAP (Fig. 9A). DMH2 at similar doses did not downregulate Id1, pTAK1, or XIAP in tumor xenografts[22]. Next, we examined the effects of JL5 (10 mg/mL) on established H1299 tumors in NSG mice treated for 21 days. From the point of maximal tumor growth on treatment day 5, JL5 induced a ~35% regression in tumor size by treatment day 14 followed by a plateau in tumor growth (Fig. 9B, C). During this same period the size of tumors in control-treated mice (DMSO) increased by 13%. No significant differences in the amount of tumor cell death or proliferation were observed in tumors examined after 21 days of treatment (Fig. 9D, E).
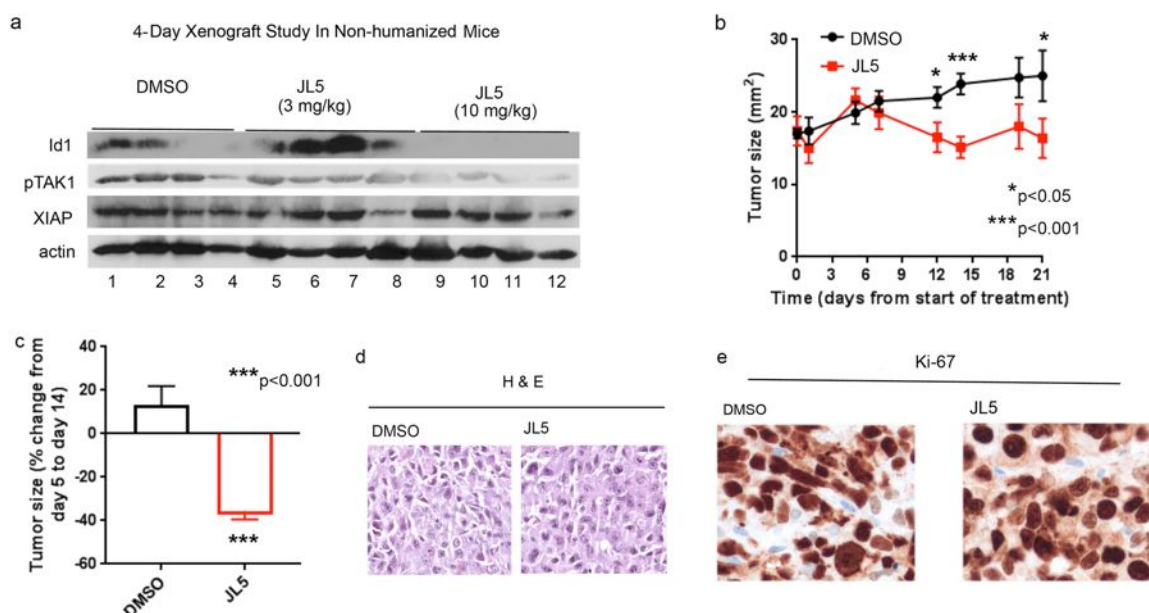
Fig. 9 JL5 suppresses BMP signaling and decreases growth of tumor xenografts in NSG mice without immune cells. (A) Western blot analysis of H1299 tumors in NSG mice without immune cells treated with JL5 for 4 days. (B-E) H1299 cells were injected intradermally into the flanks of NSG mice. Five days later after tumors had reached ~5 mm² mice were treated with DMSO or 10 mg/kg JL5 (twice daily) (n = 8 mice for each group) for 21 days. Growth curves of tumors treated for 21 days (B). Fold change in tumor growth from day 5 post-treatment to day 14 (C). DMSO-treated tumors increased in size while JL5-treated tumors demonstrate tumor regression. H&E staining of tumors shows no significant differences in the cell death (D) and IHC for the proliferation marker Ki67 on treatment day 21 show no significant differences between groups (E).

JL5 induces the influx of immune cells into the tumor microenvironment and induces tumor regression in immune-reconstituted NSG mice

Since NSG mice do not have immune cells, they accept human donor immune cells without rejection. To investigate the anti-tumor effects of JL5 in the presence of immune cells, NSG mice were reconstituted with HLA-compatible patient-derived immune cells (humanized) and xenografts then established with H1299 cells. After the tumors had reached ~5 mm^2 in size the mice were treated with JL5. JL5 caused a reduction in tumor size in humanized mice treated for 21 days (Fig. 10A). From the point of maximal tumor growth on treatment day 7, JL5 again induced an ~35% regression in tumor size by post-treatment day 12 (Fig. 10A, B). After the tumor regression, the tumors then began to grow, suggesting that the immune cells had a growth-promoting role (Fig. 10A). There were no noteworthy histomorphological differences in cell death by H&E staining (Fig. 10C) but there was a significant reduction in proliferation of tumor cells in mice treated with JL5 (Fig. 10D).

To determine the effect of JL5 treatment on immune cells, we examined the presence of immune cells within the tumors. There were significantly more immune cells within the tumor microenvironment in tumors treated with JL5 in comparison to DMSO controls (Fig. 10E). Quantitative image analysis demonstrated that JL5 induced a 67% increase in CD3+ cells and 80% increase in CD4+ cells in comparison to the DMSO control (Fig. 10F).
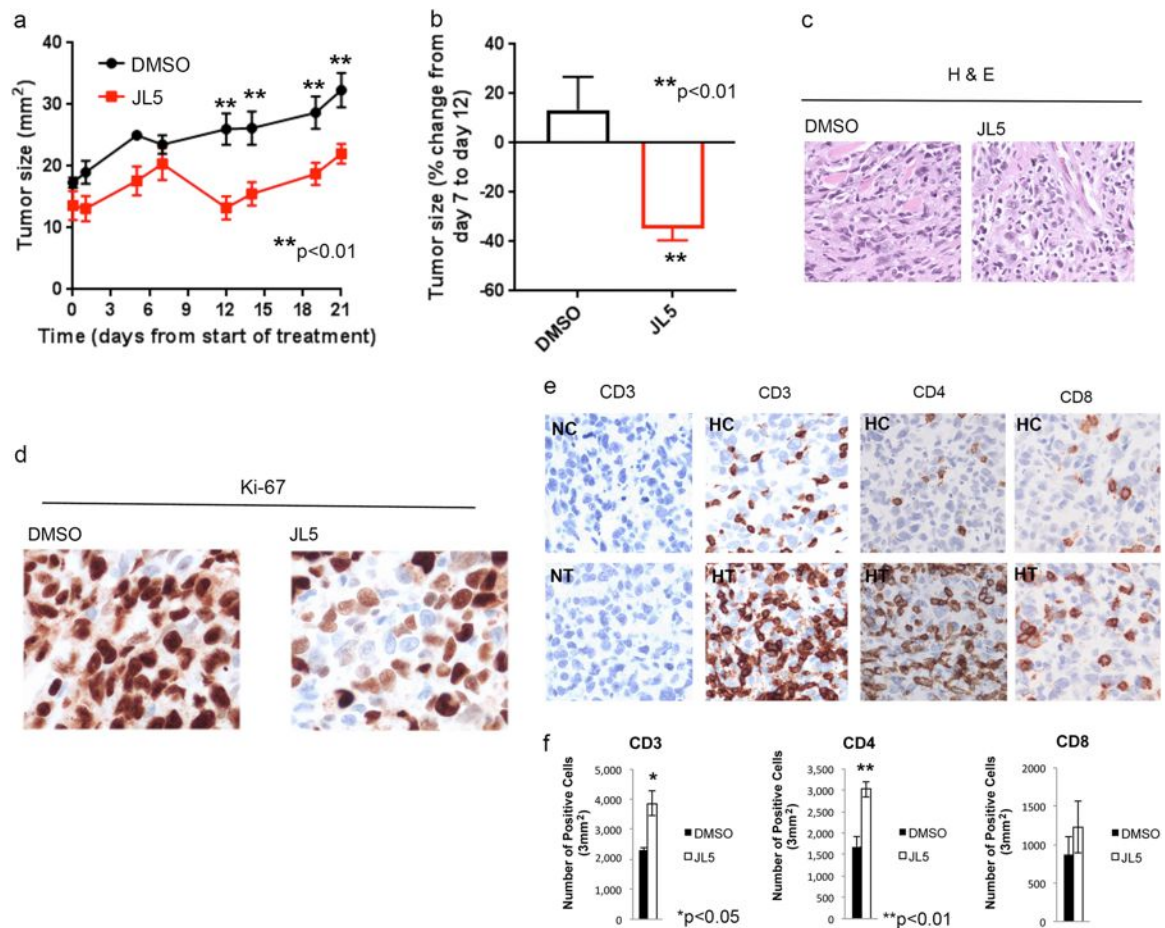
Fig. 10 JL5 suppresses growth of tumor xenografts in NSG mice with immune cells and induces infiltration of immune cells. (A-E) NSG mice received adoptively transferred human immune cells and then H1299 cells were injected intradermally into the flanks. Five days later after tumors had reached ~5 mm^2 mice were treated with DMSO or 10 mg/kg JL5 (twice daily) ($n = 8$ mice for each group) for 21 days. Growth curves of tumors treated for 21 days (A). Percent change in tumor growth from day 7 post-treatment to day 12 (B). DMSO-treated tumors increase in size while JL5-treated tumors demonstrate tumor regression. H&E staining of tumors shows no significant differences in the number of death cells (C). IHC for the proliferation marker Ki67 on treatement day 21 demonstrates a significant decrease in proliferation in tumors treated with JL5 (D). IHC staining of tumors on treatment day 21 shows that JL5 increases the number of immune cells within the tumor microenvironment (E). Tumors formed in mice that did not receive immune cells were used as controls. NC and NT = non-humanized mice treated with DMSO control or JL5, respectively. HC and HT = humanized mice treated with DMSO control or JL5, respectively. (F) IHC slides were scanned and the mean number of immune cells quantified using imaging software ($n = 3$ in each group)

JL5 induces tumor necrosis on treatment day 13

Since we did not see cell death after 21 days of treatment despite both the
humanized and non-humanized xenografts demonstrating tumor regression after ~13 days
of treatment, we repeated the humanized xenograft study but analyzed the tumors after 13
days of treatment with JL5. Again, a significant difference in the size and weight of the
tumors of mice treated with JL5 compared to vehicle control was observed (Fig. 11A, B).
The amount of tumor regression was equivalent to that seen in the prior experiments on
treatment day 15. Histological examination revealed increased necrosis in tumors treated
with JL5 compared to controls at this timepoint (Fig. 11C). Two independent pathologists
agreed on this finding. Computer-based image analysis using morphometrics software of
the H&E slides was used to examine necrosis within the tumor. JL5-treated tumors
exhibited twice the number of necrotic cells compared to control tumors (Fig. 11D).
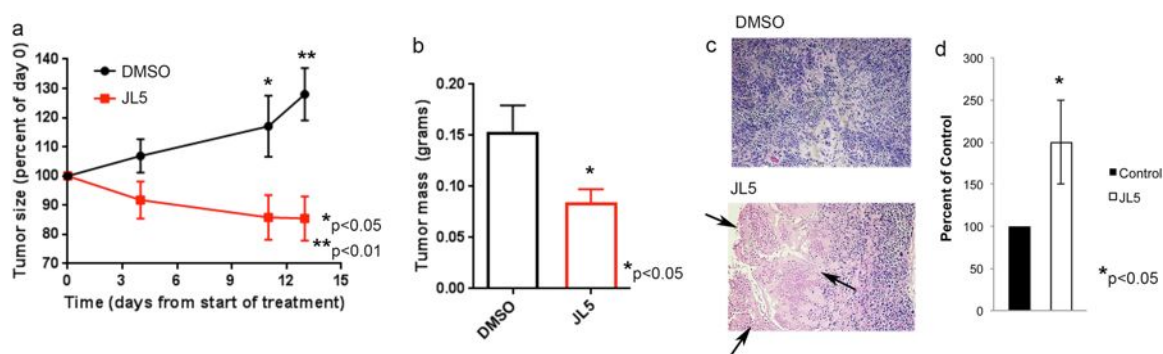
Fig. 11 JL5 induces death of cancer cells on treatment day 13. NSG mice
received adoptively transferred human immune cells and then H1299 cells were
injected intradermally into the flanks. Five days later after tumors had reached
~5 mm² mice were treated with DMSO or 10 mg/kg JL5 (twice daily) ($n = 7$
mice for each group) for 13 days. (A, B) Growth curves of tumors (A) and
tumor weights of xenograft tumors on treatment day 13 (B). (C) H&E staining
demonstrating significantly more cell death of cancer cells (pink cells shown by
arrows) of tumors treated with JL5. (D) The H&E slides were scanned and the

percentage of dead cells within each tumor determined using imaging software. Data represents the mean of 7 tumors depicted as the percent of control

DISCUSSION

Drugs targeting specific receptors are frequently only effective if that receptor has an activating mutation. Activating ROS-1 or epidermal growth factor mutations occur in 1% and 13% of NSCLC, respectively[38]. Targeted therapy is also limited by the deletion of the receptor or development of mutations that are not recognized by the drug[39]. Mutations of downstream effector genes can also render a drug inactive[39]. Our analysis supports that BMP signaling cascade is active in the majority of NSCLCs and genetic alterations are unlikely to induce resistance to small molecules targeting the BMP receptors. Expression of BMP ligands and receptors is highly redundant in NSCLC. Ten different BMP ligands were expressed in NSCLC. All three BMP type I and type II receptors were expressed in all of the NSCLC examined. We have shown that all three of the type I BMP receptors can effectively induce downstream signaling in lung cancer cell lines[40]. The mutation rate of the BMP receptors is low (<5%) and no tumor had mutations in all three of the type I or type II BMP receptors. The very low incidence of amplification of XIAP, TAK1, or Id1 suggests that these downstream effectors would not provide a mechanism inducing resistance to BMP targeted therapy. Overall, these data suggest that targeting the BMP signaling cascade will not be limited by genetic alterations found in either squamous cell carcinomas or adenocarcinomas of the lung.

There are only a few studies examining the effects of BMP receptor inhibitors in tumor xenografts. The BMP inhibitors most frequently used have been DMH1, DMH2, and LDN. Our studies have shown that DMH2 in vitro is significantly more potent than

DMH1 or LDN in decreasing the downstream targets Id1, TAK1, and XIAP and inducing cell death of cancer cells[22]. DMH1 and LDN in tumor xenograft studies reduce metastasis but have not demonstrated tumor regression or significant death of cancer cells[7,41]. DMH2 has a half-life of only 60 min with a low volume of distribution. Surprisingly, DMH2 causes an increase in Id1 expression in tumor xenografts likely from low level of suppression of BMP signaling allowing for activation of TAK1, which can cause a feed-forward activation of BMP signaling[22]. Substituting a carbon for the oxygen on the morphine side-chain improved the stability of DMH2 and resulted in a new compound, JL5. The potency of JL5 to inhibit BMP receptors and regulate BMP signaling of cancer cells is very similar to that of DMH2. Although the serum half-life was not improved, the volume of distribution was significantly better than that DMH2, which likely contributed to the improved anti-tumor effects seen in our studies. It is likely that further improvements in the pharmacokinetic properties of JL5 and the future development of other potent BMP inhibitors will produce even more pronounced in vivo anti-tumor effects.

We show for the first time that a BMP inhibitor induces tumor regression and causes significant cell death in human tumor xenografts in mice. This was associated with a downregulation of Id1 and TAK1 but not XIAP. The binding of XIAP to the BMP receptors stabilizes XIAP leading to increased expression. XIAP can be stabilized by other pathways, including by binding to survivin and phosphorylation by PI-3 kinase[42]. XIAP is an upstream activator of TAK1, which can phosphorylate Smad-1/5 leading to the activation of BMP signaling[22,44]. The ability to downregulate XIAP is likely to further inhibit BMP signaling leading to greater cell death. During apoptotic cell death smac is

released from the mitochondria, which binds and inactivates inhibitor of apoptosis proteins[43]. Smac mimetics have been designed to bind and inactivate inhibitor of apoptosis proteins IAP-1, IAP-2, and XIAP[44]. Combinational therapies utilizing inhibitors of survivin, PI-3 kinase, or smac mimetics should be explored as a potential strategy to further enhance the downregulation of BMP signaling in cancer cells.

The immune system can induce or inhibit the growth of tumors. In our humanized mouse tumor model the immune cells appeared to have a growth-promoting role. This finding argues the importance of including immune cells in preclinical tumor xenograft models to better delineate therapeutic strategies to treat cancer. Importantly, despite the growth-promoting effect of immune cells, JL5 still caused tumor regression. However, tumor regression was not sustained in the presence of immune cells. Surprisingly, only in tumors with immune cells did JL5 decrease proliferation of cancer cells. Immune cells are known to secrete BMP ligands[45]. An increase in the number of immune cells secreting BMP ligands could enhance the proliferation of tumor cells and suppress the cytotoxic effects of JL5. A more potent BMP receptor inhibitor with a longer duration of action may be able to counter act the growth-promoting effects of immune cells. A potential strategy that could be utilized is to activate cytotoxic immune cells that have become 'exhausted'. Inhibitors of the immune blockade have demonstrated sustained tumor regression in lung and other tumors[46,47]. However, the response rate is only 20%. The presence of immune cells within the tumor microenvironment is reported to be the best predictor of PD-L1 blockade inducing a response[48]. Further studies are needed to determine whether the enhanced influx of immune cells induced by BMP receptor

inhibition can be used to enhance the effects of immunotherapy directed at PD-1 or PD-L1.

BMP signaling is active in the majority of lung cancers and genetic mutations in NSCLC are unlikely to mitigate the effects of BMP receptor inhibitors. The development of JL5 provides a useful tool to examine the mechanisms in vivo by which the BMP signaling regulates the survival of cancer cells and to develop therapeutic strategies. Since JL5 induces the influx of immune cells into the tumor microenvironment, without causing their death, raising the possibility it can be used in conjunction with checkpoint inhibitors. These studies demonstrate that BMP signaling is growth-promoting in cancer, but is targetable supporting the need for further drug development and design of therapeutic strategies.

METHODS

Cell culture and reagents

The A549 and H1229 lung cancer cell lines were cultured in Dulbecco's modified Eagle's medium (DMEM, Sigma Aldrich, St Louis, MO, USA) with 5% fetal bovine serum (FBS)[49]. DMH2 and JL5 were synthesized at Rutgers-New Jersey Medical School (Dave Augeri). Z-VAD-FMK and necrostatin-1 were obtained from Sigma-Aldrich, and utilized as per manufacture instructions.

Western blot analysis

Total cellular protein was prepared as previously described and the protein concentration determined using the BCA assay[3]. Protein was separated by SDS-PAGE then transferred to nitrocellulose (Schleicher and Schuell, Keene, NH). The blots were blocked for at least 2 h then incubated overnight at 4 °C with the appropriate primary antibody. Secondary antibodies were applied for 1 h at room temperature. Proteins were detected using the enhanced chemiluminescence system (Amersham, Arlington Heights, IL). The primary antibodies used were rabbit monoclonal anti-pTAK1, rabbit monoclonal XIAP, rabbit monoclonal anti-activated caspase-3, rabbit monoclonal anti-PARP (Cell signaling Technology, Danvers MA), rabbit monoclonal anti-Id1(Calbioreagents, San Mateo, CA), rabbit anti-actin, an affinity isolated antigen specific antibody (Sigma, Saint Louis, MO), and rabbit polyclonal anti-GAPDH (Sigma, St. Louis, MO).

Chemical synthesis of JL5

To synthesize 4-(6-bromopyrazolo[1,5-*a*]pyrimidin-3-yl)quinolone, a solution of 4-(quinolin-4-yl)-1*H*-pyrazol-3-amine (535 mg, 2.54 mmol, 1 eq) in acetic acid (20 ml) was added 2-bromomalonaldehyde (383 mg, 2.54 mmol, 1 eq). After stirring for 16 h at room temperature, the reaction was diluted in water up to 150 ml total solvent. The solution was adjusted to a pH of 5–6 with careful addition of sodium hydroxide when a solid began to precipitate. After 30 min, the suspended solid was subjected to sonication, filtered and washed with water. The solid was recrystallized in MeOH to yield the title compound (752 mg, 91% yield) as a white solid. ^{1}H NMR (500 MHz, DMSO-d_6) 9.77 (d, $J = 2.2$ Hz, 1H), 8.94 (d, $J = 4.5$ Hz, 1H), 8.78–8.71 (m, 1H), 8.69 (s, 1H), 8.09 (td, $J = 8.3$, 1.4 Hz, 2H), 7.78 (ddd, $J = 8.2$, 6.7, 1.4 Hz, 1H), 7.71 (d, $J = 4.4$ Hz, 1H), 7.58 (ddd, $J = 8.3$, 6.8, 1.3 Hz, 1H). MS: 324.75, 326.80 $[M + H]^+$.

To synthesize 4-(3-(4-(4,4,5,5-tetramethyl-1,3,2-dioxaborolan-2-yl)phenyl)propyl)morpholino, a solution of 4-(3-(4-bromophenyl)propyl)morpholine (110 mg, 0.387 mmol, 1 eq), bis(pinacolato)diboron (147 mg, 0.581 mmol, 1.5 eq), $PdCl_2$(dppf)CH_2Cl_2 (16 mg, 0.0194 mmol, 0.05 eq), and KOAc (104 mg, 1.16 mmol, 3 eq) in dioxane (4 ml) was heated in a microwave reactor for 15 min at 130 °C. The crude reaction was diluted in hexanes and filtered over a pad of celite to remove inorganics. The filtrate was purified by silica gel chromatography (50% → 100% EtOAc/Hex) and concentrated to afford the title compound (115 mg, 90%) as an oil that was used in the subsequent coupling without further purification. MS: 332.05 $[M + H]^+$.

To synthesize JL5, a mixture of 4-(6-bromopyrazolo[1,5-*a*]pyrimidin-3-yl)quinolone (300 mg, 0.810 mmol, 1 eq), 4-(3-(4-(4,4,5,5-tetramethyl-1,3,2-dioxaborolan-2-yl)phenyl)propyl)morpholine (402 mg, 1.22 mmol, 1.5 eq), $PdCl_2(PPh_3)_2$ (28 mg, 0.405 mmol, 0.05 eq) in dioxane (9 ml) and 2 M aqueous Na_2CO_3 (6 ml) was heated in a microwave reactor for 10 min at 130 °C. The reaction was partitioned in EtOAc and water followed by filtration over celite to remove insoluble impurities. The filtered organic was separated and the filtered aqueous was extracted 2× EtOAc. The combined organic was dried over Na_2SO_4, filtered and concentrated. The residue was dissolved in dilute aqueous HCl and washed 2× DCM. The acidic aqueous was made basic with 1 M NaOH and extracted 4× CM. The combined organic was dried over Na_2SO_4, filtered and concentrated. The residue was purified by silica gel chromatography (2% → 5% MeOH/DCM) and product containing fractions were combined and concentrated. Recrystallization from EtOAc afforded the title compound (175 mg, 48%) as a white solid.

Evaluation of genetic abnormalities of BMP signaling in NSCLC

We used The Cancer Genome Atlas (TCGA) database available through cBioportal (http://www.cbioportal.org/public-portal/; accessed on 18 March 2016), a publicly available data portal to investigate the frequency of alterations and expression of the BMP family ligands, receptors, transcription factors, and BMP downstream mediated targets regulating cell survival[50,51]. Data sets were queried for lung adenocarcinoma and lung squamous cell cancers (provisional for both). Only cases with complete data on mutations, copy-number alterations, and mRNA expression were included. Alterations in BMP signaling in NSCLC cell lines (CCLE, Cancer Cell Line Encyclopedia) were

queried through cBioportal[52]. Dysregulated gene expression was defined by $Z > 2$ (over-expression) or $Z \leq 2$ (reduced expression). Software tools embedded within cBioPortal were used to determine the proportion of samples within each dataset with alterations or up/downregulation.

Cell viability

Lung cancer cells were plated into six-well plates. The following day cells were treated with the BMP inhibitor for the designated amount of time. The live and dead cells were determined using the Vi-CELL cell analyzer (Beckman Coulter). Vi-CELL cell analyzer examined 500 cells per sample and uses utilizes trypan blue dye exclusion to determine the number of dead cells.

Annexin V staining

To assess apoptotic cell death, H1299 cells in six-well plates were treated with DMSO or JL5 2.5 µM for 48 h. Cells were then stained with labeled Annexin V and 7-AAD as per manufacturer's instructions (Thermo Fisher Scientific). Cells were then analyzed by flow cytometry.

IC$_{50}$ kinase assay

IC$_{50}$ assays were performed for alk2, alk3, alk6, alk5, BMPRII, and TGFβ for JL5 and JL12 (Reaction Biology Corporation, Malvern, PA). This was a 10-point assay ranging from 100 µM to 100 nM performed in duplicate with the ATP concentration of 10 µM.

Plasma protein binding

Mouse protein plasma binding for JL5 was performed using equilibrium dialysis (Sai Life Sciences Limited, Pune India).

Metabolic stability

Mouse liver microsomes were treated with DMSO or JL5 for 0.5, 15, 30, and 60 min. The plates were centrifuged and 100 µL aliquots analyzed by liquid chromatography-mass spectrometry (LC-M/MS) (Sai Life Sciences Limited, Pune India).

Pharmacokinetics

The pharmacokinetics of JL5 was examined in BALB/c mice following intravenous and intraperitoneal (i.p.) administration (Sai Life Sciences Limited, Pune India). Blood samples were taken 0.08, 0.25, 0.5, 1, 2, 4, 8, 12, and 24 h and analyzed with LC/MS/MS. Plasma half-life, clearance, AUC, and volume of distribution were then determined (Sai Life Sciences Limited, Pune India).

Luciferase assay

H1299 cells were stably transfected with the Id-1 promoter, which drives the expression of the luciferase reporter. Cells were treated with BMP inhibitors for 48 h then cells lysed and luminescence measured by the TD-20/20 Luminometer (Turner Designs/Turner BioSystems, Sunnyvale, CA)[22].

Humanized and non-humanized tumor xenograft studies

Tumor xenografts from H1299 cells were established by injection of 2 million cells into the intradermal space of the flanks of NOD-*scid* IL2Rgamma[null] (NSG) mice (bred in-house and randomly assigned to groups without blinding). When tumors reached approximately 4 mm × 4 mm, mice were treated with 3 or 10 mg/kg of JL5 twice daily (or DMSO control) for four days. In some experiment, the NSG mice also received adoptive transfer (via intravenous injection, as previously described[53-55] of 1–2 million cells donor HLA-compatible human peripheral blood immune cells per mouse and were treated with 10 mg/kg of JL5 twice daily (or DMSO control) for 13 or 21 days, as described for each set of experiments. Tumors were measured using electronic calipers and dissected and processed at the end of each study, as previously described[56-58]. For each experiment, 7–8 mice per group were included (as detailed for each individual experiment) a sample size powered to identify statistical significance with a minimal number of mice. The power calculation applies to the tumor size at the final time point. Experiments were conducted in compliance with ethical regulations and approved by Rutgers IACUC.

Quantifying tumor necrosis

To quantify necrosis H&E-stained slides from each tumor were analyzed using CellSens imaging software (Olympus Life Science). Necrotic and viable tissue areas were manually delineated to calculate percent necrosis.

Toxicity studies

Mice treated with DMSO, 3 mg/kg, and 10 mg/kg of JL5 twice daily for four days were euthanized and postmortem examinations were performed at the scheduled necropsy. At

the time of necropsy, lungs, kidneys, and livers were collected and fixed in 10% neutral-buffered formalin. Histomorphological examination of hematoxylin and eosin (H&E)-stained paraffin sections were performed by a board certified veterinary pathologist. Mice in 21-day repeat-dose toxicity studies treated with DMSO (vehicle) or 10 mg/kg of JL5 were examined four times weekly for lethargy, weight loss, and loss of appetite.

Statistical analysis

The means of the control group and treated groups were compared using a two-sided paired Student t-test assuming unequal variances. Error bars represent standard error of the mean. A p-value < 0.05 was considered statistically significant.

REFERENCES

1) Sountoulidis A, *et al*. (2012) Activation of the canonical bone morphogenetic protein (BMP) pathway during lung morphogenesis and adult lung tissue repair. *PLoS One* 7:e41460.

2) Weaver M, Yingling JM, Dunn NR, Bellusci S, Hogan BL (1999). Bmp signaling regulates proximal-distal differentiation of endoderm in mouse lung development. *Development* 126:4005–15.

3) Langenfeld EM, Calvano SE, Abou-Nukta F, Lowry SF, Amenta P, Langenfeld J (2003). The mature bone morphogenetic protein-2 is aberrantly expressed in non-small cell lung carcinomas and stimulates tumor growth of A549 cells. *Carcinogenesis* 24:1445–54.

4) Langenfeld EM, Bojnowski J, Perone J, Langenfeld J (2005). Expression of bone morphogenetic proteins in human lung carcinomas. *Annals of Thoracic Surgery* 80:1028–32.

5) Lai TH, Fong YC, Fu WM, Yang RS, Tang CH (2008). Osteoblasts-derived BMP-2 enhances the motility of prostate cancer cells via activation of integrins. *Prostate* 68:1341–53.

6) Clement JH, Raida M, Sanger J, Bicknell R, Liu J, Naumann A, et al. (2005) Bone morphogenetic protein 2 (BMP-2) induces in vitro invasion and in vivo hormone independent growth of breast carcinoma cells. *International Journal of Oncology* 27:401–7.

7) Owens P, Pickup MW, Novitskiy SV, Giltnane JM, Gorska AE, Hopkins CR, et al. (2015) Inhibition of BMP signaling suppresses metastasis in mammary cancer. *Oncogene* 34:2437–49.

8) Kleeff J, Maruyama H, Ishiwata T, Sawhney H, Friess H, Buchler MW, et al. (1999) Bone morphogenetic protein 2 exerts diverse effects on cell growth in vitro and is expressed in human pancreatic cancer in vivo. *Gastroenterology* 116:1202–16.

9) Rothhammer T, Poser I, Soncin F, Bataille F, Moser M, Bosserhoff AK (2005) Bone morphogenic proteins are overexpressed in malignant melanoma and promote cell invasion and migration. *Cancer Research* 65:448–56.

10) Nguyen A, Scott MA, Dry SM, James AW (2014) Roles of bone morphogenetic protein signaling in osteosarcoma. *International Orthopaedics* 38:2313–22.

11) Langenfeld EM, Langenfeld J. Bone morphogenetic protein-2 stimulates angiogenesis in developing tumors (2004) *Molecular Cancer Research* 2:141–9.

12) Langenfeld EM, Kong Y, Langenfeld J (2006) Bone morphogenetic protein 2 stimulation of tumor growth involves the activation of Smad-1/5. *Oncogene* 25:685–92.

13) Le Page C, Puiffe ML, Meunier L, Zietarska M, de Ladurantaye M, Tonin PN, et al. (2009) BMP-2 signaling in ovarian cancer and its association with poor prognosis. *Journal of Ovarian Research*. 2:4.

14) Ye L, Mason MD, Jiang WG (2011) Bone morphogenetic protein and bone metastasis, implication and therapeutic potential. *Frontiers in Bioscience* 16:865–97.

15) Nickel J, Sebald W, Groppe JC, Mueller TD (2009) Intricacies of BMP receptor assembly. *Cytokine Growth Factor Reviews* 20:367–77.

16) Attisano L, Wrana JL (2002) Signal transduction by the TGF-beta superfamily. *Science* (New Y, NY). 296:1646–7.

17) Hollnagel A, Oehlmann V, Heymer J, Ruther U, Nordheim A (1999). Id genes are direct targets of bone morphogenetic protein induction in embryonic stem cells. *Journal of Biological Chemistry* 274:19838–45.

18) Katagiri T, Imada M, Yanai T, Suda T, Takahashi N, Kamijo R (2002) Identification of a BMP-responsive element in Id1, the gene for inhibition of myogenesis. *Genes to Cells* 7:949–60.

19) Korchynskyi O, ten Dijke P (2002) Identification and functional characterization of distinct critically important bone morphogenetic protein-specific response elements in the Id1 promoter. *Journal of Biological Chemistry* 277:4883–91.

20) Kurooka H, Nakahiro T, Mori K, Sano K, Yokota Y (2012) BMP signaling is responsible for serum-induced Id2 expression. *Biochemical and Biophysical Research Communications* 420:281–7.

21) Lyden D, Young AZ, Zagzag D, Yan W, Gerald W, O'Reilly R, et al. (1999) Id1 and Id3 are required for neurogenesis, angiogenesis and vascularization of tumour xenografts. *Nature* 401:670–7.

22) Augeri DJ, Langenfeld E, Castle M, Gilleran JA, Langenfeld J (2016) Inhibition of BMP and of TGFbeta receptors downregulates expression of XIAP and TAK1 leading to lung cancer cell death. *Molecular Cancer* 15:27.

23) Liu Z, Shen J, Pu K, Katus HA, Ploger F, Tiefenbacher CP, et al. (2009) GDF5 and BMP2 inhibit apoptosis via activation of BMPR2 and subsequent stabilization of XIAP. *Biochimica et Biophysica Acta* 1793:1819–27.

24) Yamaguchi K, Nagai S, Ninomiya-Tsuji J, Nishita M, Tamai K, Irie K, et al. (1999) XIAP, a cellular member of the inhibitor of apoptosis protein family, links the receptors to TAB1-TAK1 in the BMP signaling pathway. *EMBO Journal* 18:179–87.

25) Obexer P, Ausserlechner MJ (2014) X-linked inhibitor of apoptosis protein—a critical death resistance regulator and therapeutic target for personalized cancer therapy. *Frontiers in Oncology* 4:197.

26) Kaufmann T, Strasser A, Jost PJ (2012) Fas death receptor signalling: roles of Bid and XIAP. *Cell Death and Differentiation*. 19:42–50.

27) Mihaly SR, Ninomiya-Tsuji J, Morioka S (2014) TAK1 control of cell death. *Cell Death and Differentiation* 21:1667–76.

28) Vanlangenakker N, Vanden Berghe T, Bogaert P, Laukens B, Zobel K, Deshayes K, et al. (2011) cIAP1 and TAK1 protect cells from TNF-induced necrosis by preventing RIP1/RIP3-dependent reactive oxygen species production. *Cell Death and Differentiation* 18:656–65.

29) Zon LI, Peterson RT (2005) In vivo drug discovery in the zebrafish. *Nature Reviews Drug Discovery* 4:35–44.

30) Hao J, Ho JN, Lewis JA, Karim KA, Daniels RN, Gentry PR, et al. (2010) In vivo structure-activity relationship study of dorsomorphin analogues identifies selective VEGF and BMP inhibitors. *ACS Chemical Biology* 5:245–53.

31) Yu PB, Deng DY, Lai CS, Hong CC, Cuny GD, Bouxsein ML, et al. (2008) BMP type I receptor inhibition reduces heterotopic [corrected] ossification. *Nature Medicine* 14:1363–9.

32) Balboni AL, Hutchinson JA, DeCastro AJ, Cherukuri P, Liby K, Sporn MB, et al. (2013) DeltaNp63alpha-mediated activation of bone morphogenetic protein signaling governs stem cell activity and plasticity in normal and malignant mammary epithelial cells. *Cancer Research* 73:1020–30.

33) Martinez VG, Hernandez-Lopez C, Valencia J, Hidalgo L, Entrena A, Zapata AG, et al. (2011) The canonical BMP signaling pathway is involved in human monocyte-derived dendritic cell maturation. *Immunology and Cell Biology* 89:610–8.

34) Martinez VG, Sacedon R, Hidalgo L, Valencia J, Fernandez-Sevilla LM, Hernandez-Lopez C, et al. (2015) The BMP pathway participates in human naive CD4+ T cell activation and homeostasis. *PloS One* 10:e0131453.

35) Robson NC, Hidalgo L, McAlpine T, Wei H, Martinez VG, Entrena A, et al. (2014) Optimal effector functions in human natural killer cells rely upon autocrine bone morphogenetic protein signaling. *Cancer Research* 74:5019–31.

36) Yu PB, Hong CC, Sachidanandan C, Babitt JL, Deng DY, Hoyng SA, et al. (2008) Dorsomorphin inhibits BMP signals required for embryogenesis and iron metabolism. *Nature Chemical Biology* 4:33–41.

37) Cuny GD, Yu PB, Laha JK, Xing X, Liu JF, Lai CS, et al. (2008) Structure-activity relationship study of bone morphogenetic protein (BMP) signaling inhibitors. *Bioorganic and Medicinal Chemistry Letters* 18:4388–92.

38) Pao W, Miller V, Zakowski M, Doherty J, Politi K, Sarkaria I, et al. (2004) EGF receptor gene mutations are common in lung cancers from "never smokers" and are associated with sensitivity of tumors to gefitinib and erlotinib. *Proceedings of the National Academy of Sciences of the USA*. 101:13306–11.

39) Zhou W, Ercan D, Chen L, Yun CH, Li D, Capelletti M, et al. (2009) Novel mutant-selective EGFR kinase inhibitors against EGFR T790M. *Nature* 462:1070–4.

40) Langenfeld E, Hong CC, Lanke G, Langenfeld J. (2013) Bone morphogenetic protein type I receptor antagonists decrease growth and induce cell death of lung cancer cell lines. *PLoS One* 8:e61256.

41) Hao J, Lee R, Chang A, Fan J, Labib C, Parsa C, et al. (2014) DMH1, a small molecule inhibitor of BMP type i receptors, suppresses growth and invasion of lung cancer. *PloS One* 9:e90748.

42) Dohi T, Okada K, Xia F, Wilford CE, Samuel T, Welsh K, et al. (2004) An IAP-IAP complex inhibits apoptosis. *Journal of Biological Chemistry* 279:34087–90.

43) de Bruin EC, Medema JP (2008) Apoptosis and non-apoptotic deaths in cancer development and treatment response. *Cancer Treatment Reviews* 34:737–49.

44) Galban S, Hwang C, Rumble JM, Oetjen KA, Wright CW, Boudreault A, et al. (2009) Cytoprotective effects of IAPs revealed by a small molecule antagonist. *Biochemical Journal* 417:765–71.

45) Martinez VG, Hidalgo L, Valencia J, Hernandez-Lopez C, Entrena A, del Amo BG, et al. (2014) Autocrine activation of canonical BMP signaling regulates PD-L1 and PD-L2 expression in human dendritic cells. *European Journal of Immunology* 44:1031–8.

46) Bobbio A, Alifano M. (2015) Immune therapy of non-small cell lung cancer. The future. *Pharmacology Research* 99:217–22.

47) Sharma P, Allison JP (2015) The future of immune checkpoint therapy. *Science (New Y, NY)*. 348:56–61.

48) Taube JM, Klein A, Brahmer JR, Xu H, Pan X, Kim JH, et al. (2014) Association of PD-1, PD-1 ligands, and other features of the tumor immune microenvironment with response to anti-PD-1 therapy. Clinical cancer research: an official journal of the American Association for. *Cancer Research* 20:5064–74.

49) Langenfeld EM, Kong Y, Langenfeld J (2005) Bone morphogenetic protein-2-induced transformation involves the activation of mammalian target of rapamycin. *Molecular Cancer Research* 3:679–84.

50) Cerami E, Gao J, Dogrusoz U, Gross BE, Sumer SO, Aksoy BA, et al. (2012) The cBio cancer genomics portal: an open platform for exploring multidimensional cancer genomics data. *Cancer Discovery* 2:401–4.

51) Gao J, Aksoy BA, Dogrusoz U, Dresdner G, Gross B, Sumer SO, et al. (2013) Integrative analysis of complex cancer genomics and clinical profiles using the cBioPortal. *Science Signaling* 6:pl1.

52) Barretina J, Caponigro G, Stransky N, Venkatesan K, Margolin AA, Kim S, et al. (2012) The Cancer Cell Line Encyclopedia enables predictive modelling of anticancer drug sensitivity. *Nature* 483:603–7.

53) Hahm E, Wei C, Fernandez I, Li J, Tardi NJ, Tracy M, et al. (2017) Bone marrow-derived immature myeloid cells are a main source of circulating suPAR contributing to proteinuric kidney disease. *Nature Medicine* 23:100–6.

54) Lu R, Wu S, Zhang Y, Xia Y, Huelsmann EJ, Lacek AT, et al. (2014) HIV infection accelerates gastrointestinal tumor outgrowth in NSG-HuPBL mice. *AIDS Research Human Retroviruses* 30:677–84.

55) Zhang YG, Wu S, Lu R, Richards MH, Huelsmann EJ, Lacek AT, et al. (2015) HIV infection leads to redistribution of leaky claudin-2 in the intestine of humanized SCID IL-2R(-/-) Hu-PBMC mice. *AIDS Research Human Retroviruses* 31:774–5.

56) Kohlhapp FJ, Broucek JR, Hughes T, Huelsmann EJ, Lusciks J, Zayas JP, et al. (2015) NK cells and CD8+ T cells cooperate to improve therapeutic responses in melanoma treated with interleukin-2 (IL-2) and CTLA-4 blockade. *Journal of Immunotherapy for Cancer* 3:18.

57) Kohlhapp FJ, Huelsmann EJ, Lacek AT, Schenkel JM, Lusciks J, Broucek JR, et al. (2016) Non-oncogenic acute viral infections disrupt anti-cancer responses and lead to accelerated cancer-specific host death. *Cell Reports* 17:957–65.

58) Zloza A, Kohlhapp FJ, Lyons GE, Schenkel JM, Moore TV, Lacek AT, et al. (2012) NKG2D signaling on CD8(+) T cells represses T-bet and rescues CD4-unhelped CD8(+) T cell memory recall but not effector responses. *Nature Medicine* 18:422–8.